Planning Against Disasters in Dynamic Production Networks

Vasco M. Carvalho, Matias Covarrubias and Galo Nuño*

September 5, 2025

Abstract

In dynamic multisector economies, the planner's optimal capital allocation can serve to minimize the aggregate impact of shocks cascading through nonlinear production networks. We show analytically that (i) optimal capital allocation under uncertainty involves deliberately over-investing in upstream sectors in order to mitigate severe economic downturns; (ii) this efficient strategy reduces the average level of consumption and gives rise to a high welfare cost of business cycles. Deploying novel deep-learning techniques in a general environment we show quantitatively that: (iii) the ergodic distribution of the simulated nonlinear economy features higher mean capital levels in key upstream sectors, lower mean levels of macroeconomic aggregates, realistic aggregate volatility and a welfare cost of business cycles one order of magnitude larger than in standard linear models.

*Vasco M. Carvalho, University of Cambridge and CEPR, Matias Covarrubias, Bank of Spain, Galo Nuño, Bank of Spain, CEMFI and CEPR. This manuscript supersedes a previous version entitled 'Nets on Nets: Amplification and Nonlinearities in Dynamic Production Networks.' The paper does not necessarily reflect the views of the Bank of Spain or Eurosystem. The authors are grateful to Isaac Baley, Luis Garicano, Basile Grassi, Ben Moll, Guillermo Ordoñez, Mathias Trabandt, Simon Scheidegger, Jaume Ventura, and Christian von Lehm for useful comments; and to Charles Parry, Jesus Villota, and Bowen Wang for excellent research assistance.

1 Introduction

Recent research on production networks has demonstrated that nonlinearities and complementarities between sectors can dramatically amplify the impact of shocks. When inputs are complementary — as is often the case with specialized components, rare materials, or energy inputs — disruptions in upstream sectors can cascade throughout the economy with outsized effects. This powerful intuition sheds light on classical issues in macroeconomics and holds the promise of better understanding, for example, the nonlinear aggregate effects of oil shocks or the origins of aggregate disaster risk.

In this paper, we confront the benevolent planner of textbook dynamic neoclassical economies with this novel logic of nonlinear production networks. We ask whether, in efficient economies, the planner's allocation of *dynamic* inputs, such as capital, can help mitigate the tail risk that has been shown to emerge in *static* networked environments. We do so both analytically, in a simplified environment, and quantitatively, in a general state-of-the-art dynamic multi-sector setup. We start by showing that optimal capital allocation under uncertainty involves over-investing in upstream sectors in order to minimize the risk of catastrophic downstream transmission.The optimal avoidance of disaster risk also leads to significant sacrifices in the average level of consumption. In the second part of the paper, we offer a quantitative benchmark. We show how to adapt and deploy frontier deep neural network tools that can capture the full nonlinear effects in a canonical dynamic production-networks setup featuring both intermediate input and investment good linkages across sectors. We find that, relative to the deterministic steady state, the ergodic distribution of the simulated nonlinear economy features higher mean capital levels in key upstream sectors, lower mean levels of output, investment and consumption, realistic aggregate volatility and, importantly, a high welfare cost of business cycles.

Analytical characterization. Our first contribution is to characterize optimal capital allocation under uncertainty in a tractable two-period, two-sector networked economy. The model features an upstream sector that produces and intermediate good and a downstream sector that serves the final demand consumption of the representative household. Crucially, both sectors also need capital to produce. Unlike most of the extant literature – which has focused on characterizing static economies – we are interested in characterizing the planner's allocation of pre-determined dynamic inputs, such as capital, across sectors and how this depends on nonlinearities and complementarities.A key focus is on what we call "pre-allocation" of capital before productivity shocks are realized, i.e., how

the allocation of capital to a particular sector compares to what would be optimal in a *deterministic* environment.

Our key analytical result shows that whenever the downstream production function features complementarity across inputs and risk aversion is not too low, the planner's allocation results in excess pre-allocation of capital to the upstream, input-supplying sector (relative to the deterministic optimum). This is because productivity shocks upstream have a nonlinear effect on aggregate output rendering possible aggregate consumption disasters for sufficiently low realizations of shocks. This, in turn, renders insurance against negative upstream shocks more valuable to the planner, who deploys capital to the input supplying sector for this purpose. Our second analytical result shows that, indeed, the elasticity of aggregate consumption with respect to negative upstream shocks is strictly smaller when the planner pursues this excess pre-allocation strategy, relative to what obtains at deterministic optimum allocations.

Our third key analytical result shows that complementarities also imply that pre-allocating capital upstream is costly in terms of lower average consumption level at the stochastic steady state (again, relative to its deterministic counterpart).[1] This is because, holding the productivity of the downstream sector fixed, the planner is: (i) allocating excess capital upstream, to be used precisely in states of the world where that sector is particularly unproductive, and (ii) allocating too little capital downstream, in states of the world where the return to investing in downstream capacity would be relatively high. Thus, in mitigating nonlinear consumption disasters, the planner faces a fundamental tradeoff in terms of the level of aggregate consumption. This result implies that the welfare cost of business cycle does not come from observable volatility of consumption or consumption disasters. As discussed, the planner is able to avert these through manipulating input allocations. Instead, the welfare cost of business cycle is associated with a reduction in average consumption.

Quantitative model. In the second part of the paper, we present a quantitative benchmark by deploying tools that can capture the full nonlinear effects of dynamic production networks. Our quantitative environment is canonical, allowing for flexible substitution possibilities in consumption, investment and production, as well as flexible adjustment-cost specifications for both primary inputs, labor and capital. In detail, our baseline

[1] The stochastic steady state is the steady state of an uncertain economy where all shocks happen to be realized at their (zero) mean. For nonlinear economies, such as ours, this will in general differ from the steady state that obtains in the corresponding deterministic economy.

environment features a representative household with GHH preferences over consumption and labor. In turn, each of these is a CES aggregate of, respectively, disaggregated final consumption goods and labor employed across the different sectors in the economy.[2] Each of the sectors is populated by a representative firm that combines labor and capital with intermediate inputs to produce sectoral gross output. The latter, in turn, can be sold as final consumption, as an intermediate input, or as an investment good. We again allow for successive CES nests, allowing for substitution/complementarity over the two primary inputs, across the intermediate inputs necessary for production, and across primary and intermediate inputs. Sector-specific capital follows a standard law of motion including sector-specific adjustment costs. Sector-specific investment combines investment goods produced by other sectors, again in a CES fashion. All uncertainty derives from sector-specific persistent productivity processes. We assume throughout a perfectly competitive market structure across all markets.

We render this complex disaggregated environment quantitative by calibrating it to data moments for 37 sectors in the US, using data spanning 1948 to 2018. We match steady-state expenditure shares in the model against time-averaged data counterparts, as well as feature empirically relevant input-output and investment linkages across sectors, while also taking into account empirical sector-specific depreciation rates for capital. Whenever possible, we set elasticities to consensus parameterizations already present in the literature.

Even for our relatively low levels of disaggregation, the global solution implies that finding an equilibrium requires solving a stochastic dynamic programming problem with 74 state variables. This is beyond what traditional nonlinear solution methods, such as those based on Chebyshev collocation, can achieve due to the 'curse of dimensionality'. Our second contribution is to show how realistically-large multi-sector general equilibrium models can be solved using deep learning techniques. We build on the 'deep equilibrium nets' method of Azinovic et al. (2022), which approximates equilibrium objects using deep neural networks. To guarantee the quality of our approximation, we have run extensive accuracy checks.

With this method in hand, our third contribution is to document quantitative features of the global solution of our baseline economy. Specifically, we can both compute the ergodic distribution by simulation, capturing how the (potentially) nonlinear propaga-

[2]The CES aggregate of labor allows us to control the degree of flexibility of labor reallocation across sectors.

tion of Gaussian shocks interacts with the anticipation effects of risk on agents, and provide generalized impulse responses at the stochastic steady state. We report five key quantitative results. Our first finding is that the mean of the ergodic distribution of key aggregates – consumption, labor, GDP, investment and total intermediates produced – is always below that of the deterministic steady state. Second, we find that the implied aggregate volatility is substantial – e.g. the standard deviation of annual GDP is 3.4%. Third, our results imply that nonlinear production network economies do not display quantitatively important higher-order moments: in the ergodic distribution, kurtosis is negligible, skewness is small throughout and, depending on the macro aggregate under consideration, can have the wrong sign relative to data. Fourth, there is substantial heterogeneity across sectors in the ergodic mean allocation, with key upstream sectors – like Mining, Oil and Gas – displaying relatively higher capital stocks, whereas downstream sectors display relatively lower capital stocks. Fifth, we also show how, in counterfactual economies with higher sectoral TFP volatility, consumption and labor volatilities increase less than one-to-one. That is, as the risks of nonlinear disasters following large shocks become material, the planner spends more resources in keeping aggregate volatility from spiraling upwards.

Taken together, these results echo our analytical findings in the first part of the paper and suggest that the planner in this dynamic, fully nonlinear economy, is redistributing capital towards upstream sectors and away from downstream sectors in order to dampen large aggregate fluctuations originating in central upstream sectors. By doing this, the planner avoids the endogenous disasters stressed elsewhere in the production networks literature, at the cost of lower mean levels of aggregates. We show how the nonlinear impulse responses to sectoral TFP shocks are attenuated in comparison to the log-linear ones.[3]

Finally, we find that the welfare costs of business cycles are substantial relative to standard calculations in the literature: our global solution implies that the representative household would do away with 1% of lifetime consumption in order to live in a counterfactual economy without shocks. Combining the results above, this large welfare cost of business cycles is largely the direct result of the mean of the ergodic distribution being below that of the deterministic economy, rather than aggregate endogenous disaster risk, which is absent.

[3]This contrasts with the nonlinear response to an unanticipated zero-probability shock, which is amplified with respect to the log-linear case, in line with the findings of Baqaee and Farhi (2019).

Related Literature Our paper relates to three different strands of literature. The first is the rapidly growing literature on production networks (see Acemoglu et al. (2012) for the seminar reference and Carvalho and Tahbaz-Salehi (2019) and Baqaee and Rubbo (2023) for recent overviews of this literature. In particular, our work relates to Baqaee and Farhi (2019) analysis of nonlinear, higher order effects in production networks. In particular, Baqaee and Farhi (2019) show how complementarity and intermediate input linkages together can generate endogenous skewness and aggregate disasters, depending on the size and location - in the production network - of micro-shocks. Relative to Baqaee and Farhi (2019) and the literature that followed – emphasizing nonlinearities in (static) production networks – our contribution is to show that in dynamic environments, the efficient allocation of predetermined inputs alters business cycle properties of these models.[4] On the one hand, we show how the pre-allocation of capital limits the extent to which aggregate nonlinearities – in the form of skewness and aggregate disasters – can emerge as important features in this class of models. On the other hand, our analysis shows that this aggregate disaster possibility and the ensuing optimal preallocation of capital yields a high welfare cost of business cycles. As a second contribution to this literature, this paper is the first to offer a quantitative framework that enables a systematic evaluation of nonlinear networks. This is because all extant quantitative characterizations either provide quantitative illustrations in *static* economies (e.g. Baqaee and Farhi, 2019) where the absence of endogenous dynamics renders it difficult to benchmark results against competing dynamic general equilibrium environments, or rely on approximation techniques such as log-linearized solution (e.g. Horvath, 2000, Atalay, 2017 and Vom Lehn and Winberry, 2022) [5], which, by definition, are ill-suited to fully capture the effects of the non-linear equilibrium dynamics that characterize these environments.

Second, our paper relates to the long-standing literature on the welfare cost of business cycles in dynamic equilibrium economies. As is well known, starting from the seminal contribution of Lucas (1987), simple textbook environments are typically thought to be unable to deliver high welfare costs of uncertainty. This realization, in turn, has motivated a long list of influential research on, for example, the role of preferences, market incompleteness, and various frictional environments or risk processes. Our main contri-

[4]Our emphasis on how predetermined inputs interact and alter other standard features of production networks is shared with Kopytov et al. (2024), who show that, with endogenous network formation but in an otherwise linear and static Cobb-Douglas environment, pre-commitment to risky suppliers may lead firms to optimally choose less risky but less productive suppliers. See also Pellet and Tahbaz-Salehi (2023) for a similar mechanism.

[5]Carvalho (2007), Foerster et al. (2011) and Liu and Tsyvinski (2024) also study dynamic environments but focus on Cobb-Douglas, linear economies.

bution is to overturn the baseline assertion in the literature: we show that a 'vanilla' real business cycle model – with no distortions, frictions, exotic preferences, or unconventional exogenous driving processes – can deliver a high welfare cost of business cycles. Further, we show that the mechanism through which the model attains this high welfare cost is related to - but distinct from - recent resolutions of the 'welfare cost puzzle' relying on disasters and higher order properties of consumption risk (e.g. Barro (2009), Martin (2008) or Jorda et al. (2024)). In particular, our novel mechanism relies on (efficient) capital reallocation across sectors – and the ensuing decline in average output and consumption *levels* – in order to *avoid* disaster risk, rather than on how large disaster realizations change welfare calculations.

Third, our paper relates to a recent literature on the use of deep learning to solve high-dimensional general equilibrium models (e.g., Maliar et al., 2021; Han et al., 2021; Gu et al., 2024).[6] To the best of our knowledge, this paper is the first to apply these techniques to multi-sector dynamic equilibrium models. We do so by extending the "deep equilibrium nets"methodology by Azinovic et al. (2022), as explained in Appendix C.

The rest of the paper proceeds as follows. In Section 2, we provide a simple two-sector model that allows us to analytically characterize capital allocation under uncertainty in a multi-sector networked economy. In Section 3, we exhibit the model and the system of equations that describe the solution. In Section 4, we discuss the calibration and the numerical method. Finally, in Section 5 we detail the results for the global solution of the model.

2 Two-sector model

In this section, we analyze a stylized two-sector model that allows us to analytically characterize capital allocation under uncertainty in a multi-sector networked economy. A key focus is on what we call "excess allocation" of capital, which refers to the allocation of capital to a particular sector that exceeds what would be optimal in a *deterministic* environment. We use this terminology because capital must be allocated before productivity shocks are realized, and uncertainty leads to systematically different capital shares compared to the deterministic optimum. Using this tractable framework, we characterize the incentives behind excess allocation of capital and explore the implications of this allocation on the severity of consumption disasters and on expected consumption. The model

[6] See Fernandez-Villaverde et al. (2024) for a recent review.

allows us to derive theoretical propositions that illuminate the economic forces at play when the planner faces uncertainty about sectoral productivities. Appendix A presents all detailed algebraic derivations and proofs.

2.1 Setting

There are two sectors. Sector 1 ("upstream") produces the intermediate good, and sector 2 ("downstream") produces the final good. Both sectors are subject to productivity shocks, A_1 for upstream and A_2 for downstream. The intermediate good is produced with capital. The final good is produced using capital and the intermediate good. The planner has one unit of a factor K that needs to be allocated to the two sectors, K_1 and K_2. The key aspect of this problem is that capital is allocated before the shocks (A_1, A_2) are realized, creating a decision under uncertainty. After the shocks are realized, there are no remaining decisions to be made, since goods produced and consumed are determined by the previously allocated capital.

Let Q_i and K_i denote gross output and capital in sector $i = \{1, 2\}$, and let C denote consumption of the final good. The problem is defined by the following equations:

$$K_1 + K_2 = 1, \qquad \text{(Resource constraint)} \quad (1)$$

$$Q_1 = A_1 K_1, \qquad \text{(Upstream production)} \quad (2)$$

$$Q_2 = A_2 \left((1 - \gamma_q) (Q_1)^{\frac{\sigma_q - 1}{\sigma_q}} + \gamma_q (K_2)^{\frac{\sigma_q - 1}{\sigma_q}} \right)^{\frac{\sigma_q}{\sigma_q - 1}}, \qquad \text{(Downstream production)} \quad (3)$$

$$C = Q_2, \qquad \text{(Consumption)} \quad (4)$$

where σ_q is the elasticity of substitution between capital in the downstream sector K_2 and the intermediate good from the upstream sector Q_1, γ_q parametrizes the share of the intermediate good in gross output, and the shocks A_1 and A_2 are independent random variables.

Each shock takes either a high value $A_H = \bar{A} + \Delta_A$ or a low value $A_L = \bar{A} - \Delta_A$. For shock A_1, the probability of the low state is p_1, while for shock A_2, the probability of the low state is p_2.

A representative household maximizes the expected utility:

$$\mathbb{E}[U(C)] = \mathbb{E}\left[\frac{C^{1-\epsilon_c^{-1}}}{1-\epsilon_c^{-1}}\right] \tag{5}$$

where the expectation is taken with respect to the random variables A_1 and A_2, and ϵ_c is the intertemporal elasticity of substitution.

We consider the first-best allocation produced by a benevolent social planner. This coincides with the allocation in the competitive equilibrium, assuming that firms in both sectors operate under perfect competition. The social planner maximizes household welfare (5) subject to the technological constraints (1)-(4),

2.2 First-order condition

We express consumption as a function of K_1 and normalize it to downstream-efficiency units, $\tilde{C} = C/A_2$. Specifically, using the resource constraint (1), we can substitute $K_2 = 1 - K_1$ to obtain:

$$\tilde{C}_{S_1} = \left((1-\gamma_q)\left(A_{1,S_1}K_1\right)^{\frac{\sigma_q-1}{\sigma_q}} + \gamma_q\left(1-K_1\right)^{\frac{\sigma_q-1}{\sigma_q}}\right)^{\frac{\sigma_q}{\sigma_q-1}}, \quad S_1 \in \{L,H\}. \tag{6}$$

Here, $\tilde{C}_{S_1}$ represents the normalized consumption level when the upstream productivity shock A_1 is in state S_1, where A_{1,S_1} denotes the realization of A_1 in state $S_1 \in \{L,H\}$. Note that S_2 does not appear as a subscript since we are normalizing by A_2.

We obtain the following expression for the first-order condition:

$$\frac{\partial \tilde{U}(\tilde{C})}{\partial K_1} = p_1 \tilde{C}_L^{-\epsilon_c^{-1}} \left(\underbrace{(1-\gamma_q)\left(\frac{A_L K_1}{\tilde{C}_L}\right)^{\frac{-1}{\sigma_q}} A_L}_{\tilde{\text{MPK}}_{1,L}} - \underbrace{\gamma_q \left(\frac{1-K_1}{\tilde{C}_L}\right)^{\frac{-1}{\sigma_q}}}_{\tilde{\text{MPK}}_{2,L}} \right) \tag{7}$$

$$+ (1-p_1)\tilde{C}_H^{-\epsilon_c^{-1}} \left(\underbrace{(1-\gamma_q)\left(\frac{A_H K_1}{\tilde{C}_H}\right)^{\frac{-1}{\sigma_q}} A_H}_{\tilde{\text{MPK}}_{1,H}} - \underbrace{\gamma_q \left(\frac{1-K_1}{\tilde{C}_H}\right)^{\frac{-1}{\sigma_q}}}_{\tilde{\text{MPK}}_{2,H}} \right) = 0. \tag{8}$$

The first-order condition for K_1 is central to our analysis of excess allocation. Each component of the sum represents the marginal utility impact of allocating capital to the upstream sector in a specific upstream productivity state, weighted by the probability of that state and the marginal utility in that state.

This expression breaks down the marginal impact of allocating more capital to the upstream sector. The first term in each state, $\tilde{\text{MPK}}_{1,S}$, represents the (per-unit of efficiency) marginal product of capital in the upstream sector, which contributes positively to consumption. The second term, $\tilde{\text{MPK}}_{2,S}$, represents the opportunity cost in terms of foregone production in the downstream sector. The total marginal product in each state is the difference between these two effects.

For the following results, we consider the case where $p_1 = p_2 = 1/2$, which gives us symmetric positive and negative productivity shocks. Also, we assume $\bar{A} = 1$.

2.3 The deterministic optimum

First, we analyze the deterministic problem, that is, the problem of allocating capital when $A_1 = A_2 = 1$. The first-order condition is:

$$\left((1-\gamma_q)\left(\frac{K_1}{\tilde{C}}\right)^{\frac{-1}{\sigma_q}} - \gamma_q \left(\frac{1-K_1}{\tilde{C}}\right)^{\frac{-1}{\sigma_q}} \right) = 0, \tag{9}$$

Solving for K_1^{determ} (the optimal capital allocation in the deterministic case):

$$K_1^{determ} = \frac{\left(1-\gamma_q\right)^{\sigma_q}}{\gamma_q^{\sigma_q} + \left(1-\gamma_q\right)^{\sigma_q}} \tag{10}$$

This expression shows that the optimal deterministic allocation depends only on the production share parameters γ_q and the elasticity of substitution σ_q. Intuitively, when γ_q is higher—that is, when downstream capital is more important in production—less capital is allocated to the upstream sector. The effect of σ_q depends on the relative magnitudes of γ_q and $(1-\gamma_q)$. In the special case where $\gamma_q = 1/2$, meaning both sectors have equal weight in production, we have $K_1^{determ} = 1/2$ regardless of the value of σ_q.

2.3.1 The impact of productivity shocks at the deterministic solution

To formally characterize the asymmetric responses of consumption to sectoral productivity shocks, we introduce notation for impulse responses and skewness measures. We write $C_{A_1A_2}(K_1)$ to denote the consumption function when the upstream productivity is A_1, the downstream productivity is A_2, and the capital allocation to the upstream sector is K_1. We use $IR^{-,\text{upst}}(K_1)$ and $IR^{+,\text{upst}}(K_1)$ to denote impulse responses of consumption to negative and positive upstream productivity shocks, respectively, as functions of the capital allocation K_1. Similarly, $IR^{-,\text{downst}}(K_1)$ and $IR^{+,\text{downst}}(K_1)$ denote impulse responses to negative and positive downstream productivity shocks. Formally:

$$\begin{aligned} IR^{+,\text{upst}}(K_1) &\equiv C_{H\bar{A}}(K_1) - C_{\bar{A}\bar{A}}(K_1), \qquad & IR^{+,\text{downst}}(K_1) &\equiv C_{\bar{A}H}(K_1) - C_{\bar{A}\bar{A}}(K_1) \\ IR^{-,\text{upst}}(K_1) &\equiv C_{\bar{A}\bar{A}}(K_1) - C_{L\bar{A}}(K_1), \qquad & IR^{-,\text{downst}}(K_1) &\equiv C_{\bar{A}\bar{A}}(K_1) - C_{\bar{A}L}(K_1) \end{aligned}$$

Note that for negative shocks, we write the impulse responses as the difference between consumption at the expected productivity level and consumption at the low productivity level. This ensures all impulse responses are measured as positive numbers, facilitating comparisons of their magnitudes.

We define the skewness coefficient as:

$$\text{Skew}^{\text{upst}}(K_1) = \frac{(IR^{+,\text{upst}}(K_1))^3 - (IR^{-,\text{upst}}(K_1))^3}{[(IR^{-,\text{upst}}(K_1))^2 + (IR^{+,\text{upst}}(K_1))^2]^{3/2}} \tag{11}$$

$$\text{Skew}^{\text{downst}}(K_1) = \frac{(IR^{+,\text{downst}}(K_1))^3 - (IR^{-,\text{downst}}(K_1))^3}{[(IR^{-,\text{downst}}(K_1))^2 + (IR^{+,\text{downst}}(K_1))^2]^{3/2}} \tag{12}$$

Using this notation, we can formally characterize the asymmetric nature of consumption responses under the deterministic allocation:

Lemma 1. *For $\sigma_q < 1$, upstream shocks generate negatively skewed responses in consumption, while downstream shocks generate symmetric impacts:*

1. *Upstream shocks (negatively skewed):*

$$IR^{-,upst}(K^{determ}) > IR^{+,upst}(K^{determ}) \implies Skew^{upst}(K^{determ}) < 0$$

2. *Downstream shocks (symmetric):*

$$IR^{-,downst}(K^{determ}) = IR^{+,downst}(K^{determ}) \implies Skew^{downst}(K^{determ}) = 0$$

Lemma 2. *In a Leontief economy, the asymmetry of upstream impulse responses equals $-1 + A_L$:*

$$\lim_{\sigma_q \to 0^+} Asymmetry^{upst}(K_1) = IR^{+,upst} - IR^{-,upst} = -IR^{-,upst} = -1 + A_L \tag{13}$$

The proof of these lemmas is presented in Appendices A.3 and A.4. These lemmas formalize a central phenomenon that emerges in production networks: when inputs are complements, negative upstream productivity shocks have disproportionately large effects on consumption compared to positive shocks of equal magnitude (Baqaee and Farhi, 2019). Lemma 2 provides additional insight by examining the limiting Leontief case, which reveals two properties of production networks with perfect complementarity in terms of capital slackness. First, the positive impulse response upstream is zero ($IR^{+,\text{upst}} = 0$) in the Leontief limit. This occurs because when the upstream sector experiences a positive shock, upstream capital becomes slack—production is constrained by the downstream sector, which becomes the binding constraint. Additional upstream productivity cannot improve overall output when the downstream complement remains

fixed. Second, the negative impulse response shows that when the upstream sector experiences a negative shock, upstream capital becomes binding while downstream capital becomes slack. In this case, production is entirely determined by the constrained upstream sector. Consequently, upstream capital allocation matters in the margin precisely when the upstream sector is unproductive.

Figure 1 shows the consumption response to productivity shocks under four different substitutability cases. Panel (a) shows that upstream shocks generate asymmetric consumption responses when inputs are complements, with the asymmetry becoming more pronounced as σ_q decreases toward the Leontief case analyzed in Lemma 2. Notably, even with substitutable inputs ($\sigma_q = 4$), some asymmetry persists, though it is much less pronounced than in the complementary cases. Panel (b) shows the contrasting behavior of downstream shocks, which generate symmetric responses regardless of the elasticity of substitution, as predicted by Lemma 1. This occurs because downstream productivity shocks operate outside the CES aggregator in our production structure, making the substitutability parameters irrelevant for the consumption response.

Figure 1: Consumption responses to productivity shocks in the deterministic solution

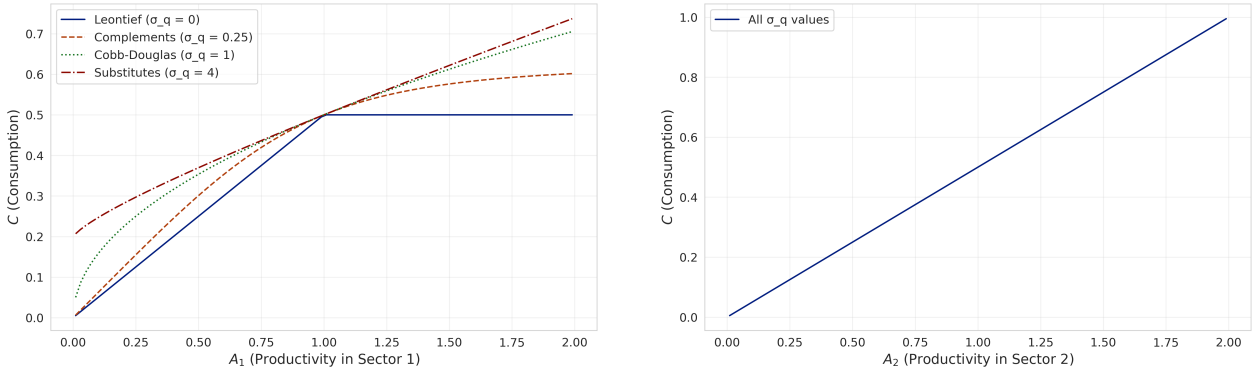

(a) Impact of upstream productivity shocks

(b) Impact of downstream productivity shocks

Note: The figure shows consumption as a function of productivity in both sectors. Panel (a) shows the impact of upstream productivity shocks across four substitutability cases: Leontief ($\sigma_q = 0$), complements ($\sigma_q = 0.25$), Cobb-Douglas ($\sigma_q = 1$), and substitutes ($\sigma_q = 4$). Panel (b) shows the impact of downstream productivity shocks; the four substitutability cases are irrelevant for the consumption response since the downstream shock is outside the CES aggregator. Assumed parameters: $\gamma_q = 0.5$, so both sectors are the same size.

2.4 The benefits and costs of excess allocation upstream

Having established the conditions under which upstream productivity shocks create asymmetric consumption effects, we now analyze the consequences of allocating excess

capital to the upstream sector beyond what would be optimal in a deterministic environment. Specifically, we examine both the insurance benefits and efficiency costs of such excess allocation. These results provide insights into how capital allocation serves as an insurance mechanism against negative upstream productivity shocks in networked production economies.

2.4.1 Insurance benefits of excess allocation upstream

Lemma 3. *If inputs are complements ($\sigma_q < 1$), then increasing capital allocation to the upstream sector beyond the deterministic optimum decreases the impulse response to negative upstream productivity shocks:*

$$\left.\frac{\partial IR^{-,upst}(K_1)}{\partial K_1}\right|_{K_1=K_1^{determ}} < 0$$

where $IR^{-,upst}(K_1)$ measures the consumption drop resulting from a negative upstream productivity shock.

The proof of this lemma is presented in Appendix A.5.

This lemma formalizes the insurance value of excess allocation upstream. When upstream and downstream sectors are complements, allocating more capital to the upstream sector than would be optimal in a deterministic environment dampens the effect of negative upstream productivity shocks on consumption. The negative derivative indicates that each additional unit of capital allocated to the upstream sector reduces the consumption drop caused by adverse shocks.

Figure 2 illustrates the economics of risk mitigation under different production structures. The figure provides a comprehensive view of consumption across all productivity states, demonstrating how the elasticity of substitution determines the optimal risk mitigation strategy. When inputs are complements ($\sigma_q < 1$), left-tail risk is attenuated by allocating more capital to the unproductive, shock-affected sector. Conversely, when inputs are substitutes ($\sigma_q > 1$), tail risk is better mitigated by strengthening the productive sectors—reflecting the essence of substitutability, where agents optimally shift resources away from low-productivity toward high-productivity inputs.

Figure 2: Impact of higher upstream capital on consumption across productivity shocks

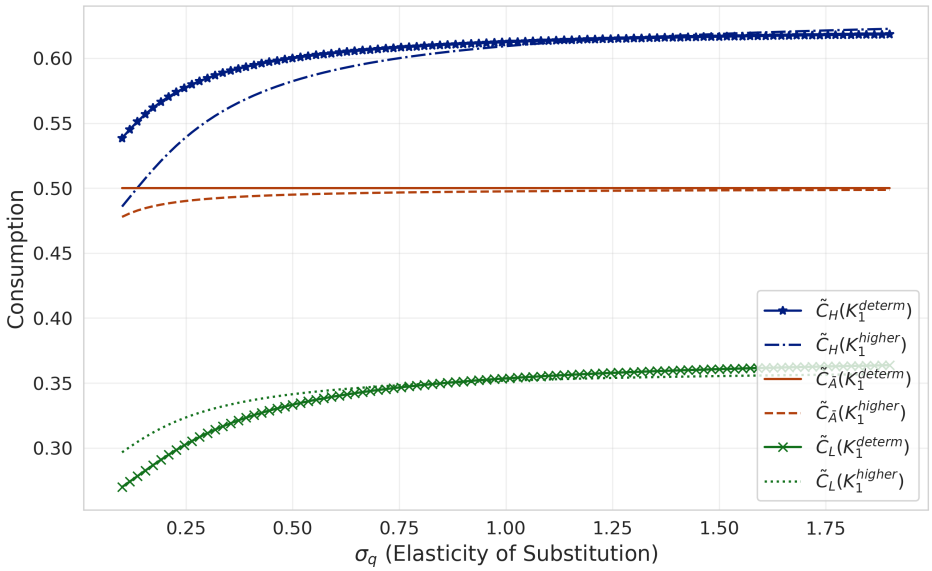

Note: The figure shows consumption as a function of σ_q for high, average, and low upstream productivity levels under two scenarios: deterministic optimal capital allocation and 10% higher upstream capital allocation. The graph shows how higher upstream capital affects consumption responses to productivity shocks. We use $\Delta_A = 0.5$ throughout.

Crucially, the figure shows that while excess upstream allocation attenuates negative impulse responses under complementarity, it comes at the cost of lower expected consumption across all states. We next characterize the productivity costs of excess allocation upstream.

2.4.2 Productivity costs of excess allocation upstream

While excess allocation upstream provides insurance benefits, it also entails costs. The next proposition show the conditions under which strengthening the upstream sector reduces expected consumption.

Proposition 1. *Up to the first-order approximation, if inputs are complements ($\sigma_q < 1$), the effect of excess allocation upstream on expected consumption depends on the relative strength of the upstream sector:*

1. *When the upstream sector is large enough ($\gamma_q < \bar{\gamma}_q(\triangle_A)$), increasing upstream capital allocation beyond the deterministic optimum decreases expected consumption:*

$$\frac{\partial \mathbb{E}\{C(A, K_1)\}}{\partial K_1}\bigg|_{K_1 = K_1^{determ}} < 0.$$

2. *When the upstream sector's role is more limited ($\gamma_q > \bar{\gamma}_q(\triangle_A)$), increasing upstream capital allocation increases expected consumption.*

The proof of this proposition is presented in Appendix A.6.

This proposition establishes the opportunity cost of allocating excess capital to the upstream sector compared to the deterministic solution. When inputs are complements and the upstream sector is not too small, allocating more capital upstream reduces expected consumption. To understand the mechanism by which expected consumption decreases, we decompose the impact of excess allocation upstream on expected consumption into marginal productivities of capital in each sector, for both states. This decomposition shows why there is an efficiency cost to providing insurance through upstream capital allocation:

$$\frac{\partial \mathbb{E}[\tilde{C}]}{\partial K_1}\bigg|_{K_1^{determ}} = p_1 \left(\underbrace{(1-\gamma_q)\left(\frac{A_L K_1^{determ}}{\tilde{C}_L}\right)^{\frac{-1}{\sigma_q}} A_L}_{\tilde{\text{MPK}}_{1,L} \quad (=(1-\gamma_q)A_L \text{ as } \sigma_q \to 0)} - \underbrace{\gamma_q \left(\frac{1-K_1^{determ}}{\tilde{C}_L}\right)^{\frac{-1}{\sigma_q}}}_{\tilde{\text{MPK}}_{2,L} \quad (=0 \text{ as } \sigma_q \to 0)} \right)$$

$$+ (1-p_1) \left(\underbrace{(1-\gamma_q)\left(\frac{A_H K_1^{determ}}{\tilde{C}_H}\right)^{\frac{-1}{\sigma_q}} A_H}_{\tilde{\text{MPK}}_{1,H} \quad (=0 \text{ as } \sigma_q \to 0)} - \underbrace{\gamma_q \left(\frac{1-K_1^{determ}}{\tilde{C}_H}\right)^{\frac{-1}{\sigma_q}}}_{\tilde{\text{MPK}}_{2,H} \quad (=\gamma_q \text{ as } \sigma_q \to 0)} \right)$$

The behavior of marginal products is presented in Figure 3. With complementarities, production is constrained by the sector with lower productivity—the "low-quantity sector." In the low upstream productivity state, the upstream sector becomes the low-quantity sector; in the high upstream productivity state, the downstream sector becomes the low-quantity sector. Everything else constant, adding resources to the constraining sector provides a high increase in the aggregate.

Figure 3: Marginal products of capital across different elasticities of substitution

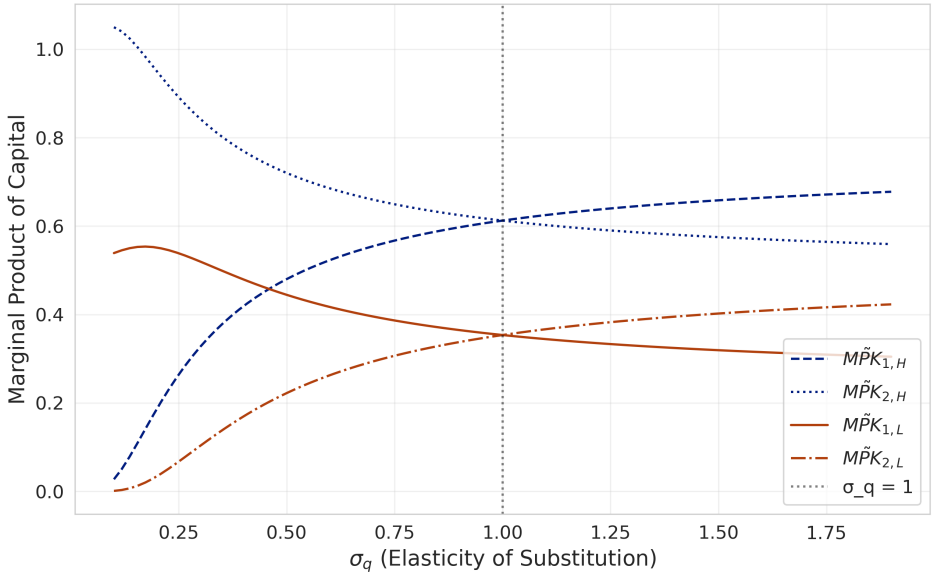

Note: The figure shows the marginal product of capital in the upstream sector ($\tilde{\text{MPK}}_1$) and downstream sector ($\tilde{\text{MPK}}_2$) under both low upstream productivity (red, intersect in the lower half) and high upstream productivity (blue, intersect in the upper half) states. All values are evaluated at the deterministic optimal capital allocation. The vertical dotted line marks $\sigma_q = 1$, the boundary between complementarity ($\sigma_q < 1$) and substitutability ($\sigma_q > 1$). Parameters: $\gamma_q = 0.5$ and $\Delta_A = 0.5$.

The Leontief case ($\sigma_q \to 0$), which corresponds to the leftmost limit of Figure 3, illustrates this constraint. When inputs are perfect complements, only the low-quantity sector matters at the margin. Thus, $\tilde{\text{MPK}}_2$ in the low upstream productivity state and $\tilde{\text{MPK}}_1$ in the high upstream productivity state both approach zero, since additional capital in the non-constraining sector yields no marginal benefit.

This insight can be described in terms of the slackness of capital under complementarity. In each state, one sector is binding and the other is slack. In the low upstream productivity state, downstream capital is slack, while upstream capital is binding but its marginal product is penalized by $A_1 = A_L$. In the high upstream productivity state, upstream capital is slack, while downstream capital is binding and enjoys full productivity, $A_2 = 1$. Strengthening the upstream sector therefore shifts units of capital away from uses that are binding and fully productive (downstream in the high upstream productivity state) toward uses that are either slack (upstream in the high upstream productivity state) or binding but penalized (upstream in the low upstream productivity state). This slackness asymmetry is visible in Figure 3: the marginal product of capital downstream in the high upstream productivity state exceeds the marginal product upstream in the low upstream

productivity state.

This insight reflects a general property of complementarities in production networks. In a multi-sector network with CES aggregation, the productivity cost of reallocating capital upstream is a generic consequence of complementarities. When the elasticity of substitution is low, shocks to any CES-linked input create consumption disasters, which makes it tempting to insure by over-allocating capital to those inputs. However, for any sector inside a CES nest, extra capital is nearly unproductive in high-productivity states because effective output is constrained by its complements, so its marginal product is concentrated in bad states. This asymmetry strengthens with upstreamness: an upstream unit of capital must be combined not only with its intra-nest complement but with the entire set of downstream complements along the chain, so in good states its marginal product is capped by multiple downstream bottlenecks, whereas in bad states it bears the full penalty of the sector's own adverse shock. As a result, the fraction of states in which upstream capital is slack rises with upstreamness, shifting its payoff toward disaster states and increasing the expected-output cost of using upstream capital to provide insurance. This represents the trade-off: insurance value rises with upstreamness, but so does the productivity cost.

Consistent with this trade-off, a risk-neutral planner who maximizes $\mathbb{E}[C]$ would not over-allocate upstream, since insurance provides no benefits, whereas sufficient risk aversion can rationalize accepting the efficiency loss for insurance value. We now characterize the conditions under which excess allocation upstream occurs.

2.5 Optimal capital allocation under uncertainty

The previous subsection established that excess allocation upstream generates two opposing effects: it provides valuable insurance against negative upstream productivity shocks by reducing their impact on consumption, but it also comes at the cost of lower expected consumption. To understand when the insurance benefits outweigh the efficiency costs, we need to characterize optimal capital allocation under uncertainty.

We cannot generally solve for the optimal level of capital allocation under uncertainty in closed form. Instead, we use the marginal expected utility $\partial \mathbb{E}[U(C)]/\partial K_1$ evaluated at the deterministic case K_1^{determ}. If the marginal expected utility of capital upstream at the deterministic allocation is positive, then it is optimal to increase the allocation of capital upstream. Our analytical strategy relies on the fact that the marginal expected utility is decreasing in K_1, which follows from the general principle of decreasing marginal returns

to inputs.

Figure 4: Marginal expected utility as a function of upstream capital allocation

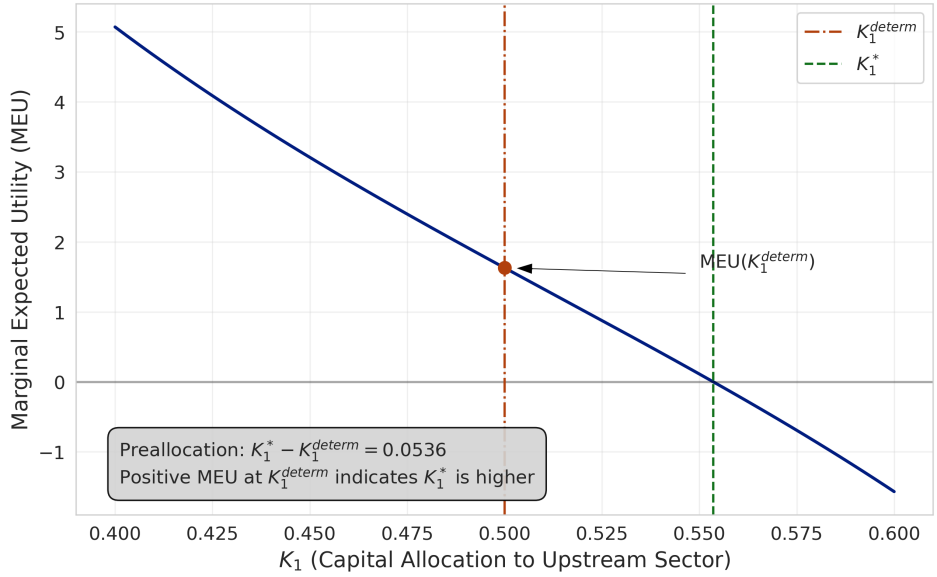

Note: This figure illustrates our proof approach: when MEU evaluated at the deterministic optimum K_1^{determ} is positive, the stochastic optimum K_1^* must be higher, resulting in excess allocation to the upstream sector. The parameters used are $\sigma_q = 0.25$, $\gamma_q = 0.5$, risk aversion $\epsilon_c^{-1} = 1$, and $\Delta_A = 0.5$. The intersection of the marginal expected utility curve with the horizontal axis determines the stochastic optimum.

Figure 4 illustrates this approach by showing the marginal expected utility curve (solid blue line) as a function of K_1, calculated assuming $\sigma_q = 0.25$, $\gamma_q = 0.5$, risk aversion $\epsilon_c^{-1} = 1$, shock distribution $p_1 = p_2 = 0.5$, and shock values $\bar{A} = 1$ and $\Delta_A = 0.5$. The intersection of this curve with the horizontal axis determines the stochastic optimum K_1^*, while the deterministic optimum K_1^{determ} is shown by the vertical dotted-dashed red line. The figure shows that when the marginal expected utility is positive at K_1^{determ}, the stochastic optimum involves higher allocation to the upstream sector. This figure represents the main idea of our proof for excess allocation upstream: the curvature and position of the marginal expected utility function determine whether and how much excess allocation occurs.

In order to evaluate the marginal expected utility of K_1 at the deterministic allocation, we first obtain consumption and the marginal productivity of K_1 evaluated at the deterministic allocation. First, we evaluate the consumption level at the deterministic allocation:

$$\tilde{C}_S\big|_{K_1^{determ}} = \left(\frac{1}{\gamma_q^{\sigma_q} + (1-\gamma_q)^{\sigma_q}}\right)\left(A_{1,S_1}^{1-\frac{1}{\sigma_q}}(1-\gamma_q)^{\sigma_q} + \gamma_q^{\sigma_q}\right)^{\frac{\sigma_q}{\sigma_q-1}}.$$

Next, we evaluate the derivative of consumption with respect to K_1 at the deterministic solution in each of the two states S:

$$\left.\frac{\partial \tilde{C}_S}{\partial K_1}\right|_{K_1^{determ}} = \frac{\left(A_{1,S_1}^{1-\frac{1}{\sigma_q}} - 1\right)}{\left(A_{1,S_1}^{1-\frac{1}{\sigma_q}}(1-\gamma_q)^{\sigma_q} + \gamma_q^{\sigma_q}\right)^{\frac{-1}{\sigma_q-1}}}$$

The FOC evaluated at the deterministic optimum is:

$$\left.\frac{\partial \mathbb{E}[U(C)]}{\partial K_1}\right|_{K_1^{determ}} \propto p_1\frac{\left(A_L^{1-\frac{1}{\sigma_q}} - 1\right)}{\left(A_L^{1-\frac{1}{\sigma_q}}(1-\gamma_q)^{\sigma_q} + \gamma_q^{\sigma_q}\right)^{\frac{\epsilon_c^{-1}\sigma_q-1}{\sigma_q-1}}} + (1-p_1)\frac{\left(A_H^{1-\frac{1}{\sigma_q}} - 1\right)}{\left(A_H^{1-\frac{1}{\sigma_q}}(1-\gamma_q)^{\sigma_q} + \gamma_q^{\sigma_q}\right)^{\frac{\epsilon_c^{-1}\sigma_q-1}{\sigma_q-1}}},$$

where we have removed the positive constant $\left[\gamma_q^{\sigma_q} + (1-\gamma_q)^{\sigma_q}\right]^{\epsilon_c^{-1}}$.

To show that we obtain excess allocation—that is, $K_1^* > K_1^{determ}$—we need to prove that the marginal expected utility with respect to K_1 is positive when evaluated at the deterministic solution, $\left.\frac{\partial \mathbb{E}[U(C)]}{\partial K_1}\right|_{K_1^{determ}} > 0$. This would indicate that the planner would increase K_1 beyond the deterministic optimum when facing uncertainty. Thus, we are trying to find parametric conditions such that:

$$(1-p_1)\frac{A_H^{1-\sigma_q^{-1}} - 1}{\left(A_H^{1-\frac{1}{\sigma_q}}(1-\gamma_q)^{\sigma_q} + \gamma_q^{\sigma_q}\right)^{\frac{\epsilon_c^{-1}\sigma_q-1}{\sigma_q-1}}} > p_1\frac{1 - A_L^{1-\sigma_q^{-1}}}{\left(A_L^{1-\frac{1}{\sigma_q}}(1-\gamma_q)^{\sigma_q} + \gamma_q^{\sigma_q}\right)^{\frac{\epsilon_c^{-1}\sigma_q-1}{\sigma_q-1}}}$$

Proposition 2. *If inputs are complements ($\sigma_q < 1$), the planner allocates excess capital to the upstream sector (that is, $K_1^* > K_1^{determ}$) under any of the following conditions, to a first-order approximation:*

1. *If risk aversion is high enough, $\epsilon_c^{-1} \geq 1$.*
2. *If risk aversion is moderate $\bar{\epsilon}_c^{-1}(\Delta_A, \gamma_q) < \epsilon_c^{-1} < 1$.*
3. *If risk aversion is low, $0 < \epsilon_c^{-1} < \bar{\epsilon}_c^{-1}(\Delta_A, \gamma_q)$, and the downstream sector's importance in production is sufficiently high, $\gamma_q > \bar{\gamma}_q(\Delta_A)$.*

The thresholds $\bar{\gamma}_q(\Delta_A)$ and $\bar{\epsilon}_c^{-1}(\Delta_A, \gamma_q)$ are determined by the size of productivity shocks and production parameters.

The proof of this proposition is presented in Appendix A.7.

This proposition clarifies the role of risk aversion in determining when excess allocation upstream is optimal. As we saw in subsection 2.4, with risk neutrality we have that excess upstream allocation would be suboptimal since insurance provides no benefits. However, a sufficiently risk-averse agent may accept this efficiency cost for the insurance value. The proposition shows that risk aversion $\epsilon_c^{-1} \geq 1$ is sufficient (but not necessary) for excess allocation upstream to occur when inputs are complements. This threshold captures the critical level of risk aversion where the marginal utility gains from insurance outweigh the marginal productivity losses from misallocation.

Figure 5 provides computational verification of this theoretical result across a wide range of parameter values. Panel (a) illustrates how excess allocation depends on the elasticity of substitution between inputs and on risk aversion: with substitutable inputs ($\sigma_q > 1$), capital is allocated in excess *downstream*, while with complementary inputs ($\sigma_q < 1$), capital is generally allocated in excess upstream except when both risk aversion and the elasticity of substitution are low. Panel (b) examines how excess allocation varies with the downstream sector's intensity share (γ_q) when inputs are complements ($\sigma_q = 0.5$). The results show that excess allocation to the upstream sector occurs across most parameter combinations, except when both risk aversion and the downstream intensity share are low. The blue regions in both panels represent parameter combinations where excess allocation to the upstream sector occurs, while the dashed black line in panel (b) shows the boundary case of zero excess allocation.

Figure 5: Excess allocation over the parameter space

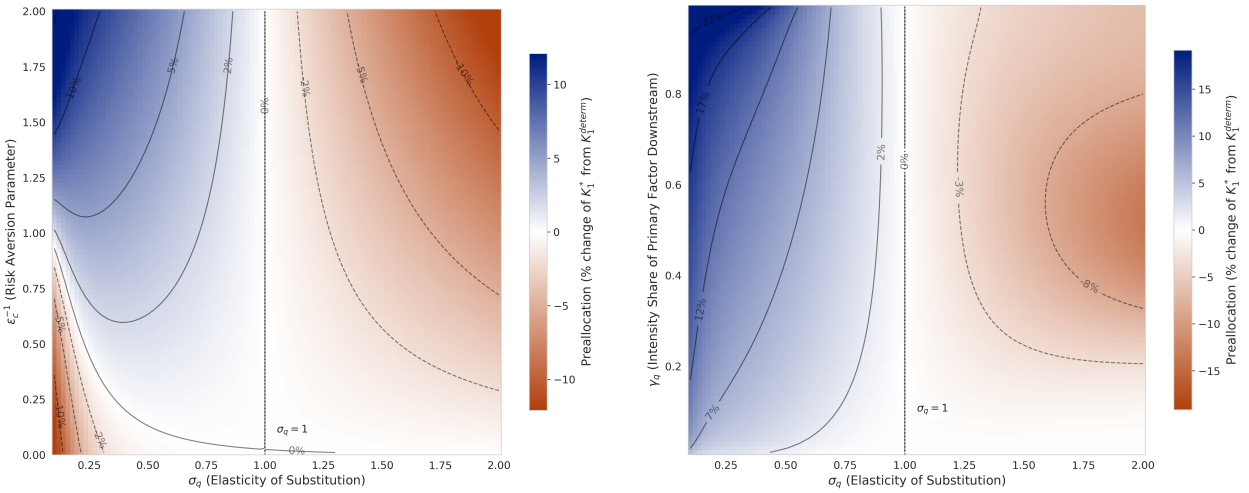

(a) Excess allocation as a function of risk aversion and elasticity of substitution

(b) Excess allocation as a function of downstream size and elasticity of substitution

Note: Excess allocation to the upstream sector. Panel (a) shows the percentage difference between stochastic optimum K_1^* and deterministic optimum K_1^{determ} across elasticity of substitution σ_q and risk aversion ϵ_c^{-1}, with $\gamma_q = 0.5$. The vertical line at $\sigma_q = 1$ marks the boundary between complementarity and substitutability. Panel (b) shows excess allocation across downstream intensity share γ_q and elasticity of substitution (σ_q), with $\epsilon_c^{-1} = 2$. In both panels, blue regions indicate positive excess allocation upstream, while red regions indicate the opposite. Contour lines show the level of excess allocation. We use $\Delta_A = 0.5$ throughout.

The analytical results in this section provide a characterization of optimal capital allocation under uncertainty in networked production economies. Lemma 1 identifies the issue with deterministic solutions: negative shocks upstream generate consumption disasters, when inputs are complements. Proposition 3 shows how to use capital allocation to attenuate consumption disasters: with complementarities, adding capital upstream increases the quantity of the unproductive sector constraining production, while with substitutability, adding capital downstream allows substitution from the unproductive to the productive sector. Proposition 1 demonstrates that for the case of complementarities, excess allocation upstream, even though it helps with consumption disasters, has a productivity cost that makes expected consumption decrease, rendering such allocation suboptimal for a risk-neutral agent. Mechanically, with complementarities, capital in sectors that have CES complements becomes slack in good states because their complements bind; for upstream sectors—whose output must be combined with both intra-nest and downstream complements—this slackness is more pervasive, so reallocating capital upstream shifts units from binding, fully productive uses to uses that are frequently slack or productivity-penalized, lowering expected consumption. Finally, Proposition 2 charac-

terizes the level of risk aversion that makes excess allocation upstream optimal, showing that risk aversion $\epsilon_c^{-1} \geq 1$ is sufficient (but not necessary) for this outcome.

Having established the theoretical foundations of capital allocation under uncertainty in a stylized two-sector framework, we now turn to a full dynamic quantitative model with input-output and investment goods networks to examine these mechanisms in a richer, more realistic setting.

3 Quantitative Model

We introduce here the full quantitative model. There are a finite number of perfectly competitive sectors indexed by $j = 1, ..., N$. A representative household consumes goods and supplies labor to firms in each sector. Time is discrete and infinite.

3.1 Households

The representative household has the following preferences over consumption of each good j, which we denote C_{jt}, and labor on industry j, which we denote L_{jt}:

$$U = \sum_{t=0}^{\infty} \beta^t \left[\frac{1}{1-\epsilon_c^{-1}} \left(C_t - \theta \frac{L_t^{1+\epsilon_l^{-1}}}{1+\epsilon_l^{-1}} \right)^{1-\epsilon_c^{-1}} \right] \quad \text{where}$$

$$C_t = \left(\sum_{j=1}^{N} \xi_j^{\frac{1}{\sigma_c}} (C_{jt})^{1-\sigma_c^{-1}} \right)^{\frac{1}{1-\sigma_c^{-1}}}, \quad \sum_{j=1}^{N} \xi_j = 1 \text{ and } L_t = \left(\sum_{j=1}^{N} (L_{jt})^{1+\sigma_l^{-1}} \right)^{\frac{1}{1+\sigma_l^{-1}}}$$

where β is the discount factor, ϵ_c is the intertemporal elasticity of substitution (or the inverse of the relative risk aversion), ϵ_l is the Frisch elasticity of labor, ξ_j captures the time-invariant preference for good j, σ_c is the elasticity of substitution across goods, σ_l controls the degree of labor reallocation between sectors, and θ is a normalization constant.

3.2 Firms

The representative firm in sector j produces gross output Q_{jt} using capital K_{jt}, labor L_{jt}, and intermediate inputs M_{jt}.[7] The production function is:

$$Q_{jt} = \left[(\mu_j)^{\sigma_q^{-1}} \left(Y_{jt}\right)^{1-\sigma_q^{-1}} + \left(1-\mu_j\right)^{\sigma_q^{-1}} \left(M_{jt}\right)^{1-\sigma_q^{-1}} \right]^{\frac{1}{1-\sigma_q^{-1}}}, \text{ where}$$
$$Y_{jt} = A_{jt} \left[(\alpha_j)^{\sigma_y^{-1}} \left(K_{jt}\right)^{1-\sigma_y^{-1}} + \left(1-\alpha_j\right)^{\sigma_y^{-1}} \left(L_{jt}\right)^{1-\sigma_y^{-1}} \right]^{\frac{1}{1-\sigma_y^{-1}}}.$$

Variable Y_{jt} denotes value-added production, α_j captures the share of capital in value-added, μ_j parametrizes the share of materials in gross output, σ_q is the elasticity of substitution between primary outputs (e.g. capital and labor) and materials, and A_{jt} is an industry-specific shock to value added productivity that follows the process

$$\log A_{jt+1} = \rho_j \log A_{jt} + \varepsilon^A_{jt+1}$$

where ρ_j represents industry-specific persistence and the shocks ε^A_{jt+1} are distributed multivariate normal with mean 0 and variance-covariance matrix Σ^A. The industry-specific productivity shocks may be correlated, that is, the variance-covariance matrix may not be diagonal.

Firms can accumulate capital by producing an industry-specific investment good I_{jt} facing capital adjustment costs denoted by Φ_{jt}:

$$K_{jt+1} = (1-\delta_j)K_{jt} + I_{jt} - \Phi_{jt},$$
$$\Phi_{jt} = \frac{\phi}{2}\left(\frac{I_{jt}}{K_{jt}} - \delta_j\right)^2 K_{jt}$$

where δ_j is the industry-specific depreciation rate, and ϕ parametrize the adjustment cost function.

The investment good is produced by bundling goods produced by other industries:

$$I_{jt} = \left(\sum_{i=1}^{N} \left(\gamma^I_{ij}\right)^{\sigma_I^{-1}} \left(I_{ijt}\right)^{1-\sigma_I^{-1}} \right)^{\frac{1}{1-\sigma_I^{-1}}}, \quad \text{where} \quad \sum_{i=1}^{N} \gamma^I_{ij} = 1$$

[7] This variable is also labeled as material in some papers (e.g., Rotemberg and Woodford, 1993).

where γ_{ij}^I represents the importance of good i in the production of the investment good for sector j, and σ_I is the elasticity of substitution between inputs of the investment bundle. In the same vein, the intermediate input is produced using the following bundle:

$$M_{jt} = \left(\sum_{i=1}^{N} \left(\gamma_{ij}^m \right)^{\sigma_m^{-1}} \left(M_{ijt} \right)^{1-\sigma_m^{-1}} \right)^{\frac{1}{1-\sigma_m^{-1}}}, \quad \text{where} \quad \sum_{i=1}^{N} \gamma_{ij}^m = 1.$$

Parameters γ_{ij}^m and σ_m are analogous to the parameters γ_{ij}^I and σ_I discussed for the investment bundle.

3.3 Market Clearing and the Planner's First Order Conditions

The market clearing conditions for each good is:

$$Q_{jt} = C_{jt} + \sum_{i=1}^{N} \left(M_{jit} + I_{jit} \right),$$

which implies that gross output equals final consumption, intermediate inputs, and investment goods.

In order to obtain the first-order conditions, we will use the fact that the model satisfies the first welfare theorem, so we can formulate the equilibrium allocations as the solution of a planning problem. The planner's Lagragian is given by:

$$\begin{aligned} \mathcal{L} = \mathbb{E}_0 \sum_{t=0}^{\infty} \beta^t \Bigg\{ & \frac{1}{1-\epsilon_c^{-1}} \left(C_t - \theta \frac{L_t^{1+\epsilon_l^{-1}}}{1+\epsilon_l^{-1}} \right)^{1-\epsilon_c^{-1}} \\ & + \sum_{j=1}^{N} P_{jt}^{\mathrm{k}} \left[I_{jt} + (1-\delta_j) K_{jt} - \Phi_{jt} - K_{jt+1} \right] \\ & + \sum_{j=1}^{N} P_{jt} \left[Q_{jt} - C_{jt} - \sum_{i=1}^{N} \left[M_{jit} + I_{jit} \right] \right] \Bigg\} \end{aligned}$$

where P_{jt}^k is the Lagrange multiplier associated to the capital accumulation constraint, P_{jt} is the Lagrange multiplier associated to the market clearing condition.

In Appendix B, we provide a detailed derivation of all first-order conditions and the resulting system of equations. We also calculate welfare, the deterministic steady state, and the closed form solution for the expenditure shares, to be used for the calibration.

4 Calibration and solution method

We calibrate the model in two steps: first, by directly setting parameters from data or existing literature, and second, by internally calibrating remaining parameters to match key empirical moments. Table 1 summarizes all parameter values and their sources.

For our dataset, we rely heavily on the empirical work of Vom Lehn and Winberry (2022).[8]. The dataset spans 1948-2018 and draws primarily from BEA Tables. The BEA Fixed Assets data is used to construct the investment network and depreciation parameters; Input-Output data provides the intermediates network parameters; and GDP-by-Industry data yields value added and employment observations. The aggregation level is $N = 37$ private non-farm sectors, with non-manufacturing sectors at the 2-digit NAICS level and manufacturing sectors at the 3-digit level.

4.1 Externally-calibrated parameters

Household preferences. At annual frequency, we set the discount factor (β) to 0.96, implying a 4% real interest rate in the deterministic steady state. The intertemporal elasticity of substitution (ϵ_c) is 0.5, corresponding to a risk aversion of 2. The Frisch Elasticity of Labor Supply (ϵ_l) is 0.5.

Elasticities of substitution. Following Atalay (2017) and Vom Lehn and Winberry (2022), we set the elasticity of substitution between intermediate goods (σ_m) to 0.1. Based on Oberfield and Raval (2021), the elasticity between capital and labor (σ_y) is 0.8. We set the elasticities between value-added and intermediates (σ_q), between investment goods (σ_I), and between consumption goods (σ_c) to 0.5.[9]

Depreciation. Capital depreciation rates (δ_j) reflect each sector's implied depreciation

[8]Data can be downloaded https://sites.google.com/site/cvomlehn/research?authuser=0 Our model generalizes some assumptions and functional forms used by Vom Lehn and Winberry (2022), so our calibration strategy differs. In particular, we have imperfect labor reallocation, and general CES for all aggregators. This mostly modify how to calibrate TFP shocks, and we need to add additional empirical targets, as explained below.

[9]Limited empirical evidence exists for these elasticities as most studies assume Cobb-Douglas. Our robustness analyses confirm that results remain qualitatively unchanged with this parameterization.

Table 1: Model Calibration

Parameter	Symbol	Value	Source
Panel A: External Parameters			
Discount factor	β	0.96	Standard
IES	ϵ_c	0.5	Standard
Frisch elasticity	ϵ_l	0.5	Standard
Intermediate elasticity	σ_m	0.1	Atalay (2017)
K-L elasticity	σ_y	0.8	Oberfield and Raval (2021)
VA-Int. elasticity	σ_q	0.5	Intermediate Value
Investment elasticity	σ_I	0.5	Intermediate Value
Consumption elasticity	σ_c	0.5	Intermediate Value
Depreciation	δ_j	By sector	BEA (1947-2018)
TFP persistence	ρ_j	By sector	Solow residuals
TFP covariance	Σ_A	By sector	Solow residuals
Panel B: Internal Parameters			
HH preferences	ξ_j	By sector	Exp. shares
VA intensity	μ_j	By sector	Exp. shares
Capital intensity	α_j	By sector	Exp. shares
Investment network	γ^I_{ij}	By sector-pair	Exp. shares
I-O network	γ^M_{ij}	By sector-pair	Exp. shares
Capital adj. cost	ϕ	Calibrated	Inv. volatility
Labor realloc.	σ_l	Calibrated	Labor volatility

Notes: Panel A shows parameters from data or literature. Panel B shows parameters matched to empirical moments. Model calibrated annually with $N = 37$ sectors (BEA 1948-2018). TFP processes detrended using fourth-order log-polynomial.

rates derived from BEA Fixed Assets data (1947-2018). Each δ_j is calculated by averaging the annual depreciation rates, weighting by the quantity of each capital good type used in sector j.

TFP. Parameters governing the TFP process (ρ_j, Σ_A) are calibrated using sector-level Solow residuals. Given our CES specification for value added, TFP variation is computed as:

$$\Delta \log A_{jt} = \log\left(\frac{Y_{jt}}{Y_{j,t-1}}\right) - \left(\frac{1}{1-\sigma_y^{-1}}\right) \log\left[\frac{\alpha_{jt}^{\sigma_y^{-1}} K_{jt}^{1-\sigma_y^{-1}} + (1-\alpha_{jt})^{\sigma_y^{-1}} L_{jt}^{1-\sigma_y^{-1}}}{\alpha_{jt}^{\sigma_y^{-1}} K_{j,t-1}^{1-\sigma_y^{-1}} + (1-\alpha_{jt})^{\sigma_y^{-1}} L_{j,t-1}^{1-\sigma_y^{-1}}}\right],$$

where α_{jt} denotes the capital share of sector j at time t. We allow factor shares to vary over time to account for technological changes, though results remain robust with constant shares. Capital input (K_{jt}) is constructed using the perpetual inventory method, with initial values from BEA nominal year-end capital stock data for 1948. We detrend sector-level TFP using a fourth-order log-polynomial, balancing nonlinearity capture against overfitting.[10]

4.2 Internally-calibrated parameters

We move now to the internally-calibrated parameters.

Expenditure shares, IO network and investment networks. Given that we have general CES aggregators at all levels, expenditure shares do not match exactly intensity shares of the corresponding CES aggregator. For example, $1 - \alpha$ is not exactly the labor share, thought it is proportional to it. This also applies to the input-output network and the investment network, which also use CES aggregators. In Appendix B.10, we describe how we can obtain an analytic expression for expenditure shares for all aggregators in the model. Using this expression, we iterate on the intensity shares of the model until the expenditure shares in the deterministic steady state matches the data. Specifically, this procedure is used to calculate the intensity parameters associated with household preferences over goods (ξ_j), value-added intensity share (μ_j), capital share(α_j), the investment network (γ^I_{ij}), and the input-output network (γ^M_{ij}).

Parameters set to match volatilities. The capital adjustment cost parameter (ϕ) matches the weighted average volatility of sectoral investment, while the labor reallocation parameter (σ_l) matches the weighted average volatility of sectoral labor.

4.3 Solution method

Our analysis of preallocation and nonlinear shock propagation requires a global solution method. With this solution in hand, we can simulate the economy to compute the ergodic distribution of sectoral and aggregate variables, capturing both nonlinear shock propagation and the anticipation effects of risk on agents' behavior. This ergodic distribution centers around the stochastic steady state (SSS)—defined as the equilibrium state where agents fully internalize the impact of future shocks on equilibrium outcomes, but current shock realizations are zero. This approach differs fundamentally from standard first-

[10] Results remain stable with lower-order polynomial detrending.

or second-order perturbation methods, which approximate the solution locally around the deterministic steady state (DSS)—a steady state where shocks are not just zero but impossible, precluding any preallocation behavior.

The global solution of our model presents a significant computational challenge. With 37 sectors and two state variables per sector (capital and TFP), we must solve a stochastic dynamic programming problem with 74 state variables —pushing the boundaries of current computational capabilities. We overcome this challenge by extending the 'deep equilibrium nets' method developed by Azinovic et al. (2022) to allow for high dimensional shocks, through the use Monte Carlo simulation to build the expectation terms that appear in theEulerr equations.

While we provide detailed technical documentation in Appendix C, the core approach can be summarized as follows: We approximate all equilibrium objects (policies and prices) as functions of the state variables using deep neural networks. The solution process then reduces to training these networks by minimizing violations of the equilibrium conditions, which consists of Euler equations and technological constraints. This is accomplished through an iterative procedure that alternates between simulation and optimization steps. In each iteration, we first simulate the economy using current network parameters, then use the simulated data to update these parameters, minimizing equilibrium condition errors. This process continues until we achieve the desired numerical precision.

5 Quantitative results

5.1 Ergodic distribution

We start by analyzing how risk can lead to preallocation in the full model. Armed with our new solution method, we consider three scenarios differing on the shock volatility. First, the baseline scenario, discussed in Section 4. Second, a *low volatility* scenario, in which the volatility of all sectoral TFP shocks is divided by two. This scenario gets us closer to the (log-)linear model.[11] Finally, a *high-volatility* scenario in which shocks are 1.5 times as volatile as in the baseline.

We solve the model nonlinearly for each of these scenarios. Then we compute the ergodic distribution by simulating 500,000 periods using in the three cases the volatility

[11]The log-linear model is computed by solving the model using a first-order perturbation method.

of the baseline scenario. That implies that the allocations in the high- and low-volatility scenarios are suboptimal, as the planner forecasts volatilities that do not materialize in the simulation. Results are displayed in Figure 6. Each panel displays the ergodic distribution of some aggregate variable, with a dashed vertical line marking the position of the DSS. Table 2 summarizes this information.

Figure 6: Ergodic distribution of key aggregate variables

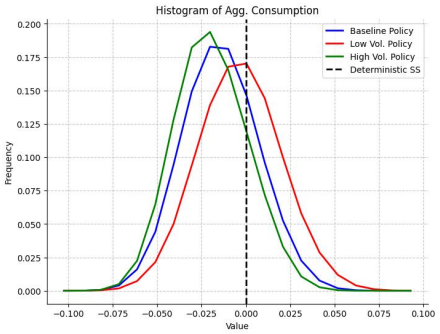

(a) Consumption

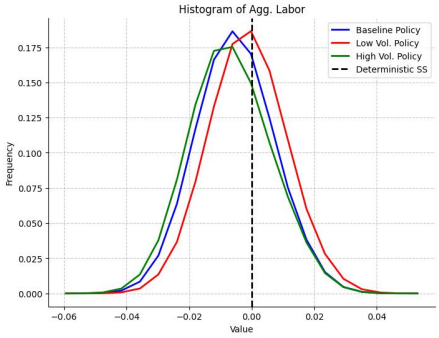

(b) Labor

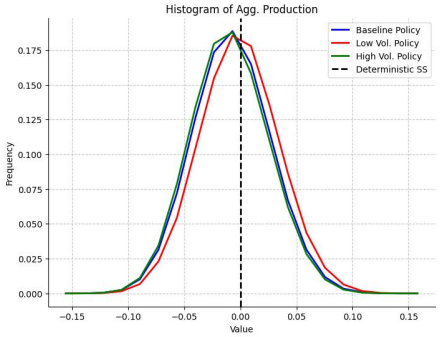

(c) GDP

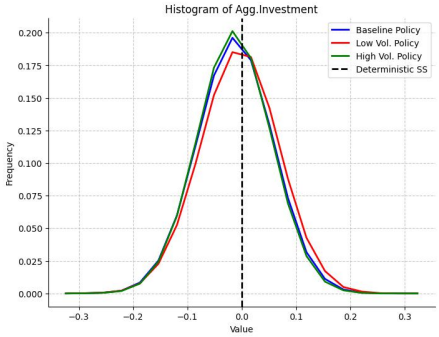

(d) Investment

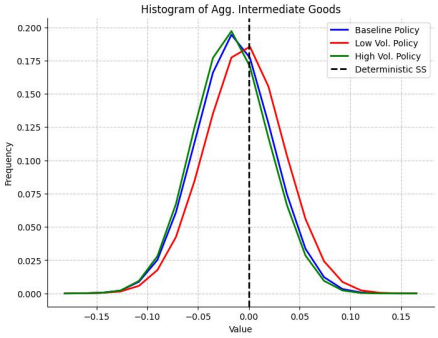

(e) Intermediates

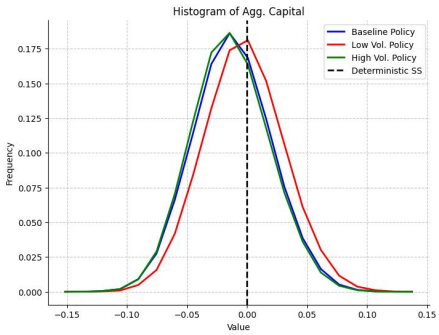

(f) Capital

Note: The figure shows the ergodic distribution of specific aggregate variables, using the 500,000 periods simulation of the global solution. For each variable, we show the case for three policy functions: baseline policy, the policy trained under low volatility (shocks scaled by 0.5), and the policy trained under high volatility (shocks scaled by 1.5). The figures are calculated using the same shocks for the four policies, that is, the only thing that varies is the policy function. The baseline volatility was used to simulate the shocks.

Variable	Policy	Mean (%)	Sd (%)	Skewness	Kurtosis
Consumption	Benchmark	-1.4	2.1	0.089	-0.102
	High volatility	-2.0	2.0	0.145	-0.193
	Low volatility	-0.3	2.3	0.067	-0.059
	Log-linear	0.0	3.1	-0.001	-0.028
Labor	Benchmark	-0.5	1.2	0.076	-0.076
	High volatility	-0.7	1.3	0.131	-0.138
	Low volatility	-0.1	1.2	0.059	-0.047
	Log-linear	0.0	1.3	-0.002	-0.019
GDP	Benchmark	-0.8	3.4	0.073	-0.062
	High volatility	-1.0	3.4	0.086	-0.102
	Low volatility	-0.1	3.5	0.064	-0.038
	Log-linear	0.0	3.8	0.000	-0.016
Investment	Benchmark	-1.3	6.9	-0.020	-0.001
	High volatility	-1.4	6.7	-0.019	-0.014
	Low volatility	-0.5	7.1	-0.035	0.001
	Log-linear	0.0	7.9	0.001	0.012
Intermediates	Benchmark	-1.5	3.7	-0.002	-0.025
	High volatility	-1.8	3.7	0.019	-0.067
	Low volatility	-0.5	3.9	-0.024	-0.005
	Log-linear	0.0	4.2	-0.002	-0.009
Capital	Benchmark	-1.2	3.3	0.056	-0.027
	High volatility	-1.4	3.2	0.083	-0.064
	Low volatility	-0.3	3.3	0.045	-0.016
	Log-linear	0.0	3.7	0.011	-0.016

Table 2: Descriptive statistics of key aggregate variables

Note: This table shows descriptive statistics of aggregate variables, using the 500,000 periods simulation of the global solution. For each variable, we show the case for the four policy functions: baseline policy, the policy trained under low volatility (shocks scaled by 0.5), the policy trained under high volatility (shocks scaled by 1.5), and the policy trained under log-linear approximation (no expected shock as it is a perturbation around the DSS). The statistics are calculated using the same shocks for the four policies, that is, the only thing that varies is the policy function. The benchmark volatility, calculated from data, was used to simulate the shocks. Mean and standard deviation are expressed in percentage deviations from the DSS for easier interpretation (for example, -1.4% means the variable is on average 1.4% below its DSS value). Skewness and kurtosis are calculated over variables expressed in log deviations from the DSS.

Several important results emerge. First, all aggregate variables display a mean below the DSS. That implies that once aggregate risk is factored in, agents find it optimal to reduce their investment and labor supply in a more volatile environment. This translates into lower capital and labor, and hence lower consumption and output. This mechanism is amplified as shock volatility increases. That showcases how the model nonlinearity becomes more prevalent as shocks are more volatile. Notice how the impact is heterogeneous across variables. While a threefold increase in volatility between the low- and high-volatility scenarios implies a sevenfold decrease in consumption, from -0.3 percent

to -2.0 percent, it is only threefold in the case of investment, from -0.5 percent to -1.3 percent.

Second, the standard deviation of all aggregate variables decreases with expected shock volatility. In other words, in counterfactual economies with higher sectoral TFP volatility, the standard deviation of key macro variables increases less than one-to-one The planner is thus trading a lower mean by a reduction in standard deviation as shock variance increases. This is in line with the theoretical results presented in Section 2. Furthermore, the implied aggregate volatility is substantial – e.g. the standard deviation of annual GDP is 3.4%.

Third, the economy displays negative excess kurtosis and a negligible degree of skewness. The negative kurtosis reflects the fact that the economy reduces large excursions from the mean, that is, the economy displays 'thinner tails' than the (log-)normal. This reflects the fact that policy functions bend for large shock values in the global solution, whereas they are (log-)linear in the linear solution (we will return to this point in subsection 5.3).

5.2 Stochastic steady state

We next analyze the SSS. A comparison between Table 2 and 3 clearly shows how the SSS is very close to the mean of the ergodic distribution. The advantage of the SSS is that it allows us to analyze in detail the sectoral characteristics of the equilibrium under the global solution.

Policy	Consumption (%)	Labor (%)	GDP (%)	Investment (%)	Intermediates (%)	Capital (%)
Low Volatility	-0.43	-0.16	-0.28	-0.37	-0.43	-0.45
Baseline	-1.56	-0.58	-1.02	-1.32	-1.50	-1.48
High Volatility	-1.89	-0.62	-1.07	-1.14	-1.47	-1.21

Table 3: Aggregate Variables in Stochastic Steady State

Note: This table shows aggregate variables in the SSS. We show the case for the baseline model, the model with low volatility (shocks scaled by 0.5), and the model with high volatility (shocks scaled by 1.5). Values are expressed as percentage deviations from the DSS (for example, -1.56% means consumption is 1.56% below its DSS value). The SSS is calculated by sampling 1,000 points from the full simulation, and simulating forward but setting shocks to zero. Then, we take the resulting 1,000 ending points, verify they are the same within 0.01% tolerance, and average them.

Figure 7 displays the capital allocation across sectors as a difference with respect to the DSS. This reflects how the anticipation of aggregate risk affects agents' decisions regarding investment.

From the aggregate results above, we know that aggregate capital is lower in the SSS than in the DSS. This result, however, masks a considerable degree of sectoral heterogeneity. In the baseline scenario, aggregate capital is 1.5 percent lower in the SSS than in the DSS. This translates into a decline in capital across most sectors of a magnitude between roughly 1-2 percent (blue). Capital is particularly penalized in Printing and Food Services. There is, however, an increase in the stock of capital in one upstream sector: Mining, Oil, and Gas.

This heterogeneous capital allocation gets much amplified in the high-volatility scenario. While most sectors experience a decline of a similar magnitude as in the baseline, the striking exceptions are Petroleum and Mining, Oil, and Gas, which get an increase larger than 2 percent compared to the DSS. The SSS does exhibit preallocation towards upstream sectors, in line with the theoretical prescriptions of Section 2.

Figure 7: Distribution of Capital in the Stochastic Steady State

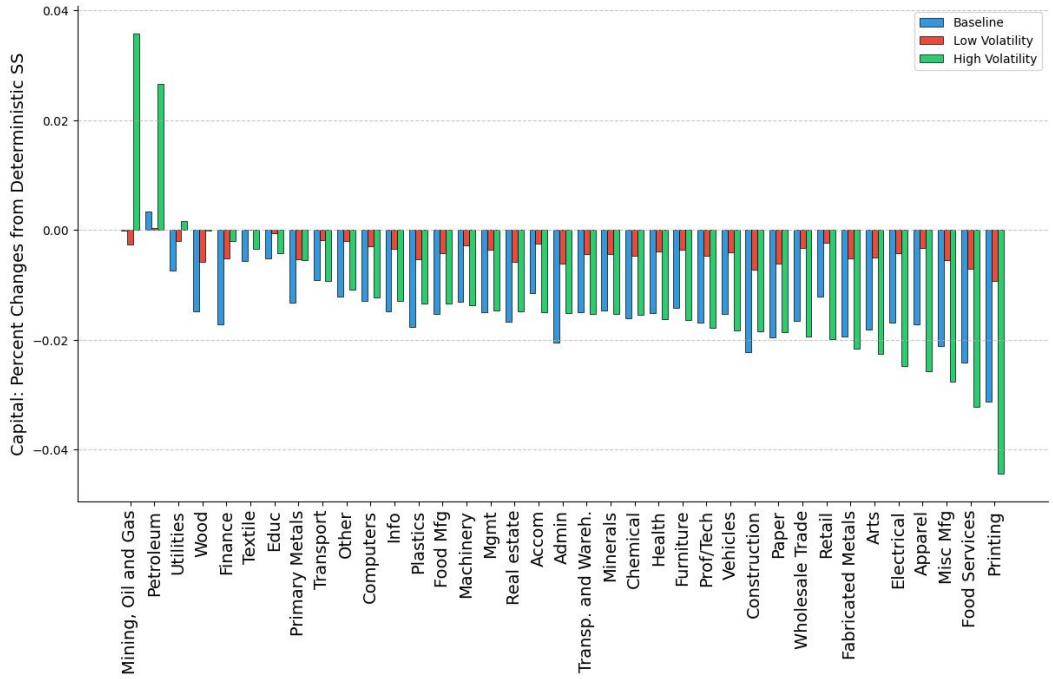

Note: This figure shows the capital of each sector in the stochastic steady state. We show the case for the baseline model, the model with low volatility (shocks scaled by 0,5), and the model with high volatility (shocks scaled by 1.5). Sectors are ordered using the value for the high volatility policy. Variables are in log deviations from the deterministic steady state, so 0.05 can be interpreted as 5% above the deterministic steady state. The stochastic steady state is calculated by sampling 1000 points from the full simulation and simulating forward trajectories with the shocks set to zero. Then, we take the resulting 1000 ending points, verify they are the same within 0.01% tolerance, and average them.

Figure 8 shows the distribution of labor in the stochastic SSS, compared to the DSS. We observe the opposite pattern compared to the distribution of capital. In the high volatility case, labor is lower in Petroleum and Mining, Oil and Gas. Notice, however, how SSS of labor is not exactly the specular image of that of capital, as Machinery and Electrical are the two sectors less penalized in terms of labor whereas Food Services are Printing were the two sectors more penalized of capital..

Figure 8: Distribution of Labor in the Stochastic Steady State

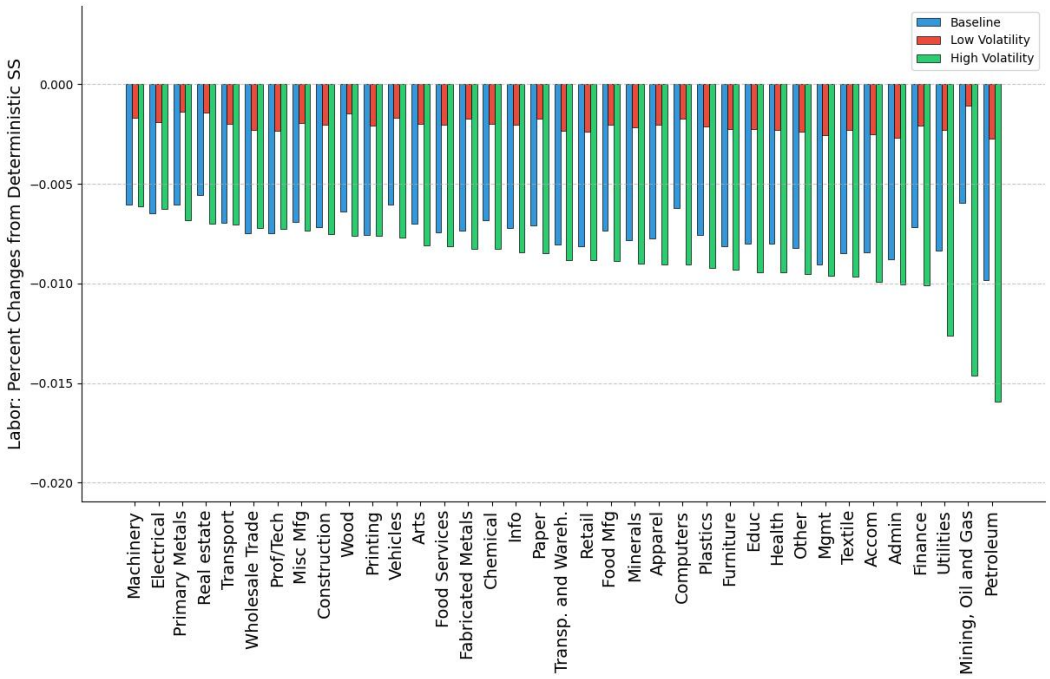

Note: This figure shows labor of each sector in the stochastic steady state. We show the case for the baseline model, the model with low volatility (shocks scaled by 0,5), and the model with high volatility (shocks scaled by 1.5). Sectors are ordered using the value for the high volatility policy. Variables are in log deviations from the deterministic steady state, so 0.05 can be interpreted as 5% above the deterministic steady state. The stochastic steady state is calculated by sampling 1000 points from the full simulation and simulating forward trajectories with the shocks set to zero. Then, we take the resulting 1000 ending points, verify they are the same within 0.01% tolerance, and average them.

Still, as we can see in Figure 9, value-added production is higher in those upstream sectors such as Mining, Oil and Gas, and Petroleum, so the higher level of capital dominates the lower level of labor.

As we discuss in Section 5.3 next, this distributional pattern in the SSS increases resilience to negative shocks, since capital takes time to accumulate and cannot be readily adjusted as a response to a negative shock, while labor can be more easily reallocated.

Figure 9: Distribution of Value Added in the Stochastic Steady State

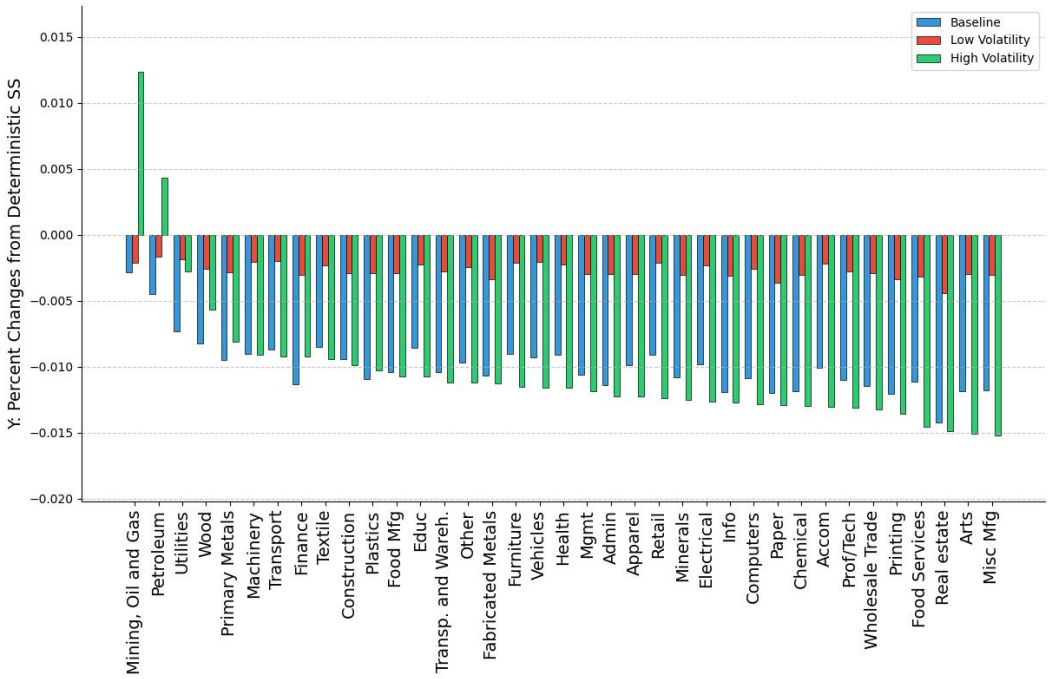

Note: This figure shows value added production of each sector in the stochastic steady state. We show the case for the baseline model, the model with low volatility (shocks scaled by 0,5), and the model with high volatility (shocks scaled by 1.5). Sectors are ordered using the value for the high volatility policy. Variables are in log deviations from the deterministic steady state, so 0.05 can be interpreted as 5% above the deterministic steady state. The stochastic steady state is calculated by sampling 1000 points from the full simulation and simulating forward trajectories with the shocks set to zero. Then, we take the resulting 1000 ending points, verify they are the same within 0.01% tolerance, and average them.

5.3 Impulse Responses

To examine the dynamic properties of the global solution, we analyze impulse response functions following a large sectoral productivity shock. Figure 10 shows how aggregate consumption responds to a negative 20% shock to the TFP of Mining, Oil, and Gas, which is a key upstream sector characterized by substantial capital preallocation, as previously discussed. The figure compares three solution methods: our global solution (black lines), a log-linear approximation (red line), and a perfect foresight solution (blue line).[12] The global solution results include the baseline (solid line), as well as the low- (dashed) and

[12]Given the nonlinearity of the model, these are *generalized* impulse responses.

high- (dotted-dashed) volatility scenarios.

Figure 10: Impulse Response of Aggregate Consumption to a Mining, Oil, and Gas Shock

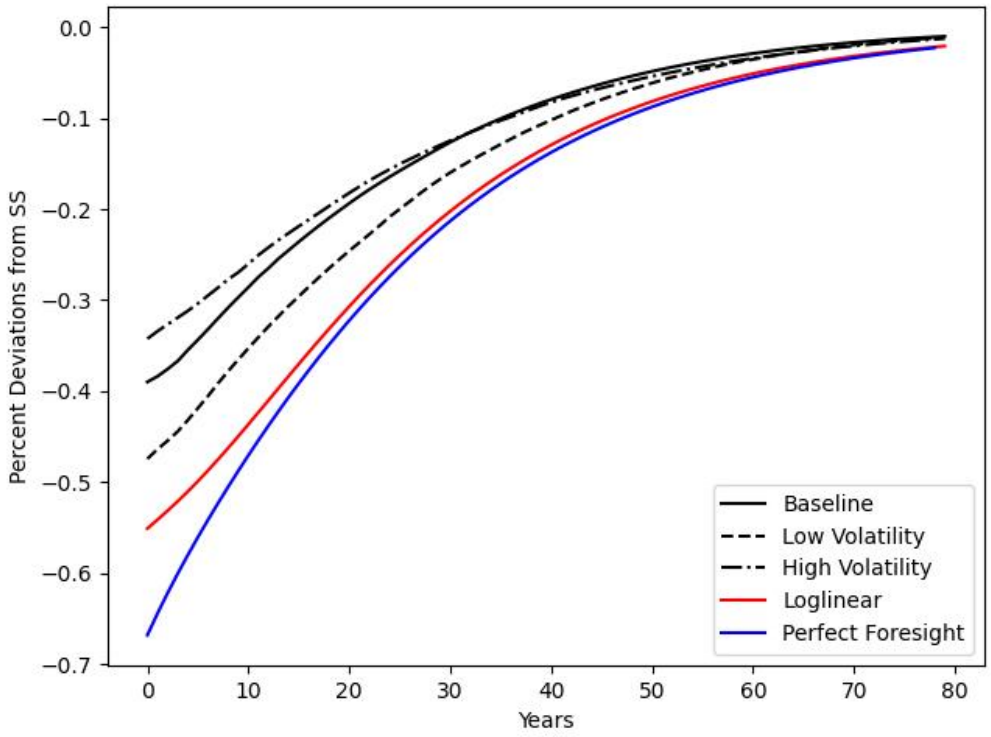

Note: This figure shows the impulse response of aggregate consumption to a 20% negative TFP shock in Mining, Oil, and Gas (an upstream sector). The black line represents the response using the global solution method, the red line shows the response using a log-linear approximation, and the blue line shows the perfect foresight solution. For the global solutions, the vertical axis shows log deviations relative to the stochastic steady state, while for the log-linear and perfect foresight solutions we show percentage deviations from the deterministic steady state.

The perfect-foresight solution evaluates transitional dynamics after an unexpected one-off 'MIT shock' when the economy starts at the DSS. It coincides with the log-linear approximation for small shocks (Boppart et al., 2018). In the case of a large shock, such as the one considered here, the two responses diverge as the perfect-foresight solution captures the nonlinear elements of the response. We see that nonlinearities amplify the impact on aggregate consumption by a 15%. This nonlinear amplification of unanticipated upstream shocks isin line with the results by Baqaee and Farhi (2019).

We also compare the perfect foresight response with that under the baseline global solution. This comparison captures the effect of input preallocation, since the baseline solution deviates from the SSS due to ex-ante uncertainty, while the perfect-foresight solution deviates from the DSS. Figure 10 shows that the baseline policy is attenuated by

50% compared to the perfect foresight solution.

The fact that the baseline model with preallocation dampens the response to sectoral shocks compared to both the linear and perfect foresight cases is similar for shocks in other sectors, both upstream and downstream, as displayed in Appendix D.[13]. The fact that the planner dampens the consumption response through capital preallocation explains why consumption volatility is lower under the global solution, as shown in Table 2 above.

5.4 Welfare Cost of Business Cycles

Finally, we conclude this section by looking at the welfare implications of business cycles under the light of our model. Table 4 reports different measures of welfare costs, always defined in consumption-equivalent terms.[14]

Policy	Full Nonlinear (%)	Loglinear (%)	C fixed at DSS (%)	L fixed at DSS (%)	Mean at DSS (%)
Low Volatility	-0.46	-0.05	0.16	-0.63	-0.03
Baseline	-1.05	-0.11	0.41	-1.51	-0.06
High Volatility	-1.50	-0.19	0.57	-2.18	-0.10

Table 4: Welfare Cost of Business Cycle

Note: This table shows the welfare cost of business cycles under different scenarios. All values are expressed as percentage changes in consumption equivalent terms (for example, -1.05% means households would need to decrease their consumption by 1.05% in the deterministic steady state to be indifferent between that and living in the stochastic economy). We show results for three cases: baseline model, model with low volatility (shocks scaled by 0.5), and model with high volatility (shocks scaled by 1.5). The welfare cost is calculated as described in subsection B.7, using 1,000 different trajectories from the full simulation, each of length 2,000 periods. We then calculate the mean welfare at the first period of each slice. The "Full Nonlinear" and "Loglinear" columns show the welfare cost using the global solution and loglinear approximation respectively. "C fixed at SS" shows the cost when labor follows the observed paths but consumption is fixed at the deterministic steady state. "L fixed at SS" fixes labor at the deterministic steady state. "Mean at SS" shows the pure effect of volatility by renormalizing the observed trajectories so their mean matches the deterministic steady state.

First, we display the losses in the global solution under the baseline calibration (1.05 percent), which are one order of magnitude larger than if the model is solved using loglinear methods (0.11 percent). This result makes evident how linear approximations may be greatly downplaying the true costs of aggregate fluctuations. This result is a direct

[13]There we show impulse responses for shocks to construction, machinery, petroleum, retail, and real estate.

[14]They are defined as the consumption amount that the representative household would be willing to pay in order to live in a counterfactual economy without shocks.

consequence of the fact that mean consumption is lower in the SSS than in the DSS, and thus the mean consumption along the business cycle falls in the global solution.

Naturally, there are two opposing effects. The SSS displays lower consumption, and lower labor supply, where the latter is welfare-improving. To capture exclusively the impact of consumption on welfare, in the second column we recompute welfare in the global solution keeping labor constant at its DSS value. Welfare now increases, reflecting the lower labor in the SSS. Conversely, if we keep labor fixed at its DSS value in the third column, welfare losses are amplified as the only effect is the fall in consumption.

The last column captures exclusively the impact of volatility on the nonlinear model, abstracting from the difference in means. It shows how welfare losses are higher under the loglinear solution, reflecting the higher volatility in that case.

Finally, we compare the low- and high- volatility scenarios. The welfare loss in the high-volatility scenario is 1.5%. This reflects both the lower mean in this case and the higher volatility.

Our results invite us to revisit the traditional view of low welfare costs of business cycles once we abandon the unrealistic assumptions of one single sector and local dynamcis around the DSS.

6 Conclusion

This paper demonstrates that, in dynamic multisector economies, optimal capital allocation by a social planner involves deliberately over-investing in upstream sectors to insure against the risk of severe economic downturns caused by sectoral shocks cascading through the network. While this strategy effectively mitigates the likelihood of catastrophic aggregate disruptions, it comes at the cost of lower average consumption, resulting in a much higher welfare cost of business cycles than predicted by standard linear models.

Using deep learning techniques to solve a high-dimensional, US-calibrated model, we show that the ergodic distribution of the economy features higher capital in key upstream sectors, realistic aggregate volatility, and a substantial welfare loss. This highlights a fundamental trade-off between resilience to rare disasters and average economic performance. Our work underscores the importance of accounting for nonlinearities and network structure in macroeconomic policy design.

References

Acemoglu, Daron, Vasco M. Carvalho, Asuman Ozdaglar, and Alireza Tahbaz-Salehi, "The Network Origins of Aggregate Fluctuations," *Econometrica*, 2012, *80* (5), 1977–2016.

Atalay, Enghin, "How important are sectoral shocks?," *American Economic Journal: Macroeconomics*, 2017, *9* (4), 254–80.

Azinovic, Marlon, Luca Gaegauf, and Simon Scheidegger, "Deep equilibrium nets," *International Economic Review*, 2022.

Baqaee, David and Elisa Rubbo, "Micro Propagation and Macro Aggregation," *Annual Review of Economics*, 2023, *15* (Volume 15, 2023), 91–123.

Baqaee, David Rezza and Emmanuel Farhi, "The macroeconomic impact of microeconomic shocks: Beyond Hulten's theorem," *Econometrica*, 2019, *87* (4), 1155–1203.

Barro, Robert J., "Rare Disasters, Asset Prices, and Welfare Costs," *American Economic Review*, March 2009, *99* (1), 243–64.

Boppart, Timo, Per Krusell, and Kurt Mitman, "Exploiting MIT shocks in heterogeneous-agent economies: the impulse response as a numerical derivative," *Journal of Economic Dynamics and Control*, 2018, *89* (C), 68–92.

Carvalho, Vasco, "Aggregate fluctuations and the network structure of intersectoral trade," Economics Working Papers 1206, Department of Economics and Business, Universitat Pompeu Fabra November 2007.

Carvalho, Vasco M. and Alireza Tahbaz-Salehi, "Production Networks: A Primer," *Annual Review of Economics*, 2019, *11* (Volume 11, 2019), 635–663.

Fernandez-Villaverde, Jesus, Galo Nuno, and Jesse Perla, "Taming the Curse of Dimensionality: Quantitative Economics with Machine Learning," Papers October 2024.

Foerster, Andrew T, Pierre-Daniel G Sarte, and Mark W Watson, "Sectoral versus aggregate shocks: A structural factor analysis of industrial production," *Journal of Political Economy*, 2011, *119* (1), 1–38.

Gu, Zhouzhou, Mathieu Lauri'ere, Sebastian Merkel, and Jonathan Payne, "Global Solutions to Master Equations for Continuous Time Heterogeneous Agent Macroeconomic Models," Papers 2406.13726, arXiv.org June 2024.

Han, Jiequn, Yucheng Yang, and Weinan E, "DeepHAM: A global solution method for heterogeneous agent models with aggregate shocks," *arXiv preprint arXiv:2112.14377*, 2021.

Horvath, Michael, "Sectoral shocks and aggregate fluctuations," *Journal of Monetary Economics*, 2000, *45* (1), 69–106.

Jorda, Oscar, Moritz Schularick, and Alan M. Taylor, "Disasters Everywhere: The Costs of Business Cycles Reconsidered," *IMF Economic Review*, March 2024, *72* (1), 116–151.

Kopytov, Alexandr, Bineet Mishra, Kristoffer Nimark, and Mathieu Taschereau-Dumouchel, "Endogenous Production Networks Under Supply Chain Uncertainty," *Econometrica*, 2024, *92* (5), 1621–1659.

Lehn, Christian Vom and Thomas Winberry, "The investment network, sectoral comovement, and the changing US business cycle," *The Quarterly Journal of Economics*, 2022, *137* (1), 387–433.

Liu, Ernest and Aleh Tsyvinski, "A Dynamic Model of Input–Output Networks," *The Review of Economic Studies*, 2024, *91* (6), 3608–3644.

Lucas, Robert E., *Models of Business Cycles*, Basil Blackwell, 1987.

Maliar, Lilia, Serguei Maliar, and Pablo Winant, "Deep learning for solving dynamic economic models.," *Journal of Monetary Economics*, 2021, *122*, 76–101.

Martin, Ian W. R., "Disasters and the Welfare Cost of Uncertainty," *American Economic Review*, May 2008, *98* (2), 74–78.

Oberfield, Ezra and Devesh Raval, "Micro data and macro technology," *Econometrica*, 2021, *89* (2), 703–732.

Pellet, Thomas and Alireza Tahbaz-Salehi, "Rigid production networks," *Journal of Monetary Economics*, 2023, *137*, 86–102.

Rotemberg, Julio J and Michael Woodford, "Dynamic general equilibrium models with imperfectly competitive product markets," 1993.

A Two sector model appendix

A.1 Setting

The full description of the model is presented in Section 2. Here we briefly summarize the key equations needed for the proofs.

This vertical network economy consists of two sectors. Sector 1 ("upstream") produces the intermediate good by using capital. In contrast, sector 2 ("downstream") produces the final good using both capital and the intermediate good. Both sectors are subject to gross-output (i.e., Hicks-neutral) productivity shocks. The planner is endowed with one unit of capital K which must be allocated between the two sectors K_1 and K_2. A key feature of the problem is that the capital allocation decision must be made before the realization of the total factor productivity shock, so we have an allocation decision under uncertainty. Once the shock is realized, no further decisions are required, as the quantities of goods produced and consumed are fully determined by the preallocated capital. Let Q_i, K_i represents gross-output and capital in sector $i = \{1, 2\}$, and C represents consumption of the final good. The problem is defined by the following equations:

$$K_1 + K_2 = 1, \quad Q_1 = A_1 K_1, \quad Q_2 = A_2 \left((1 - \gamma_q) (Q_1)^{\frac{\sigma_q - 1}{\sigma_q}} + \gamma_q (K_2)^{\frac{\sigma_q - 1}{\sigma_q}} \right)^{\frac{\sigma_q}{\sigma_q - 1}}, \quad C = Q_2$$

where A_1 and A_2 are independent random productivity for sectors 1 and 2 respectively. Both random variables take either a low value $A_L = \bar{A} - \Delta_A$ or a high value $A_H = \bar{A} + \Delta_A$. For shock A_1, the probability of low state is p_1, while for shock A_2, the probability of the low state is p_2. Unless stated otherwise, we assume that $p_1 = p_2 = 1/2$ in the proofs below. σ_q is the elasticity of substitution in production between the two goods. The planner maximizes:

$$\mathbb{E}[U(C)] = \mathbb{E}\left[\frac{C^{1 - \epsilon_c^{-1}}}{1 - \epsilon_c^{-1}} \right]$$

where ϵ_c is the intertemporal elasticity of substitution (so ϵ_c^{-1} is risk aversion).

A.2 First-order Conditions and Steady-state Solution

If we replace $K_2 = 1 - K_1$, we have an unconstrained problem with one control variable, K_1. Following our definition of normalized aggregate consumption $\tilde{C} = C/A_2$, normalized consumption in each scenario can be written as

$$\tilde{C}_S = \left((1-\gamma_q) \left(A_s K_1\right)^{\frac{\sigma_q - 1}{\sigma_q}} + \gamma_q \left(1 - K_1\right)^{\frac{\sigma_q - 1}{\sigma_q}} \right)^{\frac{\sigma_q}{\sigma_q - 1}}, \quad S \in \{L, H\}$$

Now we can write the expected utility in terms of per-unit-of-efficiency consumption $\tilde{C}_{S_1}$:

$$\begin{aligned}
\mathbb{E}[U(C)] &= \mathbb{E}\left[\frac{C^{1-\epsilon_c^{-1}}}{1-\epsilon_c^{-1}}\right] \\
&= \mathbb{E}\left[p_1 A_2^{1-\epsilon_c^{-1}} \frac{\tilde{C}_L^{1-\epsilon_c^{-1}}}{1-\epsilon_c^{-1}} + (1-p_1) A_2^{1-\epsilon_c^{-1}} \frac{\tilde{C}_H^{1-\epsilon_c^{-1}}}{1-\epsilon_c^{-1}}\right] \\
&= \left[p_1 p_2 A_{2,L}^{1-\epsilon_c^{-1}} \frac{\tilde{C}_L^{1-\epsilon_c^{-1}}}{1-\epsilon_c^{-1}} + p_1(1-p_2) A_{2,H}^{1-\epsilon_c^{-1}} \frac{\tilde{C}_L^{1-\epsilon_c^{-1}}}{1-\epsilon_c^{-1}}\right. \\
&\quad \left. + (1-p_1) p_2 A_{2,L}^{1-\epsilon_c^{-1}} \frac{\tilde{C}_H^{1-\epsilon_c^{-1}}}{1-\epsilon_c^{-1}} + (1-p_1)(1-p_2) A_{2,H}^{1-\epsilon_c^{-1}} \frac{\tilde{C}_H^{1-\epsilon_c^{-1}}}{1-\epsilon_c^{-1}}\right] \\
&= \left(p_2 A_{2,L}^{1-\epsilon_c^{-1}} + (1-p_2) A_{2,H}^{1-\epsilon_c^{-1}}\right) \frac{1}{1-\epsilon_c^{-1}} \left[\left(p_1 \tilde{C}_L^{1-\epsilon_c^{-1}} + (1-p_1) \tilde{C}_H^{1-\epsilon_c^{-1}}\right)\right].
\end{aligned}$$

Let Φ be the positive constant outside the brackets.[15] Since Φ is constant, we can simplify our analysis by defining a normalized utility function $\tilde{U}(\tilde{C}) = U(\tilde{C})/\Phi$. Maximizing $\mathbb{E}[U(C)]$ is equivalent to maximizing $\mathbb{E}[\tilde{U}(\tilde{C})]$.

Before we calculate the first order condition (F.O.C.), we will calculate the derivative of

[15] $\Phi = \left(p_2 A_{2,L}^{1-\epsilon_c^{-1}} + (1-p_2) A_{2,H}^{1-\epsilon_c^{-1}}\right) \frac{1}{1-\epsilon_c^{-1}}$

$\tilde{C}_S$ with respect to K_1:

$$\begin{aligned}
\frac{\partial \tilde{C}_S}{\partial K_1} &= \frac{\sigma_q}{\sigma_q - 1}\left((1-\gamma_q)\left(A_S K_1\right)^{\frac{\sigma_q-1}{\sigma_q}} + \gamma_q\left(1-K_1\right)^{\frac{\sigma_q-1}{\sigma_q}}\right)^{\frac{\sigma_q}{\sigma_q-1}-1} \\
&\quad \times \left(\frac{\sigma_q - 1}{\sigma_q}\right)\left((1-\gamma_q)\left(A_S K_1\right)^{\frac{-1}{\sigma_q}} A_S - \gamma_q\left(1-K_1\right)^{\frac{-1}{\sigma_q}}\right) \qquad , \quad S \in \{L, H\} \\
&= \tilde{C}_S^{\frac{1}{\sigma_q}}\left((1-\gamma_q)\left(A_S K_1\right)^{\frac{-1}{\sigma_q}} A_S - \gamma_q\left(1-K_1\right)^{\frac{-1}{\sigma_q}}\right) \qquad , \quad S \in \{L, H\} \\
&= \left((1-\gamma_q)\left(\frac{A_S K_1}{\tilde{C}_S}\right)^{\frac{-1}{\sigma_q}} A_S - \gamma_q\left(\frac{1-K_1}{\tilde{C}_S}\right)^{\frac{-1}{\sigma_q}}\right) \qquad , \quad S \in \{L, H\}
\end{aligned}$$

Then, the F.O.C. is:

$$\begin{aligned}
\frac{\partial \mathbb{E}[U(C)]}{\partial K_1} &= \left\{ p_1 \frac{1}{\tilde{C}_L^{\epsilon_c^{-1}}}\left((1-\gamma_q)\left(\frac{A_L K_1}{\tilde{C}_L}\right)^{\frac{-1}{\sigma_q}} A_L - \gamma_q\left(\frac{1-K_1}{\tilde{C}_L}\right)^{\frac{-1}{\sigma_q}}\right)\right. \\
&\quad \left. + (1-p_1)\frac{1}{\tilde{C}_H^{\epsilon_c^{-1}}}\left((1-\gamma_q)\left(\frac{A_H K_1}{\tilde{C}_H}\right)^{\frac{-1}{\sigma_q}} A_S - \gamma_q\left(\frac{1-K_1}{\tilde{C}_H}\right)^{\frac{-1}{\sigma_q}}\right)\right\} \times \mathbb{E}\{A_2^{1-\varepsilon_c^{-1}}\} \\
&= 0
\end{aligned}$$

We can then pin down steady-state solution.

$$\left((1-\gamma_q)\left(\frac{K_1}{\tilde{C}_S}\right)^{\frac{-1}{\sigma_q}} \bar{A}^{\frac{\sigma_q-1}{\sigma_q}} - \gamma_q\left(\frac{1-K_1}{\tilde{C}_S}\right)^{\frac{-1}{\sigma_q}}\right) = 0$$

or

$$
\begin{aligned}
(1-\gamma_q)\left(\frac{K_1^{determ}}{\tilde{C}_S}\right)^{\frac{-1}{\sigma_q}}\bar{A}^{\frac{\sigma_q-1}{\sigma_q}} &= \gamma_q\left(\frac{1-K_1^{determ}}{\tilde{C}_S}\right)^{\frac{-1}{\sigma_q}},\\
\left(\frac{K_1^{determ}}{1-K_1^{determ}}\right)^{\frac{-1}{\sigma_q}} &= \frac{\gamma_q}{1-\gamma_q}\bar{A}^{\frac{1-\sigma_q}{\sigma_q}},\\
\frac{K_1^{determ}}{1-K_1^{determ}} &= \left(\frac{1-\gamma_q}{\gamma_q}\right)^{\sigma_q}\bar{A}^{\sigma_q-1},\\
K_1^{determ} &= \left(\frac{1-\gamma_q}{\gamma_q}\right)^{\sigma_q}\bar{A}^{\sigma_q-1} - K_1^{determ}\left(\frac{1-\gamma_q}{\gamma_q}\right)^{\sigma_q}\bar{A}^{\sigma_q-1},\\
K_1^{determ} &= \frac{\left(\frac{1-\gamma_q}{\gamma_q}\right)^{\sigma_q}\bar{A}^{\sigma_q-1}}{\left(\frac{1-\gamma_q}{\gamma_q}\right)^{\sigma_q}\bar{A}^{\sigma_q-1}+1},\\
K_1^{determ} &= \frac{\left(1-\gamma_q\right)^{\sigma_q}\bar{A}^{\sigma_q-1}}{\gamma_q^{\sigma_q}\bar{A}^{\sigma_q-1}+\left(1-\gamma_q\right)^{\sigma_q}}.
\end{aligned}
$$

When we assume $\bar{A}=1$

$$
K_1^{determ} = \frac{\left(1-\gamma_q\right)^{\sigma_q}}{\gamma_q^{\sigma_q}+\left(1-\gamma_q\right)^{\sigma_q}}
$$

A.3 Proof for Lemma 1: Asymmetric Impacts of Negative and Positive Shocks

We firstly establish a baseline result that around the deterministic allocation of capital, negative upstream shocks have larger effects than positive ones, whereas downstream shocks exhibit symmetric effects.

Lemma. *For $\sigma_q < 1$, upstream shocks generate negatively skewed responses in consumption while downstream shocks generate symmetric impact:*

1. *Upstream shocks (negatively skewed):*

$$
IR^{-,upst}(K^{determ}) > IR^{+,upst}(K^{determ}) \implies Skew^{upst}(K^{determ}) < 0
$$

2. *Downstream shocks (symmetric):*

$$
IR^{-,downst}(K^{determ}) = IR^{+,downst}(K^{determ}) \implies Skew^{downst}(K^{determ}) = 0
$$

Proof. **Downstream Shock.** We start the proof by discussing the symmetric result for downstream shock.. The IRFs for negative downstream shock a.nd positive upstream shock are given by

$$\begin{aligned} IR^{-,\text{downst}}(K_1^{determ}) &\equiv \left| C_{\bar{A}L}(K_1^{determ}) - C_{\bar{A}\bar{A}}(K_1^{determ}) \right| = C_{\bar{A}\bar{A}}(K_1^{determ}) - C_{\bar{A}L}(K_1^{determ}) \\ &= \Delta_A \tilde{C}_{\bar{A}}(K_1^{determ}) \end{aligned}$$

$$\begin{aligned} IR^{+,\text{downst}}(K_1^{determ}) &\equiv \left| C_{\bar{A}H}(K_1^{determ}) - C_{\bar{A}\bar{A}}(K_1^{determ}) \right| = C_{\bar{A}H}(K_1) - C_{\bar{A}\bar{A}}(K_1^{determ}) \\ &= \Delta_A \tilde{C}_{\bar{A}}(K_1^{determ}) \end{aligned}$$

Therefore, two IRFs have the same size.

$$IR^{+,\text{downst}}(K_1^{determ}) - IR^{-,\text{downst}}(K_1^{determ}) = 0.$$

Upstream Shock. Around the deterministic allocation of capital, the IRF for negative upstream shock and that for positive upstream shock are given by

$$IR^{-,\text{upst}}(K_1^{determ}) \equiv \left| C_{L\bar{A}}(K_1^{determ}) - C_{\bar{A}\bar{A}}(K_1^{determ}) \right| = C_{\bar{A}\bar{A}}(K_1^{determ}) - C_{L\bar{A}}(K_1^{determ})$$

$$IR^{+,\text{upst}}(K_1^{determ}) \equiv \left| C_{H\bar{A}}(K_1^{determ}) - C_{\bar{A}\bar{A}}(K_1^{determ}) \right| = C_{H\bar{A}}(K_1) - C_{\bar{A}\bar{A}}(K_1^{determ})$$

Recall that the steady-state capital allocation is given by

$$K_1^{determ} = \frac{(1-\gamma_q)^{\sigma_q}}{(1-\gamma_q)^{\sigma_q} + \gamma_q^{\sigma_q}}$$

Therefore,

$$\begin{aligned} &C_{\bar{A}\bar{A}}(K_1^{determ}) \\ &= \bar{A} \left((1-\gamma_q) \left(K_1^{determ} \right)^{\frac{\sigma_q - 1}{\sigma_q}} \bar{A}^{\frac{\sigma_q - 1}{\sigma_q}} + \gamma_q \left(1 - K_1^{determ} \right)^{\frac{\sigma_q - 1}{\sigma_q}} \right)^{\frac{\sigma_q}{\sigma_q - 1}} \end{aligned}$$

$$C_{L\bar{A}}(K_1^{determ}) = \bar{A} \left((1-\gamma_q) \left(K_1^{determ} \right)^{\frac{\sigma_q - 1}{\sigma_q}} (A_L)^{\frac{\sigma_q - 1}{\sigma_q}} + \gamma_q \left(1 - K_1^{determ} \right)^{\frac{\sigma_q - 1}{\sigma_q}} \right)^{\frac{\sigma_q}{\sigma_q - 1}}$$

$$C_{H\bar{A}}(K_1^{determ}) = \bar{A} \left((1-\gamma_q) \left(K_1^{determ} \right)^{\frac{\sigma_q - 1}{\sigma_q}} (A_H)^{\frac{\sigma_q - 1}{\sigma_q}} + \gamma_q \left(1 - K_1^{determ} \right)^{\frac{\sigma_q - 1}{\sigma_q}} \right)^{\frac{\sigma_q}{\sigma_q - 1}}$$

We need to show that when $\sigma_q < 1$,

$$\begin{aligned} C_{\bar{A}\bar{A}}(K_1^{determ}) - C_{L\bar{A}}(K_1^{determ}) &> C_{H\bar{A}}(K_1^{determ}) - C_{\bar{A}\bar{A}}(K_1^{determ}) \\ C_{\bar{A}\bar{A}}(K_1^{determ}) &> \frac{1}{2}C_{H\bar{A}}(K_1^{determ}) + \frac{1}{2}C_{L\bar{A}}(K_1^{determ}) \\ C_{\bar{A}\bar{A}}K_1^{determ}) &> \mathbb{E}_{\mathbb{P}(A_1=A_H)=\frac{1}{2}}\{C_{S\bar{A}}(K_1^{determ})\} \end{aligned}$$

Since

$$\begin{aligned} &\frac{\partial\left((1-\gamma_q)\left(K_1^{determ}\right)^{\frac{\sigma_q-1}{\sigma_q}}\left(A_1\right)^{\frac{\sigma_q-1}{\sigma_q}}+\gamma_q\left(1-K_1^{determ}\right)^{\frac{\sigma_q-1}{\sigma_q}}\right)^{\frac{\sigma_q}{\sigma_q-1}}}{\partial A_1} \\ &= (1-\gamma_q)\left(K_1^{determ}\right)^{\frac{\sigma_q-1}{\sigma_q}} A_1^{\frac{-1}{\sigma_q}}\left((1-\gamma_q)\left(K_1^{determ}\right)^{\frac{\sigma_q-1}{\sigma_q}}\left(A_1\right)^{\frac{\sigma_q-1}{\sigma_q}}+\gamma_q\left(1-K_1^{determ}\right)^{\frac{\sigma_q-1}{\sigma_q}}\right)^{\frac{1}{\sigma_q-1}} \\ &= (1-\gamma_q)\left(K_1^{determ}\right)^{\frac{\sigma_q-1}{\sigma_q}}\left((1-\gamma_q)\left(K_1^{determ}\right)^{\frac{\sigma_q-1}{\sigma_q}}+\gamma_q\left(1-K_1^{determ}\right)^{\frac{\sigma_q-1}{\sigma_q}}\left(A_1\right)^{\frac{1-\sigma_q}{\sigma_q}}\right)^{\frac{1}{\sigma_q-1}} \end{aligned}$$

We have

$$\begin{aligned} &\frac{\partial^2\left((1-\gamma_q)\left(K_1^{determ}\right)^{\frac{\sigma_q-1}{\sigma_q}}\left(A_1\right)^{\frac{\sigma_q-1}{\sigma_q}}+\gamma_q\left(1-K_1^{determ}\right)^{\frac{\sigma_q-1}{\sigma_q}}\right)^{\frac{\sigma_q}{\sigma_q-1}}}{\partial A_1^2} \\ &= (-\frac{1}{\sigma_q})(1-\gamma_q)\left(K_1^{determ}\right)^{\frac{\sigma_q-1}{\sigma_q}}\gamma_q\left(1-K_1^{determ}\right)^{\frac{\sigma_q-1}{\sigma_q}} A_1^{\frac{1-2\sigma_q}{\sigma_q}} \\ &\times\left((1-\gamma_q)\left(K_1^{determ}\right)^{\frac{\sigma_q-1}{\sigma_q}}+\gamma_q\left(1-K_1^{determ}\right)^{\frac{\sigma_q-1}{\sigma_q}}\left(A_1\right)^{\frac{1-\sigma_q}{\sigma_q}}\right)^{\frac{2-\sigma_q}{\sigma_q-1}} \end{aligned}$$

Therefore, $C_{S\bar{A}}(K_1^{determ})$ is concave in A_1 (as long as $\sigma_q > 0$) and thus Jensen inequality gives us the ideal result.

□

A.4 Proof for Lemma 2: Impact of Preallocation on IRFs in Leontief Economy

We define an asymmetry index as the difference between the impulse responses to positive and negative shocks, which also depend on the capital allocation K_1:

$$\text{Asymmetry}^{\text{upst}}(K_1) = IR^{+,\text{upst}}(K_1) - IR^{-,\text{upst}}(K_1) \tag{14}$$

$$\text{Asymmetry}^{\text{downst}}(K_1) = IR^{+,\text{downst}}(K_1) - IR^{-,\text{downst}}(K_1) \tag{15}$$

Positive asymmetry indicates that positive shocks have larger impacts than negative shocks, while negative asymmetry indicates that negative shocks have larger impacts. The asymmetry index is connected to the skewness of the consumption function.

The asymmetry index is an order-preserving (monotonic) transformation of the statistical skewness.[16] Therefore, $\text{Asymmetry}^{\text{upst}}(K_1)$ and $\text{Skew}^{\text{upst}}(K_1)$ always have the same sign and their derivatives with respect to any parameter have the same sign.

Lemma. *In Leontief economy, the asymmetry of upstream IRFs equal to* $-1 + A_L$

$$\lim_{\sigma_q \to 0^+} \textit{Asymmetry}^{\textit{upst}}(K_1) = -1 + A_L$$

Proof. By taking limit, we have

$$\lim_{\sigma_q \to 0^+} \frac{\partial IR^{-,\text{upst}}(K_1^{determ})}{\partial K_1}\Big|_{K_1 = K_1^{determ}}$$
$$= \lim_{\sigma_q \to 0^+} -\frac{\left((1-\triangle_A)^{1-\frac{1}{\sigma_q}} - 1\right)}{\left((1-\triangle_A)^{1-\frac{1}{\sigma_q}}\left(1-\gamma_q\right)^{\sigma_q} + \gamma_q^{\sigma_q}\right)^{\frac{-1}{\sigma_q - 1}}}.$$

As $\sigma_q \to 0^+$, notice that

$$\lim_{\sigma_q \to 0^+} \left((1-\triangle_A)^{1-\frac{1}{\sigma_q}} - 1\right) = (1-\triangle_A)^{1-\lim_{\sigma_q \to 0}\frac{1}{\sigma_q}} - 1 = \infty,$$

[16] This follows because $(IR^+)^3 - (IR^-)^3 = (IR^+ - IR^-) \times [(IR^+)^2 + IR^+ \cdot IR^- + (IR^-)^2]$, where the second factor is always positive.

$$\lim_{\sigma_q \to 0^+} \left((1-\triangle_A)^{1-\frac{1}{\sigma_q}} \left(1-\gamma_q\right)^{\sigma_q} + \gamma_q^{\sigma_q} \right)^{\frac{-1}{\sigma_q - 1}} = \infty.$$

We thus have indeterminate from for negative shock. Further calculation gives us

$$\begin{aligned}
&\lim_{\sigma_q \to 0^+} -\frac{\left((1-\triangle_A)^{1-\frac{1}{\sigma_q}} - 1 \right)}{\left((1-\triangle_A)^{1-\frac{1}{\sigma_q}} \left(1-\gamma_q\right)^{\sigma_q} + \gamma_q^{\sigma_q} \right)^{\frac{-1}{\sigma_q - 1}}} \\
&= -\lim_{\sigma_q \to 0^+} \frac{1-(1-\triangle_A)^{\frac{1}{\sigma_q}-1}}{\left((1-\triangle_A)^{1-\frac{1}{\sigma_q}} \left(1-\gamma_q\right)^{\sigma_q} (1-\triangle_A)^{\frac{(1-\sigma_q)^2}{\sigma_q}} + (1-\triangle_A)^{\frac{(1-\sigma_q)^2}{\sigma_q}} \gamma_q^{\sigma_q} \right)^{\frac{-1}{\sigma_q - 1}}} \\
&= -\frac{1-0}{(1-\triangle_A)^{-1}+0} \\
&= -(1-\triangle_A).
\end{aligned}$$

where

$$\lim_{\sigma_q \to 0^+} (1-\triangle_A)^{1-\frac{1}{\sigma_q}+\frac{(1-\sigma_q)^2}{\sigma_q}} = \lim_{\sigma_q \to 0^+} (1-\triangle_A)^{1+\frac{(1-\sigma_q)^2-1}{\sigma_q}} = (1-\triangle_A)^{-1}.$$

$$\lim_{\sigma_q \to 0^+} (1-\triangle_A)^{\frac{1}{\sigma_q}-1} = (1-\triangle_A)^{(\lim_{\sigma_q \to 0^+} \frac{1}{\sigma_q})-1} = 0$$

and

$$\lim_{\sigma_q \to 0^+} (1-\triangle_A)^{\frac{(1-\sigma_q)^2}{\sigma_q}} \gamma_q^{\sigma_q} = (1-\triangle_A)^{\lim_{\sigma_q \to 0^+} \frac{(1-\sigma_q)^2}{\sigma_q}} = 0$$

For a positive shock, we have

$$\begin{aligned}
\lim_{\sigma_q \to 0^+} \frac{\partial IR^{+,\text{upst}}(K_1^{determ})}{\partial K_1}|_{K_1 = K_1^{determ}} &= \lim_{\sigma_q \to 0^+} -\frac{\left((1+\triangle_A)^{1-\frac{1}{\sigma_q}} - 1 \right)}{\left((1+\triangle_A)^{1-\frac{1}{\sigma_q}} \left(1-\gamma_q\right)^{\sigma_q} + \gamma_q^{\sigma_q} \right)^{\frac{-1}{\sigma_q - 1}}} \\
&= 1,
\end{aligned}$$

where we have applied

$$\lim_{\sigma_q \to 0^+} \left((1+\triangle_A)^{1-\frac{1}{\sigma_q}} - 1 \right) = (1+\triangle_A)^{1-\lim_{\sigma_q \to 0} \frac{1}{\sigma_q}} - 1 = -1.$$

$$\lim_{\sigma_q \to 0^+} \left((1 + \triangle_A)^{1 - \frac{1}{\sigma_q}} (1 - \gamma_q)^{\sigma_q} + \gamma_q^{\sigma_q} \right)^{\frac{-1}{\sigma_q - 1}} = (1 + 0 \times 1)^1 = 1.$$

Therefore, we have

$$\lim_{\sigma_q \to 0^+} \frac{\partial IR^{-,\text{upst}}(K_1^{determ})}{\partial K_1}|_{K_1 = K_1^{determ}} = -(1 - \triangle_A) = A_L$$

$$\lim_{\sigma_q \to 0^+} \frac{\partial IR^{+,\text{upst}}(K_1^{determ})}{\partial K_1}|_{K_1 = K_1^{determ}} = -1,$$

so that,

$$\lim_{\sigma_q \to 0^+} \text{Asymmetry}^{\text{upst}}(K_1) = -1 + A_L.$$

□

A.5 Proof for Lemma 3: Preallocation upstream reduces the impact of negative shocks

Next, we will analyze the implications of preallocating capital upstream for the impact of upstream productivity shock. We define a negative productivity shock as moving from $\bar{A} = \mathbb{E}[A]$ to A_L. Furthermore, we define the absolute value of the impulse response of consumption to a negative upstream productivity shock, as a function of original capital stock in sector 1, as:

$$IR^{-,\text{upst}}(K_1^{determ}) \equiv \left| C_{L\bar{A}}(K_1^{determ}) - C_{\bar{A}\bar{A}}(K_1^{determ}) \right| = C_{\bar{A}\bar{A}}(K_1^{determ}) - C_{L\bar{A}}(K_1^{determ})$$

Following this definition, we will prove in our next proposition that the absolute value of the impulse response of consumption to a negative shock is smaller when we set capital to the optimum under uncertainty (K_1^*) versus the deterministic optimum (K_1^{determ}). To do that, we evaluate the derivative of $IR^{-,\text{upst}}(K_1^{determ})$ with respect to K_1 at the deterministic optimum K_1^{determ}, and show that when $\sigma_q < 1$, we have that $\left.\frac{\partial IR^{-,\text{upst}}(K_1^{determ})}{\partial K}\right|_{K_1 = K_1^{determ}} < 0$. The interpretation of this result is that preallocation towards the upstream sector reduces the impact of negative shocks in consumption.

Lemma. *If inputs are complements ($\sigma_q < 1$), then increasing capital allocation to the upstream sector beyond the deterministic optimum decreases the impulse response to negative upstream*

productivity shocks:

$$\left.\frac{\partial IR^{-,upst}(K_1)}{\partial K_1}\right|_{K_1=K_1^{determ}} < 0$$

where $IR^{-,upst}(K_1)$ measures the consumption drop resulting from a negative upstream productivity shock.

Proof. We start by building $\left.\frac{\partial IR^{-,\text{upst}}(K_1^{determ})}{\partial K_1}\right|_{K_1=K_1^{determ}}$ using our expression for $C_{S\bar{A}}(K_1^{determ})$:

$$\begin{aligned}
\left.\frac{\partial IR^{-,\text{upst}}(K_1^{determ})}{\partial K_1}\right|_{K_1=K_1^{determ}} &= \left.\frac{\partial C_{\bar{A}\bar{A}}(K_1^{determ})}{\partial K_1}\right|_{K_1=K_1^{determ}} - \left.\frac{\partial C_{L\bar{A}}(K_1^{determ})}{\partial K_1}\right|_{K_1=K_1^{determ}} \\
&= \frac{\left(\bar{A}^{1-\frac{1}{\sigma_q}}-1\right)}{\left(\bar{A}^{1-\frac{1}{\sigma_q}}\left(1-\gamma_q\right)^{\sigma_q}+\gamma_q^{\sigma_q}\right)^{\frac{-1}{\sigma_q-1}}} - \frac{\left(A_L^{1-\frac{1}{\sigma_q}}-1\right)}{\left(A_L^{1-\frac{1}{\sigma_q}}\left(1-\gamma_q\right)^{\sigma_q}+\gamma_q^{\sigma_q}\right)^{\frac{-1}{\sigma_q-1}}} \\
&= -\frac{\left(A_L^{1-\frac{1}{\sigma_q}}-1\right)}{\left(A_L^{1-\frac{1}{\sigma_q}}\left(1-\gamma_q\right)^{\sigma_q}+\gamma_q^{\sigma_q}\right)^{\frac{-1}{\sigma_q-1}}}.
\end{aligned}$$

Since $A_L \in (0,1)$, we have that

$$\sigma_q < 1 \Leftrightarrow 1-\sigma_q^{-1} < 0 \Leftrightarrow \left(A_L^{1-\sigma_q^{-1}}-1\right) > 0 \Leftrightarrow \left.\frac{\partial IR(K_1,A_L)}{\partial K_1}\right|_{K_1=K_1^{determ}} < 0.$$

□

In the case of positive shocks

$$\begin{aligned}
\left.\frac{\partial IR^{+,\text{upst}}(K_1^{determ})}{\partial K_1}\right|_{K_1=K_1^{determ}} &= \left.\frac{\partial C_{H\bar{A}}(K_1^{determ})}{\partial K_1}\right|_{K_1=K_1^{determ}} - \left.\frac{\partial C_{\bar{A}\bar{A}}(K_1^{determ})}{\partial K_1}\right|_{K_1=K_1^{determ}} \\
&= \frac{\left(A_H^{1-\frac{1}{\sigma_q}}-1\right)}{\left(A_H^{1-\frac{1}{\sigma_q}}\left(1-\gamma_q\right)^{\sigma_q}+\gamma_q^{\sigma_q}\right)^{\frac{-1}{\sigma_q-1}}} - \frac{\left(\bar{A}^{1-\frac{1}{\sigma_q}}-1\right)}{\left(\bar{A}^{1-\frac{1}{\sigma_q}}\left(1-\gamma_q\right)^{\sigma_q}+\gamma_q^{\sigma_q}\right)^{\frac{-1}{\sigma_q-1}}} \\
&= \frac{\left(A_H^{1-\frac{1}{\sigma_q}}-1\right)}{\left(A_H^{1-\frac{1}{\sigma_q}}\left(1-\gamma_q\right)^{\sigma_q}+\gamma_q^{\sigma_q}\right)^{\frac{-1}{\sigma_q-1}}},
\end{aligned}$$

and using a similar reasoning as above, we get

$$\sigma_q < 1 \Leftrightarrow \left(A_H^{1-\sigma_q^{-1}}-1\right) < 0 \Leftrightarrow \left.\frac{\partial IR^{+,\text{upst}}(K_1^{determ})}{\partial K_1}\right|_{K_1=K_1^{determ}} < 0.$$

Therefore preallocating capital upstream also dampens the effect of positive shocks.

A.6 Proof for Proposition 1: Preallocation upstream reduces the expected consumption

Moreover, we can explore how preallocation towards upstream sector affects the mean of aggregate consumption under different conditions by following the same strategy of proof.

Proposition. *Up to the first-order approximation, if inputs are complements ($\sigma_q < 1$), the effect of upstream preallocation on expected consumption depends on the relative strength of the upstream sector:*

1. *When the upstream sector is large enough ($\gamma_q < \bar{\gamma}_q(\triangle_A)$), increasing upstream capital allocation beyond the deterministic optimum decreases expected consumption:*

$$\left.\frac{\partial \mathbb{E}\{C(A_1, A_2, K_1)\}}{\partial K_1}\right|_{K_1=K_1^{determ}} < 0.$$

2. *When the upstream sector's role is more limited ($\gamma_q > \bar{\gamma}_q(\triangle_A)$), increasing upstream*

capital allocation increases expected consumption.

Proof. We start by showing that

$$\begin{aligned}
\mathbf{E}\{C(A_1, A_2, K_1)\} &= \mathbf{E}\{A_2\}\left[p\tilde{C}_L(K_1) + (1-p)\tilde{C}_H(K_1)\right] \\
\frac{\partial \mathbf{E}\{C(A_1, A_2, K_1)\}}{\partial K_1}|_{K_1=K_1^{determ}} &= p_1 \frac{\partial \tilde{C}_L(K_1)}{\partial K_1}|_{K_1=K_1^{determ}} + (1-p_1)\frac{\partial \tilde{C}_H(K_1)}{\partial K_1}|_{K_1=K_1^{determ}} \\
&= p_1 \frac{\left(A_L^{1-\frac{1}{\sigma_q}} - 1\right)}{\left(A_L^{1-\frac{1}{\sigma_q}}(1-\gamma_q)^{\sigma_q} + \gamma_q^{\sigma_q}\right)^{\frac{-1}{\sigma_q - 1}}} \\
&+ (1-p_1)\frac{\left(A_H^{1-\frac{1}{\sigma_q}} - 1\right)}{\left(A_H^{1-\frac{1}{\sigma_q}}(1-\gamma_q)^{\sigma_q} + \gamma_q^{\sigma_q}\right)^{\frac{-1}{\sigma_q - 1}}}
\end{aligned}$$

Following our previous assumption, we set $p_1 = 1/2$, thus our target is to analyze the sign of

$$F \equiv \frac{\left(A_H^{1-\frac{1}{\sigma_q}} - 1\right)}{\left(A_H^{1-\frac{1}{\sigma_q}}(1-\gamma_q)^{\sigma_q} + \gamma_q^{\sigma_q}\right)^{\frac{-1}{\sigma_q - 1}}} + \frac{\left(A_L^{1-\frac{1}{\sigma_q}} - 1\right)}{\left(A_L^{1-\frac{1}{\sigma_q}}(1-\gamma_q)^{\sigma_q} + \gamma_q^{\sigma_q}\right)^{\frac{-1}{\sigma_q - 1}}}$$

Notice that this is a special case of proposition 2 below, where $\epsilon_c^{-1} = 0$. By taking a second-order local approximation for F around $\sigma_q = 1$, as the appendix **??** shows, we have

$$\lim_{\sigma_q \to 1} F = 0$$

and

$$\frac{\partial}{\partial \sigma_q} F|_{\sigma_q=1} = (1+\triangle_A)^{1-\gamma_q}\log(1+\triangle_A) + (1-\triangle_A)^{1-\gamma_q}\log(1-\triangle_A)$$

By Intermediate Value Theorem, there exists a unique threshold value $\bar{\gamma}_q(\triangle_A)$ such that

$$\frac{\partial}{\partial \sigma_q} F|_{\sigma_q=1} \begin{cases} > 0 & \text{if } \gamma_q < \bar{\gamma}_q(\triangle_A) \\ = 0 & \text{if } \gamma_q = \bar{\gamma}_q(\triangle_A) \\ < 0 & \text{if } \gamma_q > \bar{\gamma}_q(\triangle_A) \end{cases}$$

Since the values on the boundary are strictly bounded away from 0, $\bar{\gamma}_q(\triangle_A) \in (0,1)$. Finally, when $\gamma_q > \bar{\gamma}_q(\triangle_A)$,

$$F \approx 0 + \underbrace{\frac{\partial}{\partial \sigma_q}|_{\sigma_q=1} F}_{<0} \times (\sigma_q - 1)$$

F is bigger than 0 if and only if $\sigma_q < 1$ up to the first-order approximation. □

A.7 Proof for Proposition 2: Preallocation toward the upstream sector

While in the optimum we have that $\partial \mathbb{E}[U(C)]/\partial K_1 = 0$, we can use the expression of the marginal expected utility to evaluate how optimal capital allocation in the uncertainty case compares to the optimum for the deterministic case. By evaluating $\tilde{C}_S(K_1)$ at the deterministic capital allocation

$$\begin{aligned}
\tilde{C}_S(K_1)\big|_{K_1^{determ}} &= \left((1-\gamma_q) \left(A_S \frac{(1-\gamma_q)^{\sigma_q}}{\gamma_q^{\sigma_q} + (1-\gamma_q)^{\sigma_q}} \right)^{\frac{\sigma_q - 1}{\sigma_q}} + \gamma_q \left(1 - \frac{(1-\gamma_q)^{\sigma_q}}{\gamma_q^{\sigma_q} + (1-\gamma_q)^{\sigma_q}} \right)^{\frac{\sigma_q - 1}{\sigma_q}} \right)^{\frac{\sigma_q}{\sigma_q - 1}} \\
&= \left(\frac{1}{\gamma_q^{\sigma_q} + (1-\gamma_q)^{\sigma_q}} \right) \left(A_S^{1-\frac{1}{\sigma_q}} (1-\gamma_q)^{\sigma_q} + \gamma_q^{\sigma_q} \right)^{\frac{\sigma_q}{\sigma_q - 1}}
\end{aligned}$$

Next, we evaluate the derivative:

$$\begin{aligned}
\left.\frac{\partial \tilde{C}_S(K_1)}{\partial K_1}\right|_{K_1^{determ}} &= \left((1-\gamma_q) \left(\frac{A_S \frac{\left(1-\gamma_q\right)^{\sigma_q}}{\gamma_q^{\sigma_q}+\left(1-\gamma_q\right)^{\sigma_q}}}{C_S} \right)^{\frac{-1}{\sigma_q}} A_S - \gamma_q \left(\frac{1 - \frac{\left(1-\gamma_q\right)^{\sigma_q}}{\gamma_q^{\sigma_q}+\left(1-\gamma_q\right)^{\sigma_q}}}{C_S} \right)^{\frac{-1}{\sigma_q}} \right) \\
&= \left[\gamma_q^{\sigma_q} + \left(1-\gamma_q\right)^{\sigma_q}\right]^{\frac{1}{\sigma_q}} \frac{\left(A_S^{1-\frac{1}{\sigma_q}} - 1\right)}{C_S^{-\frac{1}{\sigma_q}}} \\
&= \left[\gamma_q^{\sigma_q} + \left(1-\gamma_q\right)^{\sigma_q}\right]^{\frac{1}{\sigma_q}} \frac{\left(A_S^{1-\frac{1}{\sigma_q}} - 1\right)}{\left(\left(\frac{1}{\gamma_q^{\sigma_q}+\left(1-\gamma_q\right)^{\sigma_q}} \right) \left(A_S^{1-\frac{1}{\sigma_q}} \left(1-\gamma_q\right)^{\sigma_q} + \gamma_q^{\sigma_q} \right)^{\frac{\sigma_q}{\sigma_q-1}} \right)^{-\frac{1}{\sigma_q}}} \\
&= \frac{\left(A_S^{1-\frac{1}{\sigma_q}} - 1\right)}{\left(A_S^{1-\frac{1}{\sigma_q}} \left(1-\gamma_q\right)^{\sigma_q} + \gamma_q^{\sigma_q} \right)^{\frac{-1}{\sigma_q-1}}}
\end{aligned}$$

The FOC evaluated at the deterministic optimum is

$$\begin{aligned}
\left.\frac{\partial \mathbb{E}[U(C)]}{\partial K_1}\right|_{K_1^{determ}} &= \mathbb{E}\{A_2\} \left\{ p_1 \frac{1}{\left.\tilde{C}_L(K_1)\epsilon_c^{-1}\right|_{K_1^{determ}}} \left.\frac{\partial \tilde{C}_L(K_1)}{\partial K_1}\right|_{K_1^{determ}} + (1-p_1) \frac{1}{\left.\tilde{C}_H(K_1)\epsilon_c^{-1}\right|_{K_1^{determ}}} \left.\frac{\partial \tilde{C}_H(K_1)}{\partial K_1}\right|_{K_1^{determ}} \right\} \\
&= p_1 \left[\gamma_q^{\sigma_q} + \left(1-\gamma_q\right)^{\sigma_q}\right]^{\epsilon_c^{-1}} \frac{\left(A_L^{1-\frac{1}{\sigma_q}} - 1\right)}{\left(A_L^{1-\frac{1}{\sigma_q}} \left(1-\gamma_q\right)^{\sigma_q} + \gamma_q^{\sigma_q} \right)^{\frac{\epsilon_c^{-1}\sigma_q - 1}{\sigma_q - 1}}} \\
&\quad + (1-p_1) \left[\gamma_q^{\sigma_q} + \left(1-\gamma_q\right)^{\sigma_q}\right]^{\epsilon_c^{-1}} \frac{\left(A_H^{1-\frac{1}{\sigma_q}} - 1\right)}{\left(A_H^{1-\frac{1}{\sigma_q}} \left(1-\gamma_q\right)^{\sigma_q} + \gamma_q^{\sigma_q} \right)^{\frac{\epsilon_c^{-1}\sigma_q - 1}{\sigma_q - 1}}}, \\
&\propto p_1 \frac{\left(A_L^{1-\frac{1}{\sigma_q}} - 1\right)}{\left(A_L^{1-\frac{1}{\sigma_q}} \left(1-\gamma_q\right)^{\sigma_q} + \gamma_q^{\sigma_q} \right)^{\frac{\epsilon_c^{-1}\sigma_q - 1}{\sigma_q - 1}}} + (1-p_1) \frac{\left(A_H^{1-\frac{1}{\sigma_q}} - 1\right)}{\left(A_H^{1-\frac{1}{\sigma_q}} \left(1-\gamma_q\right)^{\sigma_q} + \gamma_q^{\sigma_q} \right)^{\frac{\epsilon_c^{-1}\sigma_q - 1}{\sigma_q - 1}}},
\end{aligned}$$

where in the last line we take out the positive constant $\left[\gamma_q^{\sigma_q} + (1-\gamma_q)^{\sigma_q}\right]^{\epsilon_c^{-1}}$.

We start proof by firstly showing an auxiliary lemma that $\frac{\partial \mathbb{E}[U(C)]}{\partial K_1}$ is decreasing in K_1 globally.

Lemma. *The expected utility of aggregate consumption is globally concave in* K_1.

$$\frac{\partial^2 \mathbb{E}\{U(C)\}}{\partial K_1^2} < 0$$

Proof. We firstly prove that the normalized aggregate consumption is globally concave in K_1.

$$\begin{aligned}
\frac{\partial^2 \tilde{C}_S(K_1)}{\partial K_1^2} = & \frac{1}{\sigma_q}(1-\gamma_q)\gamma_q A_S^{\frac{\sigma_q-1}{\sigma_q}} \left((1-\gamma_q)A_S^{\frac{\sigma_q-1}{\sigma_q}} + \gamma_q(\frac{1-K_1}{K_1})^{\frac{\sigma_q-1}{\sigma_q}}\right)^{\frac{2-\sigma_q}{\sigma_q-1}} (\frac{1-K_1}{K_1})^{\frac{-1}{\sigma_q}}(-\frac{1}{K_1^2}) \\
& - \gamma_q(1-\gamma_q)A_S^{\frac{\sigma_q-1}{\sigma_q}} A_S^{\frac{\sigma_q-1}{\sigma_q}} \left((1-\gamma_q)A_1^{\frac{\sigma_q-1}{\sigma_q}}(\frac{K_1}{1-K_1})^{\frac{\sigma_q-1}{\sigma_q}} + \gamma_q\right)^{\frac{2-\sigma_q}{\sigma_q-1}} (\frac{K_1}{1-K_1})^{\frac{-1}{\sigma_q}} \frac{1}{(1-K_1)^2} \\
& < 0
\end{aligned}$$

Then, it's straightforward to show that the expected utility of aggregate consumption is globally concave in K_1.

$$\begin{aligned}
\frac{\partial \mathbb{E}\{U(C)\}}{\partial K_1} &= \mathbb{E}\{C^{-\epsilon_c^{-1}}\frac{\partial C}{\partial K_1}\} \\
\frac{\partial^2 \mathbb{E}\{U(C)\}}{\partial K_1^2} &= \underbrace{\mathbb{E}\{(-\epsilon_c^{-1})\underbrace{C^{-\epsilon_c^{-1}-1}\frac{\partial C}{\partial K_1}}_{>0}\}}_{<0} + \mathbb{E}\{C^{-\epsilon_c^{-1}}\underbrace{\frac{\partial^2 C}{\partial K_1^2}}_{<0}\} \\
&< 0
\end{aligned}$$

□

Given the lemma above, if the derivative of upstream capital on expected utility, evaluated at the deterministic allocation, is positive, then it is optimal for the social planner to allocate more capital to the upstream sector. Thus, by setting $p_1 = 1 - p_1 = \frac{1}{2}$, the

necessary and sufficient condition for allocating extra capital to sector 1 is

$$\frac{(1+\Delta_A)^{1-\sigma_q^{-1}}-1}{\left[(1+\Delta_A)^{1-\sigma_q^{-1}}\left(1-\gamma_q\right)^{\sigma_q}+\gamma_q^{\sigma_q}\right]^{\frac{\epsilon_c^{-1}\sigma_q-1}{\sigma_q-1}}} > \frac{1-(1-\Delta_A)^{1-\sigma_q^{-1}}}{\left[(1-\Delta_A)^{1-\sigma_q^{-1}}\left(1-\gamma_q\right)^{\sigma_q}+\gamma_q^{\sigma_q}\right]^{\frac{\epsilon_c^{-1}\sigma_q-1}{\sigma_q-1}}}. \quad (16)$$

The following proposition 2 fully characterizes the conditions for the above inequality to hold when $\sigma_q < 1$.

Proposition. *If inputs are complements ($\sigma_q < 1$), the planner preallocates capital to the upstream sector (that is, $K_1^* > K_1^{determ}$) under any of the following conditions, up to the first-order approximation:*

1. *If risk aversion is high enough, $\epsilon_c^{-1} \geq 1$.*
2. *If risk aversion is moderate $\bar{\epsilon}_c^{-1}(\triangle_A, \gamma_q) < \epsilon_c^{-1} < 1$.*
3. *If risk aversion is low, $0 < \epsilon_c^{-1} < \bar{\epsilon}_c^{-1}(\triangle_A, \gamma_q)$, and the downstream sector's importance in production is sufficiently high, $\gamma_q > \bar{\gamma}_q(\triangle_A)$.*

The thresholds $\bar{\gamma}_q(\triangle_A)$ and $\bar{\epsilon}_c^{-1}(\triangle_A, \gamma_q)$ are determined by the size of productivity shocks and production parameters.

Proof. Given the auxiliary lemma, our target is to discuss the conditions for the following inequality to hold when $\sigma_q < 1$.

$$F \equiv \frac{\left((1-\triangle_A)^{1-\frac{1}{\sigma_q}}-1\right)}{\left((1-\triangle_A)^{1-\frac{1}{\sigma_q}}\left(1-\gamma_q\right)^{\sigma_q}+\gamma_q^{\sigma_q}\right)^{\frac{\epsilon_c^{-1}\sigma_q-1}{\sigma_q-1}}} + \frac{\left((1+\triangle_A)^{1-\frac{1}{\sigma_q}}-1\right)}{\left((1+\triangle_A)^{1-\frac{1}{\sigma_q}}\left(1-\gamma_q\right)^{\sigma_q}+\gamma_q^{\sigma_q}\right)^{\frac{\epsilon_c^{-1}\sigma_q-1}{\sigma_q-1}}} > 0$$

We apply first-order approximation around $\sigma_q = 1$ and proceed with the whole proof in two general steps.

1. Firstly, we show that in a Cobb-Douglass economy,

$$\lim_{\sigma_q \to 1} F = 0$$

Extra allocation of capital to certain sector does not exist.

2. Secondly, given the first-order approximation,

$$F \approx 0 + \frac{\partial}{\partial \sigma_q} F|_{\sigma_q=1}(\sigma_q - 1)$$

it suffices to discuss the conditions for the following to hold

$$\frac{\partial}{\partial \sigma_q} F|_{\sigma_q=1} < 0$$

Step 1 Firstly, $\forall \epsilon_c^{-1} \geq 0$,

$$\lim_{\sigma_q \to 1^+} \left((1-\triangle_A)^{1-\frac{1}{\sigma_q}} (1-\gamma_q)^{\sigma_q} + \gamma_q^{\sigma_q} \right)^{\frac{\epsilon_c^{-1}\sigma_q - 1}{\sigma_q - 1}} < \infty \; ; \; \lim_{\sigma_q \to 1^-} \left((1-\triangle_A)^{1-\frac{1}{\sigma_q}} (1-\gamma_q)^{\sigma_q} + \gamma_q^{\sigma_q} \right)^{\frac{\epsilon_c^{-1}\sigma_q - 1}{\sigma_q - 1}} < \infty$$

The same holds for $A = 1 + \triangle_A$. We therefore have

$$\lim_{\sigma_q \to 1^+} F = 0 = \lim_{\sigma_q \to 1^-} F \;\; \forall \epsilon_c^{-1} \geq 0$$

Step 2 we then discuss the sign of the limit of the derivative of our objective function F by rewriting it as the sum of the limits of two derivatives.

$$\begin{aligned} \frac{\partial}{\partial \sigma_q} F|_{\sigma_q=1} &= \lim_{\sigma_q \to 1} \left\{ \frac{\partial}{\partial \sigma_q} \frac{(1+\triangle_A)^{1-\sigma_q^{-1}} - 1}{\left[(1+\triangle_A)^{1-\sigma_q^{-1}} (1-\gamma_q)^{\sigma_q} + \gamma_q^{\sigma_q} \right]^{\frac{\epsilon_c^{-1}\sigma_q - 1}{\sigma_q - 1}}} + \frac{\partial}{\partial \sigma_q} \frac{(1-\triangle_A)^{1-\sigma_q^{-1}} - 1}{\left[(1-\triangle_A)^{1-\sigma_q^{-1}} (1-\gamma)^{\sigma_q} + \gamma^{\sigma_q} \right]^{\frac{\epsilon^{-1}\sigma_q - 1}{\sigma_q - 1}}} \right\} \\ &= \lim_{\sigma_q \to 1} \frac{\Omega_1^1 - \Omega_2^1}{D_1^2} + \lim_{\sigma_q \to 1} \frac{\Omega_1^2 - \Omega_2^2}{D_2^2} \end{aligned} \tag{17}$$

where we define

$$\begin{aligned} D_1 &\equiv \left[(1+\triangle_A)^{1-\sigma_q^{-1}} (1-\gamma_q)^{\sigma_q} + \gamma_q^{\sigma_q} \right]^{\frac{\epsilon_c^{-1}\sigma_q - 1}{\sigma_q - 1}} \quad , \quad D_2 \equiv \left[(1-\triangle_A)^{1-\sigma_q^{-1}} (1-\gamma_q)^{\sigma_q} + \gamma_q^{\sigma_q} \right]^{\frac{\epsilon_c^{-1}\sigma_q - 1}{\sigma_q - 1}} \\ \Omega_1^1 &\equiv [\frac{\partial}{\partial \sigma_q}((1+\triangle_A)^{1-\sigma_q^{-1}} - 1)] D_1 \quad , \quad \Omega_1^2 \equiv [\frac{\partial}{\partial \sigma_q}((1-\triangle_A)^{1-\sigma_q^{-1}} - 1)] D_2 \\ \Omega_2^1 &\equiv ((1+\triangle_A)^{1-\sigma_q^{-1}} - 1)(\frac{\partial}{\partial \sigma_q} D_1) \quad , \quad \Omega_2^2 \equiv ((1-\triangle_A)^{1-\sigma_q^{-1}} - 1)(\frac{\partial}{\partial \sigma_q} D_2) \end{aligned}$$

The following proof of is proceeded by firstly calculating the two limits separately and then discussing the conditions for their sum to be positive. WLOG, we offer a detailed

explanation for finding the limits of $D_1, \Omega_1^1, \Omega_2^1$ as $\sigma_q \to 1^+$. The symmetric result then follows for $\sigma_q \to 1^-$ and for $D_2, \Omega_1^2, \Omega_2^2$.

We start by calculating the limit for D_1. Due to L'hospital rule,

$$\lim_{\sigma_q \to 1} D_1 = \exp\Big\{ \frac{\log(\gamma_q)\gamma_q + \Big[\log(1-\gamma_q)(1-\gamma_q) + \log(1+\triangle_A)(1-\gamma_q)\Big]}{(\epsilon_c^{-1}-1)^{-1}} \Big\}$$

We therefore have

$$\lim_{\sigma_q \to 1} \Omega_1^1 = \lim_{\sigma_q \to 1} \log(1+\triangle_A)(1+\triangle_A)^{1-\sigma_q^{-1}} \sigma_q^{-2} D_1 = \log(1+\triangle_A) \lim_{\sigma_q \to 1} D_1$$

Moreover, we have

$$\begin{aligned}
&\frac{\partial}{\partial \sigma_q} D_1 \\
&= \underbrace{\exp\Big\{ \frac{\epsilon_c^{-1}\sigma - 1}{\sigma_q - 1} \log\Big[(1+\triangle_A)^{1-\sigma_q^{-1}}(1-\gamma_q)^{\sigma_q} + \gamma_q^{\sigma_q}\Big] \Big\}}_{g_1^1(\sigma_q) = D_1} \\
&\times \Bigg\{ \underbrace{\frac{\epsilon_c^{-1}(\sigma-1) - (\epsilon_c^{-1}\sigma_q - 1)}{(\sigma_q-1)^2} \log\Big[(1+\triangle_A)^{1-\sigma_q^{-1}}(1-\gamma_q)^{\sigma_q} + \gamma_q^{\sigma_q}\Big]}_{g_2^1(\sigma_q)} \\
&+ \underbrace{\frac{\epsilon_c^{-1}\sigma_q - 1}{\sigma_q - 1} \frac{\Big[\log(\gamma_q)\gamma_q^{\sigma_q} + \log(1-\gamma_q)(1-\gamma_q)^{\sigma_q}(1+\triangle_A)^{1-\sigma_q^{-1}} + \log(1+\triangle_A)(1-\gamma_q)^{\sigma_q}(1+\triangle_A)^{1-\sigma_q^{-1}}(\sigma_q^{-2})\Big]}{(1+\triangle_A)^{1-\sigma_q^{-1}}(1-\gamma_q)^{\sigma_q} + \gamma_q^{\sigma_q}}}_{g_3^1(\sigma_q)} \Bigg\}
\end{aligned}$$

So we can express the limit of Ω_2^1 as

$$\lim_{\sigma_q \to 1} \Omega_2^1 = \lim_{\sigma \to 1} D_1 \lim_{\sigma_q \to 1} \Big[\underbrace{((1+\triangle_A)^{1-\sigma_q^{-1}} - 1) g_2^1(\sigma_q)}_{(1)} + \underbrace{((1+\triangle_A)^{1-\sigma_q^{-1}} - 1) g_3^1(\sigma_q)}_{(2)} \Big]$$

We first discuss the limit of component (1) from both sides. By applying L'hospital rule,

$$
\begin{aligned}
&(1-\epsilon_c^{-1}) \lim_{\sigma_q \to 1^+} \frac{\overbrace{\Big[(1+\triangle_A)^{1-\sigma_q^{-1}}-1\Big]}^{0^+} \overbrace{\log\Big[(1+\triangle_A)^{1-\sigma_q^{-1}}(1-\gamma_q)^{\sigma_q}+\gamma_q^{\sigma}\Big]}^{0^-}}{\underbrace{(\sigma_q-1)^2}_{0^+}} \\
&= (1-\epsilon_c^{-1}) \log(1+\triangle_A) \lim_{\sigma_q \to 1} \frac{\log\Big[(1+\triangle_A)^{1-\sigma_q^{-1}}(1-\gamma_q)^{\sigma_q}+\gamma_q^{\sigma_q}\Big]}{2(\sigma_q-1)} + (1-\epsilon_c^{-1}) \lim_{\sigma_q \to 1} g_4^1 \frac{\Big[(1+\triangle_A)^{1-\sigma_q^{-1}}-1\Big]}{2(\sigma_q-1)} \\
&= \frac{1}{2}(1-\epsilon_c^{-1}) \log(1+\triangle_A) \lim_{\sigma_q \to 1} g_4^1 + \frac{1}{2}(1-\epsilon^{-1}) \lim_{\sigma_q \to 1} g_4^1 \lim_{\sigma_q \to 1} \log(1+\triangle_A)(1+\triangle_A)^{1-\sigma_q^{-1}}(\sigma_q^{-2}) \\
&= (1-\epsilon_c^{-1}) \log(1+\triangle_A) \lim_{\sigma_q \to 1} g_4^1
\end{aligned}
$$

where

$$
g_4^1 = \frac{1}{(1+\triangle_A)^{1-\sigma_q^{-1}}(1-\gamma_q)^{\sigma_q}+\gamma^{\sigma}} \left\{ \log(\gamma_q)\gamma_q + \Big[\log(1-\gamma_q)(1-\gamma_q) + \log(1+\triangle_A)(1-\gamma_q)\Big] \right\}
$$

The same applies for $\sigma_q \to 1^-$.

We then discuss the limit of component (2) from both sides. Here we apply L'hospital rule twice.

$$
\begin{aligned}
&\lim_{\sigma_q \to 1^+} \Big[(1+\triangle_A)^{1-\sigma_q^{-1}}-1\Big] g_3^1(\sigma_q) \\
&= \lim_{\sigma_q \to 1^+} \frac{\Big\{\log(\gamma_q)\gamma_q^{\sigma_q} + \Big[\log(1-\gamma_q)(1-\gamma_q)^{\sigma_q}(1+\triangle_A)^{1-\sigma_q^{-1}} + \log(1+\triangle_A)(1-\gamma_q)^{\sigma_q}(1+\triangle_A)^{1-\sigma_q^{-1}}(\sigma_q^{-2})\Big]\Big\}}{(1+\triangle_A)^{1-\sigma_q^{-1}}(1-\gamma_q)^{\sigma_q}+\gamma_q^{\sigma_q}} \\
&\times \lim_{\sigma_q \to 1^+} \frac{\overbrace{\Big[(1+\triangle_A)^{1-\sigma_q^{-1}}-1\Big]}^{0}}{\underbrace{\frac{\sigma_q-1}{\epsilon_c^{-1}\sigma_q-1}}_{0}} \\
&= \left\{ \log(\gamma_q)\gamma_q + \Big[\log(1-\gamma_q)(1-\gamma_q) + \log(1+\triangle_A)(1-\gamma_q)\Big] \right\} \frac{\log(1+\triangle_A)(1+\triangle_A)^{1-\sigma_q^{-1}}(\sigma_q^{-2})}{\frac{\epsilon_c^{-1}-1}{(\epsilon_c^{-1}\sigma_q-1)^2}} \\
&= -\lim_{\sigma_q \to 1} g_4^1 \frac{\log(1+\triangle_A)}{\frac{1}{1-\epsilon_c^{-1}}}
\end{aligned}
$$

The same applies for $\sigma_q \to 1^-$.

And, the calculations for (limits of) $D_1, \Omega_1^1, \Omega_2^1$ can also apply to $D_2, \Omega_1^2, \Omega_2^2$. Therefore, by combining the above results,

$$\lim_{\sigma_q \to 1} \Omega_2^1 = \lim_{\sigma_q \to 1} g_1^1(\sigma_q) \Big[\log(1+\triangle_A) \frac{\lim_{\sigma_q \to 1} g_4^1}{\frac{1}{1-\epsilon_c^{-1}}} - \log(1+\triangle_A) \frac{\lim_{\sigma_q \to 1} g_4^1}{\frac{1}{1-\epsilon_c^{-1}}} \Big] = 0$$

$$\lim_{\sigma_q \to 1} \Omega_2^2 = \lim_{\sigma_q \to 1} g_1^2(\sigma_q) \Big[\log(1-\triangle_A) \frac{\lim_{\sigma_q \to 1} g_4^2}{\frac{1}{1-\epsilon_c^{-1}}} - \log(1-\triangle_A) \frac{\lim_{\sigma_q \to 1} g_4^2}{\frac{1}{1-\epsilon_c^{-1}}} \Big] = 0$$

All of the results above hold for all $\epsilon_c^{-1} \geq 0$

Based on the previous calculation, our original target equation 17 in step 2 is reduced to

$$\begin{aligned}
\frac{\partial}{\partial \sigma_q} F|_{\sigma_q=1} &= \lim_{\sigma_q \to 1} \frac{\Omega_1^1 - \Omega_2^1}{D_1^2} + \lim_{\sigma_q \to 1} \frac{\Omega_1^2 - \Omega_2^2}{D_2^2} \\
&= \lim_{\sigma_q \to 1} \frac{\Omega_1^1}{D_1^2} + \lim_{\sigma_q \to 1} \frac{\Omega_1^2}{D_2^2} \\
&= (1+\triangle_A)^{(1-\epsilon_c^{-1})(1-\gamma_q)} \frac{\log(1+\triangle_A)}{D(\epsilon_c^{-1}, \gamma_q)} + (1-\triangle_A)^{(1-\epsilon_c^{-1})(1-\gamma_q)} \frac{\log(1-\triangle_A)}{D(\epsilon_c^{-1}, \gamma_q)}
\end{aligned}$$

where $D(\epsilon_c^{-1}, \gamma_q) \equiv \exp\Big(\frac{\log(\gamma_q)\gamma_q + \log(1-\gamma_q)(1-\gamma_q)}{(\epsilon_c^{-1}-1)^{-1}} \Big)$ is strictly positive for any $(\epsilon_c^{-1}, \gamma_q) \in [0,1] \times [0,1]$. Therefore, the sign of the first-order derivative depends on the values of $\triangle_A$, γ_q, and ϵ_c^{-1}.

When $\epsilon_c^{-1} = 1$, due to the strict concavity of log function, given $\triangle_A \in (0,1)$

$$\frac{\partial}{\partial \sigma_q} F|_{\sigma_q=1} = \log(1+\triangle_A) + \log(1-\triangle_A) < 1$$

When $\epsilon_c^{-1} > 1$,

$$\begin{aligned}\frac{\partial}{\partial \sigma_q} F|_{\sigma_q=1} &< (1-\triangle_A)^{(1-\epsilon_c^{-1})(1-\gamma_q)} \frac{\log(1+\triangle_A)}{D} + (1-\triangle_A)^{(1-\epsilon_c^{-1})(1-\gamma_q)} \frac{\log(1-\triangle_A)}{D} \\ &= (1-\triangle_A)^{(1-\epsilon_c^{-1})(1-\gamma_q)} \Big[\frac{\log(1+\triangle_A)}{D} + \frac{\log(1-\triangle_A)}{D}\Big] \\ &< (1-\triangle_A)^{(1-\epsilon_c^{-1})(1-\gamma_q)} \Big[\frac{\log(1)}{D} + \frac{\log(1)}{D}\Big] = 0\end{aligned}$$

Since $\log(1+\triangle_A) > 0 > \log(1-\triangle_A)$ and $(1-\triangle_A)^{(1-\epsilon_c^{-1})(1-\gamma_q)} > (1+\triangle_A)^{(1-\epsilon_c^{-1})(1-\gamma_q)}$, by adding more positive numbers, we get the first inequality. The second strict inequality is again due to the strict concavity of log function.

Lastly, when $\epsilon_c^{-1} < 1$, we first note that

$$\lim_{\gamma_q \to 0} \lim_{\epsilon_c^{-1} \to 0^+} \frac{\partial}{\partial \sigma_q} F|_{\sigma_q=1} > 0, \quad \lim_{\gamma_q \to 0} \lim_{\epsilon_c^{-1} \to 1^-} \frac{\partial}{\partial \sigma_q} F|_{\sigma_q=1} < 0 \ \text{ (Opposite Signs on } \epsilon_c^{-1}\text{'s boundary)}$$

$$\lim_{\gamma_q \to 0} \lim_{\epsilon_c^{-1} \to 0^+} \frac{\partial}{\partial \sigma_q} F|_{\sigma_q=1} > 0, \quad \lim_{\gamma_q \to 1} \lim_{\epsilon_c^{-1} \to 0^+} \frac{\partial}{\partial \sigma_q} F|_{\sigma_q=1} < 0 \ \text{ (Opposite Signs on } \gamma_q\text{'s boundary)}$$

These two pairs of opposite signs indicate the existence of threshold values for γ_q and ϵ_c^{-1}. Notice that $\frac{\partial}{\partial \sigma_q} F|_{\sigma_q=1}$ is continuously differentiable and strictly monotone in ϵ_c^{-1} and γ_q when $\triangle_A \in (0,1)$. Therefore, we can apply Intermediate Value Theorem (IVT) to show that given any $\triangle_A \in (0,1)$, there exists a unique threshold value $\bar{\gamma}_q(\triangle_A)$ such that

1. if $\gamma_q > \bar{\gamma}_q(\triangle_A)$, $\frac{\partial}{\partial \sigma_q} F|_{\sigma_q=1} < 0$ when $\epsilon_c^{-1} < 1$. Together with previous discussion, $\frac{\partial}{\partial \sigma_q} F|_{\sigma_q=1} < 0 \ \forall \epsilon_c^{-1} \geq 0$.

2. if $\gamma_q \leq \bar{\gamma}_q(\triangle_A)$, by applying IVT again, there exists a unique threshold value $\bar{\epsilon}_c^{-1}(\triangle_A, \gamma_q) \in (0,1)$ such that

$$\frac{\partial}{\partial \sigma_q} F|_{\sigma_q=1} \begin{cases} > 0 & \forall \epsilon_c^{-1} < \bar{\epsilon}_c^{-1}(\gamma_q, \triangle_A) \\ = 0 & \forall \epsilon_c^{-1} = \bar{\epsilon}_c^{-1}(\gamma_q, \triangle_A) \\ < 0 & \forall \epsilon_c^{-1} \in (\bar{\epsilon}_c^{-1}(\gamma_q, \triangle_A), 1) \end{cases}$$

Finally,

$$F \approx 0 + \frac{\partial}{\partial \sigma_q} F|_{\sigma_q=1} \times (\sigma_q - 1)$$

When either $\gamma_q > \bar{\gamma}_q(\triangle_A)$ or $[\gamma_q \leq \bar{\gamma}_q(\triangle_A)] \wedge [\epsilon_c^{-1} \in (\bar{\epsilon}_c^{-1}(\gamma_q, \triangle_A), 1)]$, $\frac{\partial}{\partial \sigma_q} F|_{\sigma_q=1} < 0$, and thus F is bigger than 0 if and only if $\sigma_q < 1$ up to the first-order approximation. $\square$

A.8 Proof for Proposition: Comparative statics of risk aversion and volatility

Proposition 3. *Up to the first-order approximation around $\sigma_q = 1$, when inputs are complements ($\sigma_q < 1$),*

1. *an increase in the degree of risk aversion leads to more allocation of capital towards sector* 1

$$\frac{\partial \frac{\partial \mathbf{E}\{U(C)\}}{\partial K_1}|_{K_1=K_1^{ss}}}{\partial \epsilon_c^{-1}} > 0 \ \ \forall \epsilon_c^{-1} \geq 0$$

2. *when $\epsilon_c^{-1} \geq 1$, an increase in sector 1's volatility certainly increases the preallocation of capital towards the it.*

$$\frac{\partial \frac{\partial \mathbf{E}\{U(C)\}}{\partial K_1}|_{K_1=K_1^{ss}}}{\partial \triangle_A} > 0$$

Proof. We prove two statements in two separate parts.

Statement 1 Our target is to prove that the following derivative is positive up to the first-order approximation around $\sigma_q = 1$.

$$\begin{aligned}\frac{\partial \frac{\partial \mathbf{E}\{U(C)\}}{\partial K_1}|_{K_1=K_1^{ss}}}{\partial \epsilon_c^{-1}} = &\log\left(\gamma_q^{\sigma_q} + (1-\gamma_q)^{\sigma_q}\right)^{\epsilon_c^{-1}} \left[\gamma_q^{\sigma_q} + (1-\gamma_q)^{\sigma_q}\right]^{\epsilon_c^{-1}} F \\ &+ \left[\gamma_q^{\sigma_q} + (1-\gamma_q)^{\sigma_q}\right]^{\epsilon_c^{-1}} \frac{\partial F}{\partial \epsilon_c^{-1}}\end{aligned}$$

where F is the objective function we define in proposition 3

$$F = p_1 \frac{\left(A_L^{1-\frac{1}{\sigma_q}} - 1\right)}{\left(A_L^{1-\frac{1}{\sigma_q}} (1-\gamma_q)^{\sigma_q} + \gamma_q^{\sigma_q}\right)^{\frac{\epsilon_c^{-1}\sigma_q - 1}{\sigma_q - 1}}} + (1-p_1) \frac{\left(A_H^{1-\frac{1}{\sigma_q}} - 1\right)}{\left(A_H^{1-\frac{1}{\sigma_q}} (1-\gamma_q)^{\sigma_q} + \gamma_q^{\sigma_q}\right)^{\frac{\epsilon_c^{-1}\sigma_q - 1}{\sigma_q - 1}}}$$

Since the mapping $x \mapsto x^y$ is decreasing in y when $x \in (0,1)$, $x^y + (1-x)^y > x + (1-x) = 1$. Then, $\log\left(\gamma_q^{\sigma_q} + (1-\gamma_q)^{\sigma_q}\right)^{\epsilon_c^{-1}} \left[\gamma_q^{\sigma_q} + (1-\gamma_q)^{\sigma_q}\right]^{\epsilon_c^{-1}} > 0$ and $\left[\gamma_q^{\sigma_q} + (1-\gamma_q)^{\sigma_q}\right]^{\epsilon_c^{-1}} \geq 0$ for any value of $\sigma_q \geq 0$. It's therefore sufficient to pin down the sign of F and $\frac{\partial F}{\partial \epsilon_c^{-1}}$ up to the first order approximation.

Based on the proof in proposition 3, the proof for F follows. For $\frac{\partial F}{\partial \epsilon_c^{-1}}$,

$$\begin{aligned}
\frac{\partial F}{\partial \epsilon_c^{-1}} &\approx \underbrace{\lim_{\sigma_q \to 1} \frac{\partial F}{\partial \epsilon_c^{-1}}}_{=0} + \left(\lim_{\sigma_q \to 1} \frac{\partial}{\partial \sigma_q} \frac{\partial F}{\partial \epsilon_c^{-1}}\right)(\sigma_q - 1) \\
&= \underbrace{\lim_{\sigma_q \to 1} \frac{\partial F}{\partial \epsilon_c^{-1}}}_{=0} + \left(\lim_{\sigma_q \to 1} \frac{\partial}{\partial \epsilon_c^{-1}} \frac{\partial F}{\partial \sigma_q}\right)(\sigma_q - 1) \quad \text{(Young's Theorem)} \\
&= \underbrace{\lim_{\sigma_q \to 1} \frac{\partial F}{\partial \epsilon_c^{-1}}}_{=0} + \left[\frac{\partial}{\partial \epsilon_c^{-1}} \left(\lim_{\sigma_q \to 1} \frac{\partial F}{\partial \sigma_q}\right)\right](\sigma_q - 1)
\end{aligned}$$

where Young's theorem and the exchange between limits and derivative hold because F is continuously differentiable in ϵ_c^{-1} and at $\sigma_q = 1$, and $\frac{\partial F}{\partial \sigma_q}$ as well as $\frac{\partial}{\partial \epsilon_c^{-1}} \frac{\partial F}{\partial \sigma_q}$ are continuous at $\sigma_q = 1$. As long as $\frac{\partial}{\partial \epsilon_c^{-1}} \left(\lim_{\sigma_q \to 1} \frac{\partial F}{\partial \sigma_q}\right) < 0$, our ideal results are established.

By defining

$$H = \gamma_q \log(\gamma_q) + (1-\gamma_q)\log(1-\gamma_q)$$

and

$$\begin{aligned}
\Lambda^+ &= -H - \log(1+\triangle_A)(1-\gamma_q) \\
&< -H - \log(1-\triangle_A)(1-\gamma_q) > 0 \\
&\equiv \Lambda^-
\end{aligned}$$

We can rewrite the derivative (defined in the proof for proposition) compactly as

$$\frac{\partial}{\partial \epsilon_c^{-1}} \left(\lim_{\sigma_q \to 1} \frac{\partial F}{\partial \sigma_q}\right) = e^{\Lambda^-(\epsilon_c^{-1}-1)} \underbrace{\left[\Lambda^- \log(1-\triangle_A) + \Lambda^+ \log(1+\triangle_A) e^{(\Lambda^+ - \Lambda^-)(\epsilon_c^{-1}-1)}\right]}_{(*)}$$

If $\Lambda^+ < 0$, then the derivative is trivially negative. If $\Lambda^+ > 0$, we then finish the proof in two general steps

1. The function in the bracket is strictly decreasing in ϵ_c^{-1}

2. The function in the bracket has maximum 0 at $\epsilon_c^{-1} = 0$

Firstly,

$$\frac{\partial(*)}{\partial \epsilon_c^{-1}} = (\underbrace{\Lambda^+ - \Lambda^-}_{<0}) \Lambda^+ \log(1 + \triangle_A) e^{(\Lambda^+ - \Lambda^-)(\epsilon_c^{-1} - 1)} < 0$$

Secondly, it's sufficient to show

$$\Lambda^- \log(1 - \triangle_A) + \Lambda^+ \log(1 + \triangle_A) e^{-(\Lambda^+ - \Lambda^-)} < 0$$
$$e^{(\Lambda^- - \Lambda^+)} \frac{\Lambda^+ \log(1 + \triangle_A)}{\Lambda^- (-\log(1 - \triangle_A))} < 1$$

where

$$\Lambda^- - \Lambda^+ = (1 - \gamma_q) \left[-\log(1 - \triangle_A) + \log(1 + \triangle_A) \right]$$

and

$$\log(\Lambda^-) - \log(\Lambda^+) < \Lambda^- - \Lambda^+$$

The key is to notice that the left-hand-side (LHS) of the ideal inequality is strictly monotone in H and in $1 - \gamma_q$.

1. Holding $(1 - \gamma_q)$ fixed, $-H \uparrow$ leads to higher LHS, so LHS is maximized, given any γ_q, at $-H = -\log(0.5) = \log(2) < 1$

2. Holding $-H$ fixed, the derivative with respect to $(1 - \gamma_q)$ is

$$\frac{\partial(*)}{\partial 1 - \gamma_q} = \underbrace{constant}_{<0} + \frac{-\log(1 + \triangle_A)}{\Lambda^+} - \frac{-\log(1 - \triangle_A)}{\Lambda^-} + \log(\frac{1 + \triangle_A}{1 - \triangle_A})$$
$$< \frac{-\log(1 + \triangle_A)}{\Lambda^+} - \frac{-\log(1 - \triangle_A)}{\Lambda^-} + \log(\frac{1 + \triangle_A}{1 - \triangle_A})$$

Let

$$\tilde{F} \equiv \frac{\log(1 + \triangle_A)}{\Lambda^+} + \frac{-\log(1 - \triangle_A)}{\Lambda^-}$$

Then, because of Jensen's inequality,

$$\frac{\tilde{F}}{\log(1+\triangle_A)-\log(1-\triangle_A)} = \frac{\log(1+\triangle_A)}{\log(1+\triangle_A)-\log(1-\triangle_A)}\frac{1}{\Lambda^+} + \left(1-\frac{\log(1+\triangle_A)}{\log(1+\triangle_A)-\log(1-\triangle_A)}\right)$$
$$> \frac{1}{\frac{\log(1+\triangle_A)}{\log(1+\triangle_A)-\log(1-\triangle_A)}\Lambda^+ + \left(1-\frac{\log(1+\triangle_A)}{\log(1+\triangle_A)-\log(1-\triangle_A)}\right)\Lambda^-}$$

Therefore,

$$\tilde{F} > \frac{[\log(1+\triangle_A)-\log(1-\triangle_A)]^2}{\log(1+\triangle_A)\Lambda^+ + (-\log(1+\triangle_A))\Lambda^-}$$

where

$$\begin{aligned}
&\log(1+\triangle_A)\Lambda^+ + (-\log(1-\triangle_A))\Lambda^- \\
&= -H\left[\log(1+\triangle_A)-\log(1-\triangle_A)\right] - \log(1+\triangle_A)^2(1-\gamma_q) + \log(1-\triangle_A)^2(1-\gamma_q) \\
&= -H\left[\log(1+\triangle_A)-\log(1-\triangle_A)\right] + (1-\gamma_q)\left(\frac{\log(1-\triangle_A)^2}{\log(1+\triangle_A)^2}-1\right) \\
&< -H\left[\log(1+\triangle_A)-\log(1-\triangle_A)\right] \\
&< \log(1+\triangle_A)-\log(1-\triangle_A)
\end{aligned}$$

So

$$\tilde{F} > \log(1+\triangle_A)-\log(1-\triangle_A)$$

Based on this inequality, we can find a strict upper bound on the derivative of $(*)$.

$$\frac{\partial(*)}{\partial 1-\gamma_q} < \left(\log(\frac{1+\triangle_A}{1-\triangle_A}) - F\right) < 0$$

Therefore, the remaining function is maximized at $1-\gamma_q$

$$\frac{\log(1+\triangle_A)}{-\log(1-\triangle_A)}\frac{-H}{-H} < 1$$
$$\log(1+\triangle_A)+\log(1-\triangle_A) < 0$$

The bracket is thus maximized at $\epsilon_c^{-1} = 0$.

So, $\max_{\epsilon_c^{-1}\geq 0}(*) < 0$. Since $e^{\Lambda^-(\epsilon_c^{-1}-1)} > 0$, then $\frac{\partial}{\partial \epsilon_c^{-1}}\left(\lim_{\sigma_q\to 1}\frac{\partial \tilde{F}}{\partial \sigma_q}\right) < 0$ and $\frac{\partial \tilde{F}}{\partial \epsilon_c^{-1}} > 0$.

Finally,

$$\frac{\partial \frac{\partial \mathbf{E}\{U(C)\}}{\partial K_1}|_{K_1=K_1^{ss}}}{\partial \epsilon_c^{-1}} = \underbrace{\log\left(\gamma_q^{\sigma_q} + (1-\gamma_q)^{\sigma_q}\right)^{\epsilon_c^{-1}} \left[\gamma_q^{\sigma_q} + (1-\gamma_q)^{\sigma_q}\right]^{\epsilon_c^{-1}}}_{>0} \underbrace{\tilde{F}}_{>0 \text{ up to first-order approximation}}$$
$$+ \underbrace{\left[\gamma_q^{\sigma_q} + (1-\gamma_q)^{\sigma_q}\right]^{\epsilon_c^{-1}}}_{>0} \underbrace{\frac{\partial \tilde{F}}{\partial \epsilon_c^{-1}}}_{>0 \text{ up to first-order approximation}}$$

Our ideal result is achieved.

Statement 2 Following the same logic in proving statement 1, because $\frac{\partial F}{\partial \sigma_q}$ and $\frac{\partial^2 F}{\partial \sigma \partial \triangle_A}$ are jointly continuous at $\sigma_q = 1$ (the following expressing can be double-checked by firstly calculate the derivative and then take first-order approximation around $\sigma_q = 1$).

$$\frac{\partial F}{\partial \triangle_A} = \underbrace{\lim_{\sigma_q \to 1} \frac{\partial F}{\partial \triangle_A}}_{=0} + \left[\frac{\partial}{\partial \triangle_A}\left(\lim_{\sigma_q \to 1} \frac{\partial F}{\partial \sigma_q}\right)\right](\sigma_q - 1)$$

It's sufficient to discuss the sign of $\frac{\partial}{\partial \triangle_A}\left(\lim_{\sigma_q \to 1} \frac{\partial F}{\partial \sigma_q}\right)$. Again, based on previous calculation,

$$\begin{aligned}
&\frac{\partial}{\partial \triangle_A}\left(\lim_{\sigma_q \to 1} \frac{\partial F}{\partial \sigma_q}\right) \\
&= D\left\{\left[(1+\triangle_A)^{(1-\epsilon^{-1})(1-\gamma)-1} - (1-\triangle_A)^{(1-\epsilon^{-1})(1-\gamma)-1}\right]\right. \\
&\left.+(1-\gamma)(1-\epsilon^{-1})\left[(1+\triangle_A)^{(1-\epsilon^{-1})(1-\gamma)-1}\log(1+\triangle_A) - (1-\triangle_A)^{(1-\epsilon^{-1})(1-\gamma)-1}\log(1-\triangle_A)\right]\right\}
\end{aligned}$$

where

$$D = \exp\left(\frac{\log(\gamma)\gamma + \log(1-\gamma)(1-\gamma)}{(\epsilon^{-1}-1)^{-1}}\right) > 0$$

Therefore, when $\epsilon^{-1} \geq 1$,

$$(1+\triangle_A)^{(1-\epsilon^{-1})(1-\gamma)-1} - (1-\triangle_A)^{(1-\epsilon^{-1})(1-\gamma)-1} < 0$$

$$(1-\epsilon^{-1})\left[(1+\triangle_A)^{(1-\epsilon^{-1})(1-\gamma)-1}\log(1+\triangle_A) - (1-\triangle_A)^{(1-\epsilon^{-1})(1-\gamma)-1}\log(1-\triangle_A)\right] < 0$$

So $\lim_{\sigma_q \to 1} \frac{\partial \left[\frac{\partial(\partial \mathbf{E}\{U(C)\}/\partial K_1|_{K_1^{ss}})}{\partial \triangle_A} \right]}{\partial \sigma_q} < 0.$

Then, based on the first-order approximation around $\sigma_q = 1$, $\epsilon^{-1} \geq 1$ is sufficient to ensure that when $\sigma_q < 1$, $\frac{\partial(\partial \mathbf{E}\{U(C)\}/\partial K_1|_{K_1^{ss}})}{\partial \triangle_A} > 0$.

□

B First-order conditions and auxiliary results regarding the full model

In this appendix, we derive the first-order conditions of the full model. We also provide some additional results

The Lagrangian of the planner is:

$$\begin{aligned}\mathcal{L} = \mathbb{E}_0 \sum_{t=0}^{\infty} \beta^t \Bigg\{ & \frac{1}{1-\epsilon_c^{-1}} \left(C_t - \theta \frac{L_t^{1+\epsilon_l^{-1}}}{1+\epsilon_l^{-1}} \right)^{1-\epsilon_c^{-1}} \\ & + \sum_{j=1}^{N} P_{jt}^{\mathrm{k}} \left[I_{jt} + (1-\delta_j) K_{jt} - \Phi_{jt} - K_{jt+1} \right] \\ & + \sum_{j=1}^{N} P_{jt} \left[Q_{jt} - C_{jt} - \sum_{i=1}^{N} \left[M_{jit} + I_{jit} \right] \right] \Bigg\},\end{aligned}$$

where

$$
\begin{aligned}
C_t &= \left(\sum_{j=1}^{N} \xi_j^{\sigma_c^{-1}} (C_{jt})^{1-\sigma_c^{-1}} \right)^{\frac{1}{1-\sigma_c^{-1}}}, \\
L_t &= \left(\sum_{j=1}^{N} (L_{jt})^{1+\sigma_l^{-1}} \right)^{\frac{1}{1+\sigma_l^{-1}}}, \\
Q_{jt} &= \left[(\mu_j)^{\sigma_q^{-1}} (Y_{jt})^{1-\sigma_q^{-1}} + (1-\mu_j)^{\sigma_q^{-1}} (M_{jt})^{1-\sigma_q^{-1}} \right]^{\frac{1}{1-\sigma_q^{-1}}}, \\
Y_{jt} &= A_{jt} \left[(\alpha_j)^{\sigma_q^{-1}} (K_{jt})^{1-\sigma_y^{-1}} + (1-\alpha_j)^{\sigma_y^{-1}} (L_{jt})^{1-\sigma_y^{-1}} \right]^{\frac{1}{1-\sigma_y^{-1}}}, \\
I_{jt} &= \left(\sum_{i=1}^{N} \left(\gamma_{ij}^{I} \right)^{\sigma_I^{-1}} (I_{ijt})^{1-\sigma_I^{-1}} \right)^{\frac{1}{1-\sigma_I^{-1}}}, \\
M_{jt} &= \left(\sum_{i=1}^{N} \left(\gamma_{ij}^{m} \right)^{\sigma_m^{-1}} (M_{ijt})^{1-\sigma_m^{-1}} \right)^{\frac{1}{1-\sigma_m^{-1}}}, \\
\Phi_{jt} &= \frac{\phi}{2} \left(\frac{I_{jt}}{K_{jt}} - \delta_j \right)^2 K_{jt}.
\end{aligned}
$$

We will start by writing down all the derivatives of the CES aggregators and the adjustment cost function. See sub-appendix B.11 to see the details of the CES algebra involved:

$$
\begin{aligned}
\frac{\partial C_t}{\partial C_{jt}} &= \left(\xi_j \frac{C_t}{C_{jt}} \right)^{\sigma_c^{-1}} & \frac{\partial L_t}{\partial L_{jt}} &= \left(\frac{L_{jt}}{L_t} \right)^{\sigma_l^{-1}} \\
\frac{\partial Q_{jt}}{\partial Y_{jt}} &= \left(\mu_j \frac{Q_{jt}}{Y_{jt}} \right)^{\sigma_q^{-1}} & \frac{\partial Q_{jt}}{\partial M_{jt}} &= \left((1-\mu_j) \frac{Q_{jt}}{M_{jt}} \right)^{\sigma_q^{-1}} \\
\frac{\partial Y_{jt}}{\partial K_{jt}} &= A_{jt}^{1-\sigma_y^{-1}} \left(\alpha_j \frac{Y_{jt}}{K_{jt}} \right)^{\sigma_y^{-1}} & \frac{\partial Y_{jt}}{\partial L_{jt}} &= A_{jt}^{1-\sigma_y^{-1}} \left((1-\alpha_j) \frac{Y_{jt}}{L_{jt}} \right)^{\sigma_y^{-1}} \\
\frac{\partial M_{jt}}{\partial M_{ijt}} &= \left(\gamma_{ij}^{M} \frac{M_{jt}}{M_{ijt}} \right)^{\sigma_m^{-1}} & \frac{\partial I_{jt}}{\partial I_{ijt}} &= \left(\gamma_{ij}^{I} \frac{I_{jt}}{I_{ijt}} \right)^{\sigma_I^{-1}} \\
\frac{\partial \Phi_{jt}}{\partial I_{jt}} &= \phi \left(\frac{I_{jt}}{K_{jt}} - \delta_j \right) & \frac{\partial \Phi_{jt}}{\partial K_{jt}} &= -\frac{\phi}{2} \left(\frac{I_{jt}^2}{K_{jt}^2} - \delta_j^2 \right).
\end{aligned}
$$

B.1 FOC for consumption

We start with

$$\frac{\partial \mathcal{L}}{\partial C_{jt}} = \beta^t \left(\left(C_t - \theta \frac{L_t^{1+\epsilon_l^{-1}}}{1+\epsilon_l^{-1}} \right)^{-\epsilon_c^{-1}} \frac{\partial C_t}{\partial C_{jt}} - P_{jt} \right) = 0.$$

Next, we replace the derivatives:

$$\left(C_t - \theta \frac{L_t^{1+\epsilon_l^{-1}}}{1+\epsilon_l^{-1}} \right)^{-\epsilon_c^{-1}} \frac{\partial C_t}{\partial C_{jt}} = P_{jt},$$
$$\left(C_t - \theta \frac{L_t^{1+\epsilon_l^{-1}}}{1+\epsilon_l^{-1}} \right)^{-\epsilon_c^{-1}} \left(\xi_j \frac{C_t}{C_{jt}} \right)^{\sigma_c^{-1}} = P_{jt}.$$

B.2 FOC for labor

We start with

$$\frac{\partial \mathcal{L}}{\partial L_{jt}} = \beta^t \left(- \left(C_t - \theta \frac{L_t^{1+\epsilon_l^{-1}}}{1+\epsilon_l^{-1}} \right)^{-\epsilon_c^{-1}} \theta \left(L_t \right)^{\epsilon_l^{-1}} \frac{\partial L_t}{\partial L_{jt}} + P_{jt} \frac{\partial Q_{jt}}{\partial L_{jt}} \right) = 0.$$

Next, we replace the derivatives, using the chain rule when needed:

$$\left(C_t - \theta \frac{L_t^{1+\epsilon_l^{-1}}}{1+\epsilon_l^{-1}} \right)^{-\epsilon_c^{-1}} \theta \left(L_t \right)^{\epsilon_l^{-1}} \frac{\partial L_t}{\partial L_{jt}} = P_{jt} \frac{\partial Q_{jt}}{\partial Y_{jt}} \frac{\partial Y_{jt}}{\partial L_{jt}},$$
$$\left(C_t - \theta \frac{L_t^{1+\epsilon_l^{-1}}}{1+\epsilon_l^{-1}} \right)^{-\epsilon_c^{-1}} \theta \left(L_t \right)^{\epsilon_l^{-1}} \left(\frac{L_{jt}}{L_t} \right)^{\sigma_l^{-1}} = P_{jt} A_{jt}^{1-\sigma_y^{-1}} \left(\mu_j \frac{Q_{jt}}{Y_{jt}} \right)^{\sigma_q^{-1}} \left(\left(1 - \alpha_j \right) \frac{Y_{jt}}{L_{jt}} \right)^{\sigma_y^{-1}}.$$

B.3 FOC with respect to capital in next period

We start with

$$\frac{\partial \mathcal{L}}{\partial K_{jt+1}} = \beta^t \left(-P_{jt}^k\right) + \beta^{t+1} \mathbb{E}_t \left(P_{jt+1}^k \left((1-\delta_j) - \frac{\partial \Phi_{jt+1}}{\partial K_{jt+1}} \right) + P_{jt+1} \frac{\partial Q_{jt+1}}{\partial K_{jt+1}} \right) = 0.$$

Next, we replace the derivatives, using the chain rule when needed:

$$\begin{aligned}
P_{jt}^k &= \beta \mathbb{E}_t \left(P_{jt+1}^k \left((1-\delta_j) - \frac{\partial \Phi_{jt+1}}{\partial K_{jt+1}} \right) + P_{jt+1} \frac{\partial Q_{jt+1}}{\partial Y_{jt+1}} \frac{\partial Y_{jt+1}}{\partial K_{jt+1}} \right), \\
P_{jt}^k &= \beta \mathbb{E}_t \left[P_{jt+1}^k \left((1-\delta_j) + \frac{\phi}{2} \left(\frac{I_{jt+1}^2}{K_{jt+1}^2} - \delta_j^2 \right) \right) \right. \\
&\quad \left. + P_{jt+1} A_{jt+1}^{1-\sigma_y^{-1}} \left(\mu_j \frac{Q_{jt+1}}{Y_{jt+1}} \right)^{\sigma_q^{-1}} \left(\alpha_j \frac{Y_{jt+1}}{K_{jt+1}} \right)^{\sigma_y^{-1}} \right].
\end{aligned}$$

B.4 FOC for intermediates and system reduction

We start with

$$\frac{\partial \mathcal{L}}{\partial M_{ijt}} = \beta^t \left(P_{jt} \frac{\partial Q_{jt}}{\partial M_{ijt}} - P_{it} \right) = 0.$$

Next, we replace the derivatives, using the chain rule when needed:

$$\begin{aligned}
P_{jt} \frac{\partial Q_{jt}}{\partial M_{jt}} \frac{\partial M_{jt}}{\partial M_{ijt}} &= P_{it}, \\
P_{jt} \left((1-\mu_j) \frac{Q_{jt}}{M_{jt}} \right)^{\sigma_q^{-1}} \left(\gamma_{ij}^M \frac{M_{jt}}{M_{ijt}} \right)^{\sigma_m^{-1}} &= P_{it}
\end{aligned}$$

We want to use this FOC to get rid of M_{ijt}. First, we solve for M_{ijt}:

$$M_{ijt} = \left(\frac{P_{jt}}{P_{it}} \right)^{\sigma_m} \left((1-\mu_j) \frac{Q_{jt}}{M_{jt}} \right)^{\frac{\sigma_m}{\sigma_q}} \gamma_{ij}^m M_{jt}$$

We solve for M_{jt} by aggregating from the solution for M_{ijt}. First, we construct the term $\left(\gamma_{ij}^{m}\right)^{\frac{1}{\sigma_m}} M_{ijt}^{1-\sigma_m^{-1}}$ that is inside the aggregator:

$$M_{ijt} = \left(\frac{P_{jt}}{P_{it}}\right)^{\sigma_m} \left((1-\mu_j)\frac{Q_{jt}}{M_{jt}}\right)^{\frac{\sigma_m}{\sigma_q}} \gamma_{ij}^{m} M_{jt},$$

$$\left(\gamma_{ij}^{m}\right)^{\frac{1}{\sigma_m}} M_{ijt}^{1-\sigma_m^{-1}} = \left(\gamma_{ij}^{m}\right)^{\frac{1}{\sigma_m}} \left(\frac{P_{it}}{P_{jt}}\right)^{1-\sigma_m} \left((1-\mu_j)\frac{Q_{jt}}{M_{jt}}\right)^{\frac{\sigma_m-1}{\sigma_q}} \left(\gamma_{ij}^{m} M_{jt}\right)^{1-\sigma_m^{-1}},$$

$$\left(\gamma_{ij}^{m}\right)^{\frac{1}{\sigma_m}} M_{ijt}^{1-\sigma_m^{-1}} = \gamma_{ij}^{m} \left(\frac{P_{it}}{P_{jt}}\right)^{1-\sigma_m} \left((1-\mu_j)\frac{Q_{jt}}{M_{jt}}\right)^{\frac{\sigma_m-1}{\sigma_q}} \left(M_{jt}\right)^{1-\sigma_m^{-1}}.$$

Next, we sum over all the goods in the aggregator:

$$\sum_{i=1}^{N} \left(\gamma_{ij}^{m}\right)^{\frac{1}{\sigma_m}} M_{ijt}^{1-\sigma_m^{-1}} = \sum_{i=1}^{N} \gamma_{ij}^{m} \left(\frac{P_{it}}{P_{jt}}\right)^{1-\sigma_m} \left((1-\mu_j)\frac{Q_{jt}}{M_{jt}}\right)^{\frac{\sigma_m-1}{\sigma_q}} M_{jt}^{1-\sigma_m^{-1}},$$

$$M_{jt}^{1-\sigma_m^{-1}} = \left(P_{jt}\right)^{\sigma_m-1} \left((1-\mu_j)\frac{Q_{jt}}{M_{jt}}\right)^{\frac{\sigma_m-1}{\sigma_q}} M_{jt}^{1-\sigma_m^{-1}} \sum_{i=1}^{N} \gamma_{ij}^{m} \left(P_{it}\right)^{1-\sigma_m},$$

$$M_{jt}^{\frac{\sigma_m-1}{\sigma_q}} = \left(\left(1-\mu_j\right) Q_{jt}\right)^{\frac{\sigma_m-1}{\sigma_q}} \left(P_{jt}\right)^{\sigma_m-1} \sum_{i=1}^{N} \left(\gamma_{ij}^{m}\right) \left(P_{it}\right)^{1-\sigma_m},$$

$$M_{jt} = \left(\left(1-\mu_j\right) Q_{jt}\right) P_{jt}^{\sigma_q} \left(\sum_{i=1}^{N} \left(\gamma_{ij}^{m}\right) \left(P_{it}\right)^{1-\sigma_m}\right)^{\frac{\sigma_q}{\sigma_m-1}}.$$

Following the CES algebra in sub-appendix B.11, we define the price index for the M_{jt} bundle as:

$$P_{jt}^{m} = \left(\sum_{i=1}^{N} \left(\gamma_{ij}^{m}\right) \left(P_{it}\right)^{1-\sigma_m}\right)^{\frac{1}{1-\sigma_m}}.$$

so we can write the FOC for M_{jt} as:

$$M_{jt} = \left(1-\mu_j\right) \left(\frac{P_{jt}^{m}}{P_{jt}}\right)^{-\sigma_q} Q_{jt}.$$

We can use this expression for M_{jt} to simplify our solution for M_{ijt}:

$$\begin{aligned}
M_{ijt} &= \left(\frac{P_{it}}{P_{jt}}\right)^{-\sigma_m} \left((1-\mu_j)\frac{Q_{jt}}{M_{jt}}\right)^{\frac{\sigma_m}{\sigma_q}} \gamma_{ij}^m M_{jt}, \\
&= \left(\frac{P_{it}}{P_{jt}}\right)^{-\sigma_m} \left((1-\mu_j)\frac{Q_{jt}}{(1-\mu_j)\left(\frac{P_{jt}^m}{P_{jt}}\right)^{-\sigma_q} Q_{jt}}\right)^{\frac{\sigma_m}{\sigma_q}} \gamma_{ij}^m M_{jt}, \\
&= \gamma_{ij}^m \left(\frac{P_{it}}{P_{jt}^m}\right)^{-\sigma_m} M_{jt}.
\end{aligned}$$

Finally, using this solution for M_{ijt}, we can calculate the supply of intermediate goods of each sector, which we denote $M_{jt}^{out} = \sum_{i=1}^N M_{jit}$:

$$M_{jt}^{out} = \sum_{i=1}^N M_{jit} = \sum_{i=1}^N \gamma_{ji}^m \left(\frac{P_{jt}}{P_{it}^m}\right)^{-\sigma_m} M_{it}.$$

B.5 FOC for investment and system reduction

We start with

$$\frac{\partial \mathcal{L}}{\partial I_{ijt}} = \beta^t \left(P_{jt}^k \left(\frac{\partial I_{jt}}{\partial I_{ijt}} - \frac{\partial \Phi_{jt}}{\partial I_{ijt}}\right) - P_{it}\right) = 0.$$

Next, we replace the derivatives, using the chain rule when needed:

$$\begin{aligned}
P_{jt}^k \left(\frac{\partial I_{jt}}{\partial I_{ijt}} - \frac{\partial \Phi_{jt}}{\partial I_{jt}}\frac{\partial I_{jt}}{\partial I_{ijt}}\right) &= P_{it}, \\
P_{jt}^k \frac{\partial I_{jt}}{\partial I_{ijt}}\left(1 - \frac{\partial \Phi_{jt}}{\partial I_{jt}}\right) &= P_{it}, \\
P_{jt}^k \left(\gamma_{ij}^I \frac{I_{jt}}{I_{ijt}}\right)^{\sigma_I^{-1}} \left(1 - \phi\left(\frac{I_{jt}}{K_{jt}} - \delta_j\right)\right) &= P_{it}.
\end{aligned}$$

We want to use this FOC to eliminate I_{ijt}. First, we solve for I_{ijt}:

$$I_{ijt} = \gamma_{ij}^{I} \left(\frac{P_{it}}{P_{jt}^{k}} \right)^{-\sigma_I} I_{jt} \left(1 - \phi \left(\frac{I_{jt}}{K_{jt}} - \delta_j \right) \right)^{\sigma_I}.$$

We solve for I_{jt} by aggregating up from the solution for I_{ijt}

$$\begin{aligned}
I_{ijt} &= \gamma_{ij}^{I} \left(\frac{P_{it}}{P_{jt}^{k}} \right)^{-\sigma_I} I_{jt} \left(1 - \phi \left(\frac{I_{jt}}{K_{jt}} - \delta_j \right) \right)^{\sigma_I}, \\
\left(\gamma_{ij}^{I} \right)^{\sigma_I^{-1}} I_{ijt}^{1-\sigma_I^{-1}} &= \left(\gamma_{ij}^{I} \right)^{\sigma_I^{-1}} \left(\frac{P_{it}}{P_{jt}^{k}} \right)^{1-\sigma_I} \left(\gamma_{ij}^{I} I_{jt} \right)^{1-\sigma_I^{-1}} \left(1 - \phi \left(\frac{I_{jt}}{K_{jt}} - \delta_j \right) \right)^{\sigma_I - 1}, \\
I_{jt}^{1-\sigma_I^{-1}} &= \sum_{i=1}^{N} \left(\gamma_{ij}^{I} \right) \left(\frac{P_{it}}{P_{jt}^{k}} \right)^{1-\sigma_I} \left(I_{jt} \right)^{1-\sigma_I^{-1}} \left(1 - \phi \left(\frac{I_{jt}}{K_{jt}} - \delta_j \right) \right)^{\sigma_I - 1}. \\
1 &= \left(P_{jt}^{k} \right)^{\sigma_I - 1} \left(1 - \phi \left(\frac{I_{jt}}{K_{jt}} - \delta_j \right) \right)^{\sigma_I - 1} \sum_{i=1}^{N} \left(\gamma_{ij}^{I} \right) \left(P_{it} \right)^{1-\sigma_I}, \\
P_{jt}^{k} &= \left(1 - \phi \left(\frac{I_{jt}}{K_{jt}} - \delta_j \right) \right)^{-1} \left(\sum_{i=1}^{N} \left(\gamma_{ij}^{I} \right) \left(P_{it} \right)^{1-\sigma_I} \right)^{\frac{1}{1-\sigma_I}}.
\end{aligned}$$

We define the frictionless price index of capital goods as

$$\tilde{P}_{jt}^{k} = \left(\sum_{i=1}^{N} \left(\gamma_{ij}^{I} \right) \left(P_{it} \right)^{1-\sigma_I} \right)^{\frac{1}{1-\sigma_I}}.$$

Then, we can write the FOC for I_{jt} as

$$P_{jt}^{k} = \tilde{P}_{jt}^{k} \left(1 - \phi \left(\frac{I_{jt}}{K_{jt}} - \delta_j \right) \right)^{-1}.$$

Next, we calculate the amount of goods of a sector that goes to other sectors as investment goods. We define

$$I_{jt}^{out} = \sum_{i=1}^{N} I_{jit}.$$

Using the FOC for I_{ijt}, we have

$$I_{jt}^{out} = \sum_{i=1}^{N} \gamma_{ji}^{I} \left(\frac{P_{jt}}{P_{it}^{k}} \right)^{-\sigma_I} I_{it} \left(1 - \phi \left(\frac{I_{it}}{K_{it}} - \delta_i \right) \right)^{\sigma_I}.$$

B.6 Full system of equations

The full system we get is:

$$
\begin{aligned}
\log A_{jt+1} &= \rho_j \log A_{jt} + \varepsilon^A_{jt+1}, \\
K_{jt+1} &= (1-\delta_j)K_{jt} + I_{jt} - \frac{\phi}{2}\left(\frac{I_{jt}}{K_{jt}} - \delta_j\right)^2 K_{jt}, \\
P_{jt} &= \left(C_t - \theta \frac{L_t^{1+\epsilon_l^{-1}}}{1+\epsilon_l^{-1}}\right)^{-\epsilon_c^{-1}} \left(\xi_j \frac{C_t}{C_{jt}}\right)^{\sigma_c^{-1}}, \\
\frac{\theta\left(L_t\right)^{\epsilon_l^{-1}}\left(\frac{L_{jt}}{L_t}\right)^{\sigma_l^{-1}}}{\left(C_t - \theta \frac{L_t^{1+\epsilon_l^{-1}}}{1+\epsilon_l^{-1}}\right)^{\epsilon_c^{-1}}} &= P_{jt} A_{jt}^{1-\sigma_y^{-1}} \left(\mu_j \frac{Q_{jt}}{Y_{jt}}\right)^{\sigma_q^{-1}} \left((1-\alpha_j)\frac{Y_{jt}}{L_{jt}}\right)^{\sigma_y^{-1}}, \\
P^k_{jt} &= \beta \mathbb{E}_t \left[P_{jt+1} A_{jt+1}^{1-\sigma_y^{-1}} \left(\mu_j \frac{Q_{jt+1}}{Y_{jt+1}}\right)^{\sigma_q^{-1}} \left(\alpha_j \frac{Y_{jt+1}}{K_{jt+1}}\right)^{\sigma_y^{-1}} \right], \\
&\quad + P^k_{jt+1}\left((1-\delta_j) + \frac{\phi}{2}\left(\frac{I^2_{jt+1}}{K^2_{jt+1}} - \delta_j^2\right)\right)\Bigg], \\
P^m_{jt} &= \left(\sum_{i=1}^N \left(\gamma^m_{ij}\right)\left(P_{it}\right)^{1-\sigma_m}\right)^{\frac{1}{1-\sigma_m}}, \\
M_{jt} &= (1-\mu_j)\left(\frac{P^m_{jt}}{P_{jt}}\right)^{-\sigma_q} Q_{jt}, \\
M^{out}_{jt} &= \sum_{i=1}^N \gamma^m_{ji}\left(\frac{P_{jt}}{P^m_{it}}\right)^{-\sigma_m} M_{it}, \\
P^k_{jt} &= \left(\sum_{i=1}^N \left(\gamma^I_{ij}\right)\left(P_{it}\right)^{1-\sigma_I}\right)^{\frac{1}{1-\sigma_I}} \left(1 - \phi\left(\frac{I_{jt}}{K_{jt}} - \delta_j\right)\right)^{-1}, \\
I^{out}_{jt} &= \sum_{i=1}^N \gamma^I_{ji}\left(\frac{P_{jt}}{P^k_{it}}\right)^{-\sigma_I} I_{it}\left(1 - \phi\left(\frac{I_{it}}{K_{it}} - \delta_i\right)\right)^{\sigma_I}, \\
Q_{jt} &= C_{jt} + M^{out}_{jt} + I^{out}_{jt}, \\
Q_{jt} &= \left[\left(\mu_j\right)^{\sigma_q^{-1}}\left(Y_{jt}\right)^{1-\sigma_q^{-1}} + \left(1-\mu_j\right)^{\sigma_q^{-1}}\left(M_{jt}\right)^{1-\sigma_q^{-1}}\right]^{\frac{1}{1-\sigma_q^{-1}}}, \\
Y_{jt} &= A_{jt}\left[\left(\alpha_j\right)^{\sigma_y^{-1}}\left(K_{jt}\right)^{1-\sigma_y^{-1}} + \left(1-\alpha_j\right)^{\sigma_y^{-1}}\left(L_{jt}\right)^{1-\sigma_y^{-1}}\right]^{\frac{1}{1-\sigma_y^{-1}}}, \\
C_t &= \left(\sum_{j=1}^N \xi_j^{\frac{1}{\sigma_c}}\left(C_{jt}\right)^{1-\sigma_c^{-1}}\right)^{\frac{1}{1-\sigma_c^{-1}}}, \\
L_t &= \left(\sum_{j=1}^N \left(L_{jt}\right)^{1+\sigma_l^{-1}}\right)^{\frac{1}{1+\sigma_l^{-1}}}.
\end{aligned}
$$

B.7 Welfare

In order to calculate welfare, we can write the intertemporal utility of the representative household as:

$$V_t = \frac{1}{1-\epsilon_c^{-1}} \left(C_t - \theta \frac{L_t^{1+\epsilon_l^{-1}}}{1+\epsilon_l^{-1}} \right)^{1-\epsilon_c^{-1}} + \beta E_t V_{t+1}.$$

Steady state welfare is:

$$\bar{V} = \frac{1}{1-\beta} \frac{1}{1-\epsilon_c^{-1}} \left(\bar{C} - \theta \frac{\bar{L}^{1+\epsilon_l^{-1}}}{1+\epsilon_l^{-1}} \right)^{1-\epsilon_c^{-1}}.$$

Then, in a given period, we can get an interpretable measure of welfare by calculating the fraction of steady-state consumption that you would need to give up to achieve that level of welfare in the steady state. We denote such consumption-equivalent welfare as $\hat{V}_t^c$:

$$V_t = \frac{1}{1-\beta} \frac{1}{1-\epsilon_c^{-1}} \left(\bar{C}(1+\hat{V}_t^c) - \theta \frac{\bar{L}^{1+\epsilon_l^{-1}}}{1+\epsilon_l^{-1}} \right)^{1-\epsilon_c^{-1}}.$$

We can solve analytically for consumption-equivalent welfare $\hat{V}_t^c$:

$$\hat{V}_t^c = \frac{1}{\bar{C}} \left[\left(V_t(1-\beta)(1-\epsilon_c^{-1}) \right)^{\frac{1}{1-\epsilon_c^{-1}}} + \theta \frac{\bar{L}^{1+\epsilon_l^{-1}}}{1+\epsilon_l^{-1}} \right] - 1.$$

We will analyze how $\hat{V}_t^c$ is affected by productivity shocks.

B.8 Vectorizations

In terms of programming, it will be useful to vectorize the equations that involve sums over sectoral variables. We will use variables in bold to denote vectors where each element represents the corresponding sectoral value, and use $*$ to denote element by element multiplication. When we raise a vector to the power of a parameter, we mean

element-to-element exponentiation. Then, we get the following equations:

$$\begin{aligned}
\boldsymbol{P_t^m} &= \left(\Gamma_M^{'} \boldsymbol{P_t}^{1-\sigma_m}\right)^{\frac{1}{1-\sigma_m}}, \\
\boldsymbol{M_t^{out}} &= \boldsymbol{P_t}^{-\sigma_m} * \Gamma_M \left(\boldsymbol{P_t^m}\right)^{\sigma_m} * \boldsymbol{M_t} \\
\boldsymbol{\tilde{P}_t^k} &= \left(\Gamma_I^{'} \boldsymbol{P_t}^{1-\sigma_I}\right)^{\frac{1}{1-\sigma_I}}, \\
\boldsymbol{\tilde{I}_t^{out}} &= \boldsymbol{P_t}^{-\sigma_I} * \Gamma_I \left(\boldsymbol{P_t^k}\right)^{\sigma_I} * \boldsymbol{I_t}.
\end{aligned}$$

B.9 Steady state

There are three dynamic equations in the model:

$$\begin{aligned}
K_{jt+1} &= (1-\delta_j)K_{jt} + I_{jt} - \frac{\phi}{2}\left(\frac{I_{jt}}{K_{jt}} - \delta_j\right)^2 K_{jt}, \\
a_{jt+1} &= \rho_j a_{jt} + \epsilon_{jt}, \\
P_{jt}^k &= \beta \mathbb{E}_t \left[P_{jt+1} A_{jt+1}^{1-\sigma_y^{-1}} \left(\mu_j \frac{Q_{jt+1}}{Y_{jt+1}}\right)^{\sigma_q^{-1}} \left(\alpha_j \frac{Y_{jt+1}}{K_{jt+1}}\right)^{\sigma_y^{-1}} \right. \\
&\qquad \left. + P_{jt+1}^k \left((1-\delta_j) + \frac{\phi}{2}\left(\frac{I_{jt+1}^2}{K_{jt+1}^2} - \delta_j^2\right)\right)\right].
\end{aligned}$$

First, notice that $I_{jt} = \delta_j K_{jt}$ implies $K_{jt+1} = K_{jt}$ and makes the adjustment costs equal to zero. Then, in the steady state we have:

$$\begin{aligned}
\bar{K} &= \bar{I}_j / \delta_j, \\
\bar{P}_j^k &= \frac{\beta}{1-\beta(1-\delta)} \bar{P}_j \left(\mu_j \frac{\bar{Q}_j}{\bar{Y}_j}\right)^{\sigma_q^{-1}} \left(\alpha \frac{\bar{Y}_j}{\bar{K}_j}\right)^{\sigma_y^{-1}}.
\end{aligned}$$

B.10 Intensity shares mapping to expenditure shares

In sub-appendix B.11, we show that for standard CES aggregators, the intensity shares (e.g., ξ_j for consumption bundle or α_j for value-added function) do not correspond to expenditure shares. In the same sub-appendix, we show that how to map expenditures shares to intensity shares once you know the steady state equilibrium variables. We use tilde notation to refer to expenditures, so $\tilde{\xi}_j$ is the consumption share of good j. Then,

for a given steady state equilibrium the relation between the expenditure share in steady state and the intensity share used to calculate the steady state is:

$$\tilde{\xi}_j = \xi_j^{\sigma_c^{-1}} \left(\frac{\bar{C}_j}{\bar{C}} \right)^{1-\sigma_c^{-1}},$$

$$\tilde{\mu}_j = \mu_j^{\sigma_q^{-1}} \left(\frac{\bar{Y}_j}{\bar{Q}_j} \right)^{1-\sigma_q^{-1}},$$

$$\tilde{\alpha}_j = \alpha_j^{\sigma_y^{-1}} \left(\frac{\bar{K}_j}{\bar{Y}_j} \right)^{1-\sigma_y^{-1}},$$

$$\tilde{\gamma}_{ij}^m = \left(\gamma_{ij}^m \right)^{\sigma_m^{-1}} \left(\frac{\bar{M}_{ij}}{\bar{M}_j} \right)^{1-\sigma_m^{-1}},$$

$$\tilde{\gamma}_{ij}^I = \left(\gamma_{ij}^I \right)^{\sigma_I^{-1}} \left(\frac{\bar{I}_{ij}}{\bar{I}_j} \right)^{1-\sigma_I^{-1}}.$$

Since we do not solve explicitly for $\bar{M}_{ij}$ and $\bar{I}_{ij}$ we are going to use the first order conditions to solve for $\bar{M}_{ij}/\bar{M}_j$ and $\bar{I}_{ij}/\bar{I}_j$. We get

$$\tilde{\gamma}_{ij}^m = \gamma_{ij}^m \left(\frac{P_{it}}{P_{jt}^m} \right)^{1-\sigma_m},$$

$$\tilde{\gamma}_{ij}^I = \gamma_{ij}^I \left(\frac{P_{it}}{P_{jt}^k} \right)^{1-\sigma_I}.$$

Given this mapping, a naive approach would be simply to replace the intensity shares with the equations that map the empirical shares with the model shares. Nevertheless, if we use this mapping equations as endogenous equations in the steady state system of equations, the output of each aggregator become indeterminate. To see why, we can replace the mapping in the consumption aggregator and rearrange to obtain:

$$C_t = \bar{C} \left(\sum_{j=1}^{N} \tilde{\xi}_j \left(\frac{C_{jt}}{\bar{C}_j} \right)^{1-\sigma_c^{-1}} \right)^{\frac{1}{1-\sigma_c^{-1}}}.$$

This equation for aggregate C cannot be used in steady state, since if we replace the time

t values for steady-state values we get a tautology ($\bar{C} = \bar{C}$). Given this, the correct approach is to include in the steady state system the difference between the model-implied expenditure shares as additional expressions to minimize.

B.11 CES algebra

The objective of this appendix is to obtain a mapping between the intensity shares (the primitive parameters that appear in the CES aggregator) and the expenditure shares (input expenditure/aggregate expenditure). We start with the common CES aggregator:

$$X = A\left(\sum_{j=1}^{N} \xi_j^{\sigma_x^{-1}} X_j^{1-\sigma_x^{-1}}\right)^{\frac{1}{1-\sigma_x^{-1}}}.$$

where A is a constant (e.g., TFP in the value added aggregator). The derivative is:

$$\begin{aligned}
\frac{\partial X}{\partial X_j} &= \frac{A}{1-\sigma_x^{-1}}\left(\sum_{j=1}^{N} \xi_j^{\sigma_x^{-1}} (X_j)^{1-\sigma_x^{-1}}\right)^{\frac{\sigma_x^{-1}}{1-\sigma_x^{-1}}} \left(\xi_j^{\sigma_x^{-1}}\left(1-\sigma_x^{-1}\right)(X_j)^{-\sigma_x^{-1}}\right), \\
&= \frac{A}{A^{\sigma_x^{-1}}} A^{\sigma_x^{-1}}\left(\sum_{j=1}^{N} \xi_j^{\sigma_q^{-1}} (X_j)^{1-\sigma_x^{-1}}\right)^{\frac{\sigma_x^{-1}}{1-\sigma_x^{-1}}} \xi_j^{\sigma_x^{-1}} (X_j)^{-\sigma_x^{-1}}, \\
&= A^{1-\sigma_x^{-1}}\left(A\left(\sum_{j=1}^{N} \xi_j^{\sigma_x^{-1}} (X_j)^{1-\sigma_x^{-1}}\right)^{\frac{1}{1-\sigma_x^{-1}}}\right)^{\sigma_x^{-1}} \xi_j^{\sigma_x^{-1}} (X_j)^{-\sigma_x^{-1}}.
\end{aligned}$$

Notice that we can now plug the definition of the aggregator. We get:

$$\begin{aligned}
\frac{\partial X_t}{\partial X_{jt}} &= A^{1-\sigma_x^{-1}} X^{\sigma_x^{-1}} \xi_j^{\sigma_x^{-1}} (X_j)^{-\sigma_x^{-1}}, \\
&= A^{1-\sigma_x^{-1}}\left(\xi_j \frac{X}{X_j}\right)^{\sigma_x^{-1}}
\end{aligned}$$

From this first-order condition, we are going to get a price aggregator. We start from the

budget constraint:

$$\sum_{j=1}^{N} P_j X_j = Y_j.$$

where Y_{jt} represents income. The optimization problem is

$$\max_{\{X_j\}_{j=1}^{N}} X \quad \text{s.t.} \quad \sum_{j=1}^{N} P_j X_j = Y_j,$$

The first-order conditions with respect to X_{jt} are:

$$\frac{\partial X}{\partial X_j} - \lambda P_j = 0.$$

So, for al goods $i \neq j$, we have:

$$\frac{\partial X}{\partial X_j}\frac{1}{P_j} = \frac{\partial X}{\partial X_i}\frac{1}{P_i},$$

$$A^{1-\sigma_x^{-1}} \left(\xi_j \frac{X}{X_j}\right)^{\sigma_x^{-1}} \frac{1}{P_j} = A^{1-\sigma_x^{-1}} \left(\xi_i \frac{X}{X_i}\right)^{\sigma_x^{-1}} \frac{1}{P_i},$$

and we get

$$X_j = \left(\frac{P_i}{P_j}\right)^{\sigma_x} \frac{\xi_j}{\xi_i} X_i.$$

Let's replace that into the aggregator:

$$\begin{aligned} X &= A \left(\sum_{j=1}^{N} \xi_j^{\sigma_x^{-1}} \left(\left(\frac{P_i}{P_j}\right)^{\sigma_x} \frac{\xi_j}{\xi_i} X_i\right)^{1-\sigma_x^{-1}}\right)^{\frac{1}{1-\sigma_x^{-1}}}, \\ &= \frac{1}{\xi_i} \left(P_i\right)^{\sigma_x} X_i A \left(\sum_{j=1}^{N} \xi_j \left(P_j\right)^{1-\sigma_x}\right)^{\frac{1}{1-\sigma_x^{-1}}}. \end{aligned}$$

We get an expression for X_i in terms of aggregates:

$$X_i = \xi_i \left(\frac{1}{P_i}\right)^{\sigma_x} X A^{-1} \left(\sum_{j=1}^{N} \xi_j^{\sigma_x} \left(P_j\right)^{1-\sigma_x}\right)^{\frac{-1}{1-\sigma_x^{-1}}}.$$

We calculate total expenditure:

$$P_i X_i = P_i^{1-\sigma_x} \xi_i X A^{-1} \left(\sum_{j=1}^{N} \xi_j \left(P_j\right)^{1-\sigma_x}\right)^{\frac{-1}{1-\sigma_x^{-1}}}.$$

Adding up all the goods:

$$\begin{aligned} Y &= X A^{-1} \left(\sum_{j=1}^{N} \xi_j \left(P_j\right)^{1-\sigma_x}\right) \left(\sum_{j=1}^{N} \xi_j \left(P_j\right)^{1-\sigma_x}\right)^{\frac{-1}{1-\sigma_x^{-1}}}, \\ &= X A^{-1} \left(\sum_{j=1}^{N} \xi_j \left(P_j\right)^{1-\sigma_x}\right)^{\frac{1}{1-\sigma_x}}. \end{aligned}$$

We can define the price aggregator

$$P = A^{-1} \left(\sum_{j=1}^{N} \xi_j \left(P_j\right)^{1-\sigma_x}\right)^{\frac{1}{1-\sigma_x}}.$$

such that $Y_t = X_t P_t$. Also, we can plug in the price aggregator in our expression for X_{it} to obtain:

$$\begin{aligned} X_i &= \xi_i \left(\frac{1}{P_i}\right)^{\sigma_x} X A^{-1} \left(\sum_{j=1}^{N} \xi_j \left(P_j\right)^{1-\sigma_x}\right)^{\frac{-1}{1-\sigma_x^{-1}}}, \\ &= \xi_i \left(\frac{P}{P_i}\right)^{\sigma_x} X. \end{aligned}$$

The problem with the standard formulation of the CES is that the taste parameters ξ_i do

not correspond to expenditure shares unless $\sigma_x = 1$:

$$\xi_i = \left(\frac{X_i}{X}\right)\left(\frac{P_i}{P}\right)^{\sigma_x}$$

Given this, we propose a mapping between intensity shares ξ_i and expenditure shares $\tilde{\xi}_i$:

$$\begin{aligned}
\xi_i &= \left(\frac{X_i}{X}\right)\left(\frac{P_i}{P}\right)^{\sigma_x}, \\
&= \left(\frac{X_i}{X}\right)\left(\frac{X}{X_i}\frac{X_i}{X}\frac{P_i}{P}\right)^{\sigma_x}, \\
&= \left(\frac{X_i}{X}\right)^{1-\sigma_x}\left(\tilde{\xi}_i\right)^{\sigma_x}.
\end{aligned}$$

This implies the following mapping from intensity shares to expenditure shares:

$$\tilde{\xi}_i = \xi_i^{\sigma_x^{-1}}\left(\frac{X_i}{X}\right)^{1-\sigma_x^{-1}}.$$

C Solution Method

To find the global solution, we adapt the Deep Equilibrium Nets method (Azinovic et al., 2022) to allow for Monte-Carlo based expectations, since our model has a large number of shocks. This method consists in using neural networks as function approximators for the policy functions that map the state variables $\{K_{jt}, Z_{jt}\}_j$ to the endogenous variables (policies and prices), which we denote as $\{X_{jt}\}_j$, and train the neural net to reduce the error in the system of equations describing the equilibrium, presented in subsection B.6. One of the key elements of this methodology is that we use the neural network to simulate the model and obtain points of the state space over which we will minimize the loss function. Also, we use the neural net to estimate the expectation terms that appear in the system of equations that describe the solution.

More specifically, the system of equations that we are trying to solve contains state and endogenous variables at time t, and expectations that depend on endogenous variables at time $t+1$. In order to evaluate the average error in the system of equations associated to some neural net parameters, we first sample points of the state space by simulating

episodes using the neural net to step the model forward. Then, we use again the neural network to get the policies at those points of the state space. Finally, to calculate the expectation terms at each point of the state space, we simulate many one-period transitions, use the neural net to recover the terms inside the expectation for each one-period ahead simulation, and then averaging them up to get the expectation. The only non-trivial part of this evaluation is to evaluate the expectation terms. For models in which we have an explicit and deterministic equation linking the endogenous state today (K_{jt}) with the endogenous state tomorrow (K_{jt+1}), such as real business cycle models, we can simulate many one-period transitions by sampling only the exogenous state, since we already know K_{jt+1}.

Before we explain formally how to calculate the expectation terms, we are going to introduce the neural net approximator. Let $S_t \in \mathbb{R}^{2N}$ be the state vector $S = [K_t, a_t]$. The neural net approximator, with L layers indexed by i, is:

$$\mathcal{F}(\{W, b_l\}_l; S_t) = \sigma_l(W_l * [K_t, a_t] + b_l)$$

Thus, the neural net is a function $\mathcal{F}(\theta_t; K_t, a_t)$ where θ_t correspond to the internal parameters of the neural net. The output of the neural net is a vector of non-negative real values. In particular, we define the policy variables as

$$X_t = \mathcal{F}(\theta_t; K_t, a_t)$$

Next, we show how to calculate the expectation function given that we are at particular point of the state space and our current policy has parameters θ_t.

C.1 The expectation function

In the system of equations presented in subsection B.6, the only expectation term appears in the F.O.C. for K_{jt+1}:

$$P_{jt}^{k} = \beta \mathbb{E}_t \left[P_{jt+1} \left(A_{jt+1} \right)^{1-\sigma_y^{-1}} \left(\mu_j \frac{Q_{jt+1}}{Y_{jt+1}} \right)^{\sigma_q^{-1}} \left(\alpha \frac{Y_{jt+1}}{K_{jt+1}} \right)^{\sigma_y^{-1}} + P_{jt+1}^{k} \left((1-\delta_k) + \frac{\phi}{2} \left(\frac{I_{jt+1}^2}{K_{jt+1}^2} - \delta_j^2 \right) \right) | K_t, a_t \right]$$

Notice that given policy parameters θ_t, K_{jt+1} is already determined, so the expectation is taken over realizations of $a_{t+1} \equiv \log(A_{t+1})$, whose conditional probability distribution is

$$p(a_{t+1}|a_t) = \mathcal{N}(\rho a_t, \Sigma^a)$$

In order to calculate our loss function, we need to calculate that expectation term at each point of the state space we visit. Next, we break down how that expectation would be constructed using a montecarlo simulation. First, given K_t and the policy parameters θ_t, we calculate next period capital:

$$K_{t+1} = (1-\delta_j) K_t + 1_{I_t}^{'} \mathcal{F}(\theta_t; K_t, a_t)$$

where $1_{I_t}^{'}$ is a vector that selects, among all the policies, the vector of sectoral investments. Second, we sample 128 realization of the shock vector using the conditional distribution $(a_{t+1}|a_t) = \mathcal{N}(\rho a_t, \Sigma^a)$. Third, we we are going to use our policy function to obtain the policies in $t+1$ for a each draw of $a_{t+1} \sim \mathcal{N}(\rho a_t, \Sigma^a)$ and the predetermined K_{t+1}:

$$X_{t+1} = \mathcal{F}(\theta_t; K_{t+1}, a_{t+1})$$

Finally, we use K_{t+1} and the policies X_{t+1} to calculate the term inside the expectation for each draw of the shock vector, and we get the expectation by taking the average across all draws.

C.2 The loss function

Now that we have solved for the expectation function $\Phi_t(K_t, a_t, \theta_t)$, we can calculate the loss function in period t. First, we specify the endogenous variables in period t given K_t, a_t and the parameters of the policy θ_t:$X_t = \mathcal{F}(\theta_t; K_t, a_t)$. Then, we calculate the period error, given as the quadratic loss in the system of equations that describe the solution. The error is written as right hand side divided by left hand side minus. For example, the loss for the market clearing equation of sector j is:

$$\mathcal{L}_{Q_j} \equiv \left(\frac{\left[(mu_j)^{\frac{1}{\sigma_q}} \left(Y_{jt}\right)^{\frac{\sigma_q - 1}{\sigma_q}} + \left(1 - \mu_j\right)^{\frac{1}{\sigma_q}} \left(M_{jt}\right)^{\frac{\sigma_q - 1}{\sigma_q}} \right]^{\frac{\sigma_q}{\sigma_q - 1}}}{Q_{jt}} \mathbf{1} \right)^2$$

then, we take this loss and square it.

C.3 Implementation

In this section, we present a step by step breakdown of the implementation. The first part of the implementation, which consists on calculating a loglinear policy using dynare, is done in Matlab. The second and third part of the implementation, which consist on pretraining the neural net to fit the log linear policy and then use that solve the full nonlinear version of the model, are coded in Python Colab Notebooks. The notebooks are publicly available at RbcProdNet_pretrain and RbcProdNet_train, and all the codes, including the notebooks, can also be found in the github page github econjax.

Before we start our three steps, we start in Matlab calculating the **steady state**, described in section B.9

C.3.1 Solve Log-linear Model

We solve a version of the model with log-linearization around the steady state using dynare. We are going to use these policies to "pre-train" the neural net (more details in next subsection). . Next, we recover the state space representation used by dynare internally. Let $X_t = \{I_t, Q_t, P_t, L_t\}$ be the vector of endogenous variables, and denote the vector with logs as x_t .s_t contains the log of the states, and the sub-index ss represents steady state values. The representation is:

$$s_{t+1} - s_{ss} = A(s_t - s_{ss}) + Be_t$$
$$x_t - x_{ss} = C(s_{t_{-1}} - s_{ss}) + De_t$$

A relevant detail of this stage is that timing conventions in dynare, and in particular the implementation of the log-linearized systems, introduce a subtle informational assumption. They write the evolution of log TFP as $a_t = \rho_t a_{t-1} + \epsilon_t$. Policies depend on $\{k_t, a_{t1}, \epsilon_t\}$, and the terms a_{t-1} and ϵ_t do not load according to the evolution of a_t. Trying to fit the neural net to these policies, conditioning only on $\{k_t, a_t\}$ leads to less than complete learning (up to 95% accuracy). Then, we will use$\{k_t, a_{t-1}, \epsilon_t\}$as an input for the neural net. We will also normalize those three vectors by subtracting the steady state and dividing by the standard deviation over dynare simulations. Thus, we denote observations as as $o_t = \{\tilde{k}_t, \tilde{a}_{t-1}, \tilde{e}_t\}$, where tildes are used to represent normalized variables. [17] As an output of this stage, which we pass to Python, we save the matrices $\{A, B, C, D\}$ and the standard deviation of all state and policy variables in the simulation. We are going to import in Python.

C.3.2 Pretrain Neural Net

Next, we "pretrain" the neural net to approximate the dynare policies. First, we simulate the model using the state space representation we extracted from dynare, and we store the states we visited and loglinear policy at each period. Second, we evaluate the neural net at the visited states, so we get the neural net policies. Third, we calculate the loss at each step, using the following loss function:

$$\mathcal{L}_t = \sum_{i=1}^{4N} (X_{it}^{neuralnet} / X_{it}^{loglinear} - 1)^2 / (4N)$$

We can also calculate the average accuracy in one period as

$$Acc_t = \sum_{i=1}^{4N} \left| \frac{X_{it}^{neuralnet} - X_{it}^{loglinear}}{X_{it}^{dynare}} \right| / (4N)$$

so 100% represents perfect fitting.

[17] Throughout the code, we will distinguish between state and observations, and normalized variables or not.

Table 5: Pretrain experiment hyperparameters

Hyperparameter	Value
Network Architecture	
NN hidden layers	[1024,1024]
Output layer	Softplus
Training Workflow	
episodes per step	1024
periods per episode	128
steps per epoch	100
number of epoches	1000
shock size scaling	1.5
Optimization	
Optimizer	Adam
Learning rate	5e-4 to 1e-5
batch size	16
Opt. Momentum	0.9
Mean gradients exp. decay	0.9
S.D. gradients exp. decay	0.999
Solution threshold	mean error $<$ 5e-6, max error $<$ 5e-5

In table 5, we show the configuration of the pre-train experiment. We will use vanilla Fully Connected Layer, also called Multi-layer Perceptron, with 2 hidden layers of 1024 nodes each. The input to the neural net is the normalized observations we just described in subsection C.3.1. We activate the output layer with a Softplus activation, which guarantees that the outputs are positive. The input to the neural net is the normalized observations we just described in subsection C.3.1. The targets that the neural net needs to hit are normalized in such a way that if the neural net outputs 1 for a variable, it is outputting the deterministic steady state of the variable. If it outputs 1.1, it is outputting a value that is 10% higher than the deterministic steady state.

In order to explain the training workflow, we need to introduce some notation. Whenever we update the neural net, we call it a step. But we let the computer to run for several steps before it gives us feedback on how the neural net is doing. We call this set of steps an epoch, so we have a parameter called steps per epoch, set to 100 in this case. Then, in a step, we are going to sample a number of episodes in parallel. An episode is a simulation of the model for a number of periods (in this case years). Hence, we have a parameter

called episodes per step, set at 1024, and another parameter called periods per episode , set at 128. For the training, we scale up the shocks by 1.5 so we have more volatility.

For the optimization, we use Adam as an optimizer with default parameters. The learning rate follows a cosine decaying schedule starting at 5e-4 and ending at 1e-5. We split randomly all the periods collected in a step in minibatches of step 16, we calculate gradients of the loss function for each minibatch, and then we average the gradients across minibatches. While we are training for a fixed number of epochs, our criteria for the problem being solved is that the mean loss is below 5e-6 and the max loss is below 5e-5.

C.3.3 Solve the Nonlinear Model

FOllowing the same notation explained in the pretraining step, the configuration of the experiment is

Table 6: Train experiment hyperparameters

Hyperparameter	Value
Network Architecture	
NN hidden layers	[1024,1024]
Output layer	Softplus
Training workflow	
episodes per step	64
periods per episode	32
steps per epoch	100
number of epoches	1000
shock size scaling	1.5
Montecarlo draws	128
Optimization	
Optimizer	Adam
Learning rate	2e-5
batch size	16
Opt. Momentum	0.9
Mean gradients exp. decay	0.9
S.D. gradients exp. decay	0.999
Solution threshold	mean error $<$ 5e-6, max error $<$ 5e-5

Given that in the training step we need to estimate the expectations at each point of the

state space that we visit, the training step is much more computationally intensive, so we have lower values for periods per episode and episodes per step. For the montecarlo estimation of expectations, we draw 128 samples of the shock vector in parallel (each shock vector has dimension 37 by 1). Since the pretraining leaves us close to the optimum, we fix the learning rate at a low value of 2e-5.

C.4 Accuracy Checks

In figure 11, we observe the histogram of period losses that result from a 10000 period simulation of the solved neural net policies. We see that most of the mass is concentrated below 5e-6.

Figure 11: Distribution of Losses over Ergodic Distribution

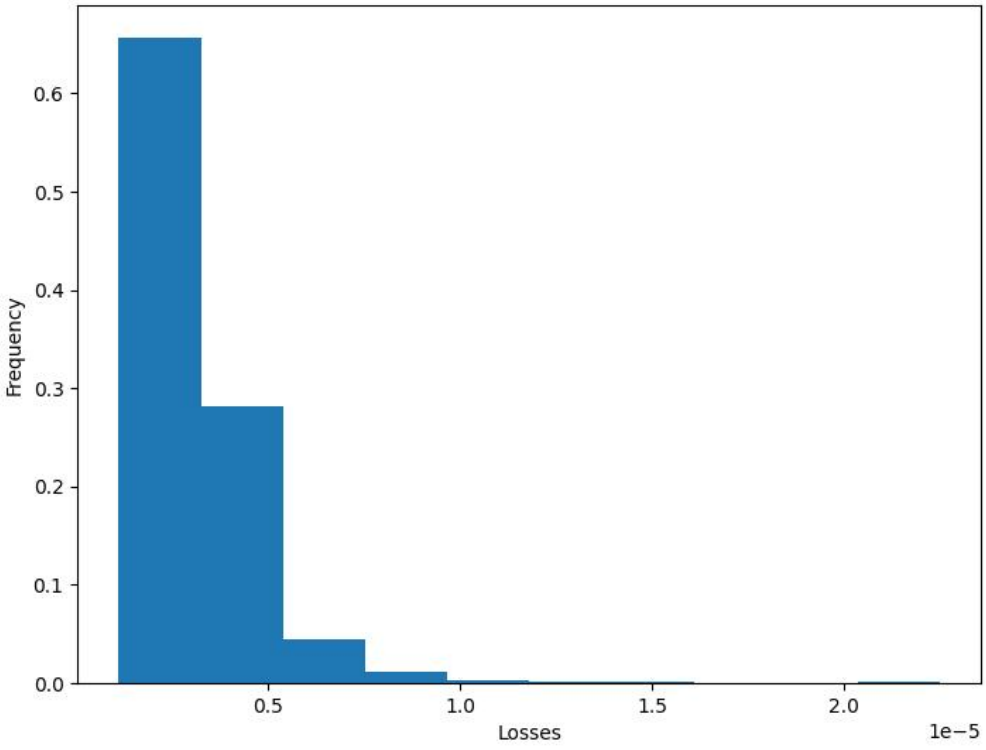

Note: This figure shows the distribution of losses over the ergodic distribution. Ir order to calculate, we simulate the global solution for 10000 periods, calculate the loss in each period, and plot the histogram.

Another accuracy metric that is important to keep track of is the error introduced by the expectation estimation via the montecarlo method. In order to do this, we use the solved neural net and we calculate the expectation terms in random points of the state space. For each point of the state space, we repeat the montecarlo simulation 1000 times with different shock realizations. In figure 12, we see the accuracy of the montecarlo estimation of the expectation terms, measured as the standard deviation divided by the mean of the error. As we can see, the error diminishes considerably as we increase the number of random draws, but at 128, the number of draws we use, the error is already below 1%.

Figure 12: Error in Montecarlo Estimation of Expectations

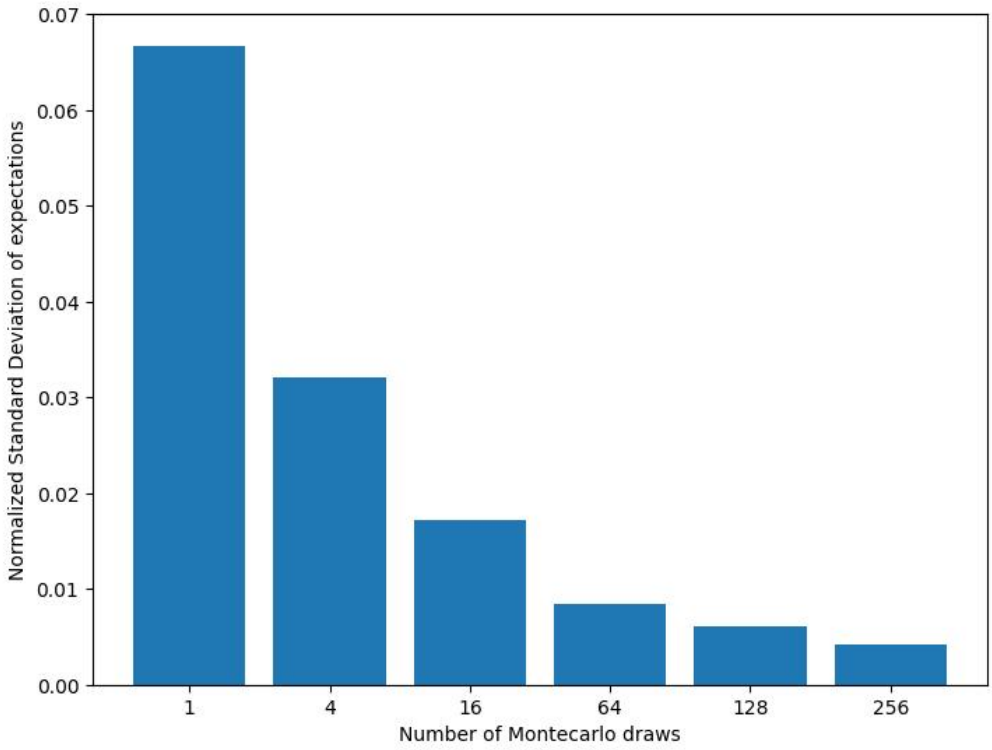

Note: This figure shows the accuracy of the montecarlo simulation method. In order to calculate it, we perform the simulation 1000 times for different draws of the shocks, and calculate accuracy statistics. In the y axis we present our measure of accuracy, that corresponds to the normalized standard deviation of the expectation estimation (standard deviation divided by the mean). The number of draws actually used in the experiments is 128.

D Auxiliary Figures for Section 5

In this appendix, we present impulse responses for additional sectors.

Figure 13: Impulse Response of Aggregate Consumption to a Construction TFP Shock

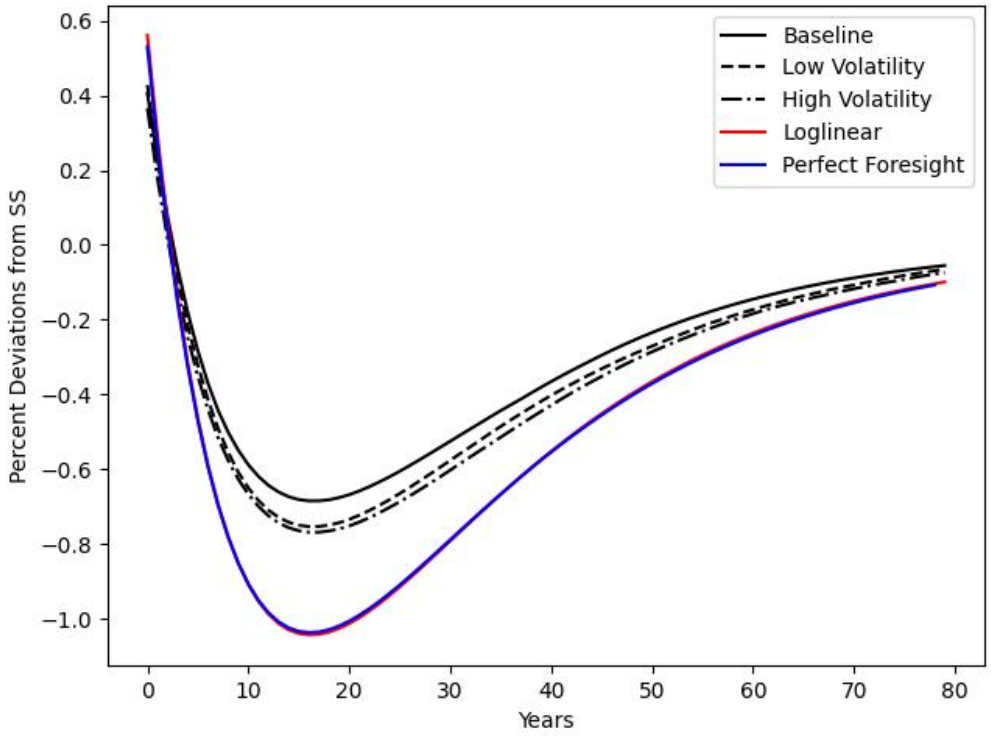

Note: This figure shows the impulse response of aggregate consumption to a 20% negative TFP shock in Construction. The black line represents the response using the global solution method, the red line shows the response using a log-linear approximation, and the blue line shows the perfect foresight solution. For the global solutions, the vertical axis shows log deviations relative to the stochastic steady state, while for the log-linear and perfect foresight solutions we show percentage deviations from the deterministic steady state.

Figure 14: Impulse Response of Aggregate Consumption to a Machinery TFP Shock

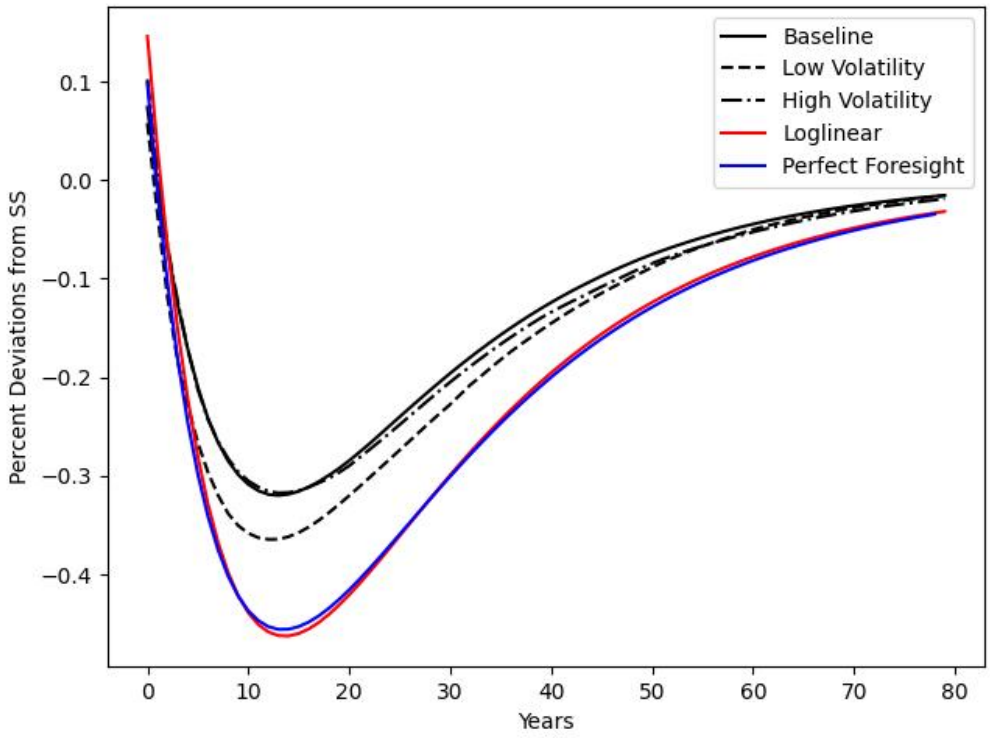

Note: This figure shows the impulse response of aggregate consumption to a 20% negative TFP shock in Machinery. The black line represents the response using the global solution method, the red line shows the response using a log-linear approximation, and the blue line shows the perfect foresight solution. For the global solutions, the vertical axis shows log deviations relative to the stochastic steady state, while for the log-linear and perfect foresight solutions we show percentage deviations from the deterministic steady state.

Figure 15: Impulse Response of Aggregate Consumption to a Petroleum TFP Shock

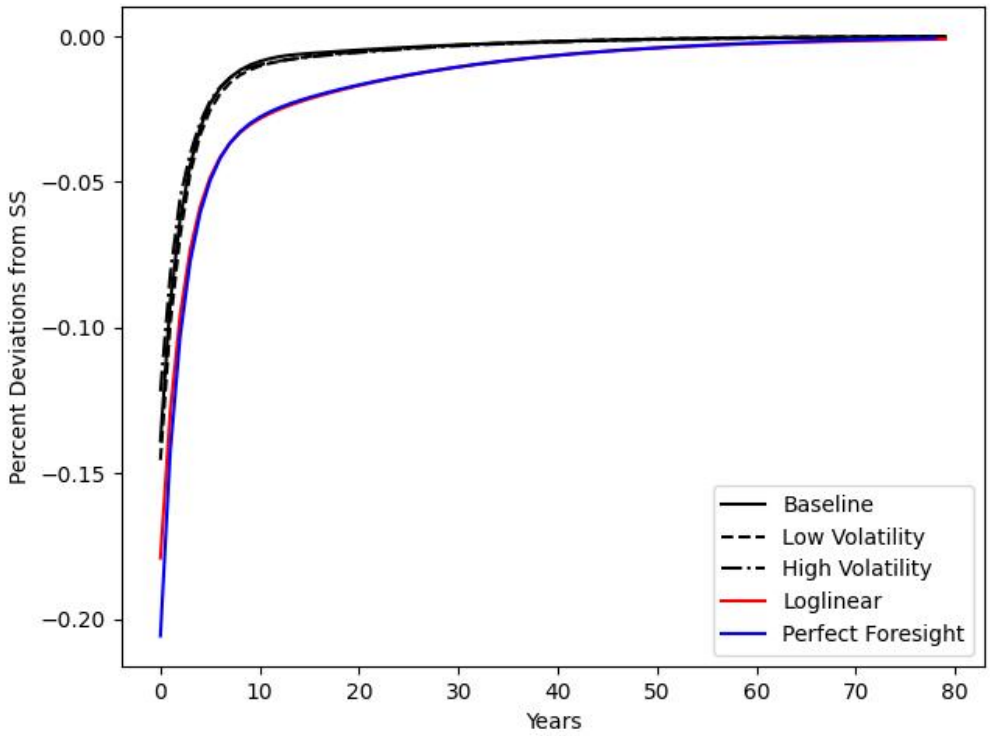

Note: This figure shows the impulse response of aggregate consumption to a 20% negative TFP shock in Petroleum. The black line represents the response using the global solution method, the red line shows the response using a log-linear approximation, and the blue line shows the perfect foresight solution. For the global solutions, the vertical axis shows log deviations relative to the stochastic steady state, while for the log-linear and perfect foresight solutions we show percentage deviations from the deterministic steady state.

Figure 16: Impulse Response of Aggregate Consumption to a Retail TFP Shock

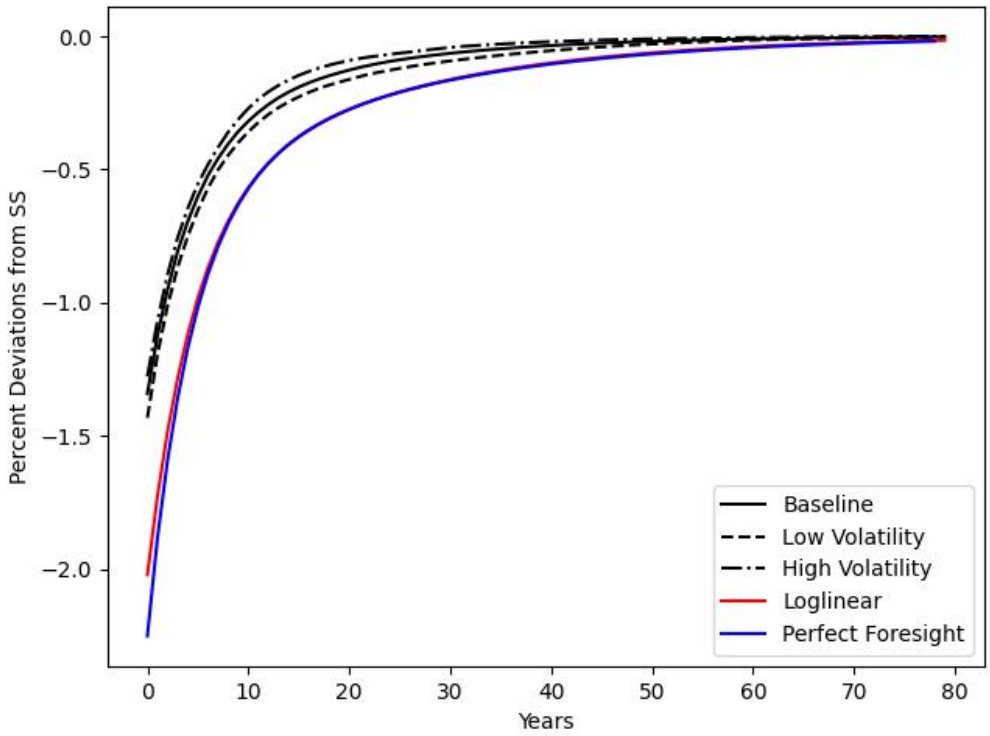

Note: This figure shows the impulse response of aggregate consumption to a 20% negative TFP shock in Retail. The black line represents the response using the global solution method, the red line shows the response using a log-linear approximation, and the blue line shows the perfect foresight solution. For the global solutions, the vertical axis shows log deviations relative to the stochastic steady state, while for the log-linear and perfect foresight solutions we show percentage deviations from the deterministic steady state.

Figure 17: Impulse Response of Aggregate Consumption to a Real Estate TFP Shock

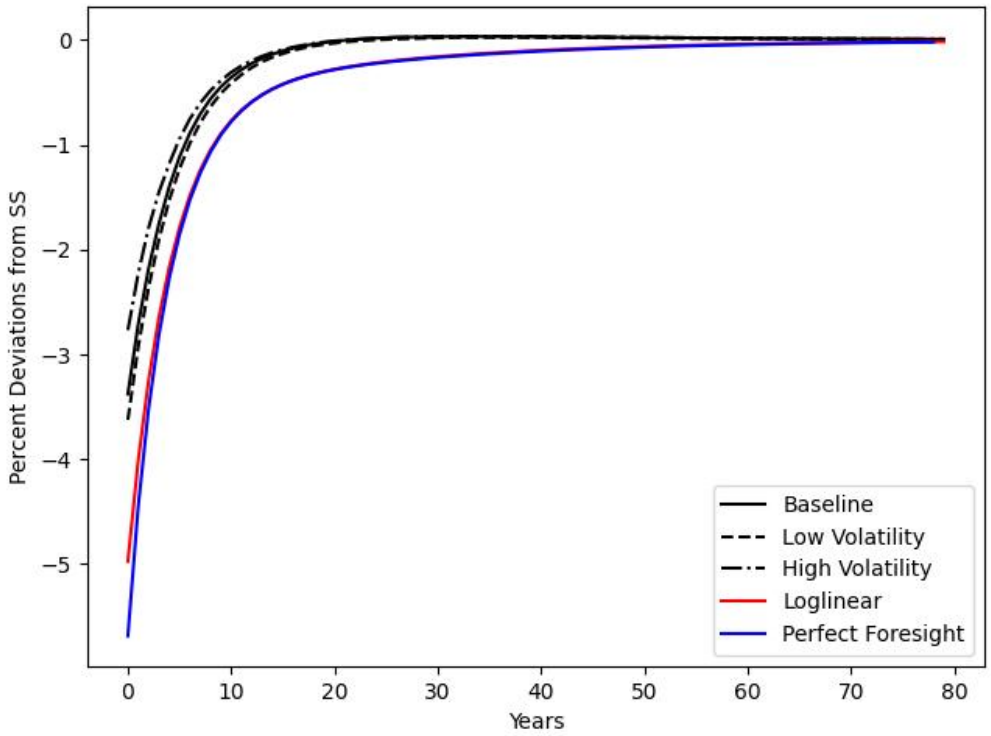

Note: This figure shows the impulse response of aggregate consumption to a 20% negative TFP shock in Real Estate. The black line represents the response using the global solution method, the red line shows the response using a log-linear approximation, and the blue line shows the perfect foresight solution. For the global solutions, the vertical axis shows log deviations relative to the stochastic steady state, while for the log-linear and perfect foresight solutions we show percentage deviations from the deterministic steady state.